BIOASSAY-GUIDED ISOLATION AND IDENTIFICATION OF BIOACTIVE COMPOUNDS FROM *LEONURUS JAPONICUS* HOUTT. EXTRACT

TRIRATH SUKTHAWEE

MASTER OF SCIENCE
IN
APPIED CHEMISTRY

SCHOOL OF SCIENCE
MAE FAH LUANG UNIVERSITY

2022

BIOASSAY-GUIDED ISOLATION AND IDENTIFICATION OF BIOACTIVE COMPOUNDS FROM *LEONURUS JAPONICUS* HOUTT. EXTRACT

TRIRATH SUKTHAWEE

THIS THESIS IS A PARTIAL FULFILLMENT OF
THE REQUIREMENTS FOR THE DEGREE OF
MASTER OF SCIENCE
IN
APPLIED CHEMISTRY

SCHOOL OF SCIENCE
MAE FAH LUANG UNIVERSITY
2022

BIOASSAY-GUIDED ISOLATION AND IDENTIFICATION OF BIOACTIVE COMPOUNDS FROM *LEONURUS JAPONICUS* HOUTT. EXTRACT

TRIRATH SUKTHAWEE

THIS THESIS HAS BEEN APPROVED
TO BE A PARTIAL FULFILLMENT OF THE REQUIREMENTS
FOR THE DEGREE OF MASTER OF SCIENCE
IN
APPLIED CHEMISTRY
2022

EXAMINATION COMMITTEE

.....CHAIRPERSON
(Asst. Prof. Cholpisut Tantapakul, Ph. D.)

Tharakorn.
.....ADVISOR
(Tharakorn Maneerat, Ph. D.)

.....CO-ADVISOR
(Assoc. Prof. Surat Laphookhieo, Ph. D.)

.....CO-ADVISOR
(Asst. Prof. Rawiwan Charoensup, Ph. D.)

Kanchana Watla-iad
.....EXAMINER
(Kanchana Watla-iad, Ph. D.)

ACKNOWLEDGEMENTS

I would like to sincerely thank my advisor, Dr. Tharakorn Maneerat, Assoc. Prof. Dr. Surat Laphookhieo, and Asst. Prof. Dr. Rawiwan Charoensup for their unwavering support of my master's degree study and research. Their patience, motivation, encouragement, support, and detailed knowledge were invaluable to me throughout the entire research and thesis-writing process.

Additionally, I would like to thank Mae Fah Luang University for its support of the scholarship. I wish to thank Prof. Dr. Lean-Teik NG for allowing me to work in his laboratory for three months and for sharing his wealth of knowledge. Moreover, I would like to thank Medicinal Plant Innovation Center (MPIC) and Technological Instruments Center (STIC) of Mae Fah Luang University, for their support in the analysis and testing of the samples, as well as all of his lab's staff for their countless hours of assistance and support during my studies.

Finally, I would like to thank you from the bottom of my heart to my parents for their financial support, never-ending love and inspiration, which gave my life meaning and happiness. Moreover, I would like to thank our members in MPIC for their support and cheer me up when I'm disappointed and sad. Together with those whose names are not mentioned here for all their support throughout this research.

Trirath Sukthawee

Thesis Title	Bioassay-Guided Isolation and Identification of Bioactive Compounds from *Leonurus japonicus* Houtt. Extract
Author	Trirath Sukthawee
Degree	Master of Science (Applied Chemistry)
Advisor	Tharakorn Maneerat, Ph. D.
Co-Advisor	Assoc. Prof. Surat Laphookhieo, Ph. D.
	Asst. Prof. Rawiwan Charoensup, Ph. D.

ABSTRACT

Leonurus japonicus (*L. japonicus*) is widely used in folk medicine to treat diabetes, menstrual irregularities, and bronchitis. This study evaluated the *α*-glucosidase inhibitory and anti-inflammatory activity of the crude extract, semipurified fractions, and isolated compounds from the areal of *L. japonicus*, through bioassay-guided testing. The crude extract was obtained with an ethanolic extract and then partitioned with ethyl acetate. Bioassay-guided fractionation of an EtOAc-soluble extract of arial of *L. japonicas* led to the isolation of six known compounds (**T-1 to T-6**). Their structures were elucidated based on data analysis, including ^{1}H NMR data, LC-QTOF-MS, ECD, UV, and FT-IR. Compounds **T-1 to T-6** exhibited *α*-glucosidase inhibitory and anti-inflammatory activity in range IC_{50} values at 143.9 - 598.4 μM and 66.9 - 285.8 μM, respectively, when compared with the positive control.

Keywords: *Leonurus japonicus*, *α*-Glucosidase Inhibitory, NO Production Inhibitory

TABLE OF CONTENTS

TABLE OF CONTENTS (continued)

LIST OF TABLES

LIST OF TABLES (continued)

LIST OF FIGURES

LIST OF FIGURES (continued)

LIST OF FIGURES (continued)

ABBREVIATION AND SYMBOL

	Nuclear Magnetic Resonance
NMR	Singlet
s	Doublet
d	Triplet
t	Multiplet
m	Doublet of doublet
dd	Chemical Shift
δ	Relative to TMS
J	Coupling constant
$[\alpha]_D^{25}$	Specific Rotation
λ_{max}	Maximum Wavelength
m/z	a Value of Mass Divided by Charge
MHz	Megahertz
LC-QTOF MS	Liquid Chromatograph Quadrupole Time-of-Flight Mass Spectrometer
CD	Circular Dichroism
UV-Vis	Ultra Violet-Visible
FT-IR	Fourier Transform Infrared
LPS	Lipopolysaccharide
NO	Nitric Oxide
IC_{50}	Half-maximal inhibitory concentration
µM	Micromolar
cm	Centimeter
mm	Milimeter
TNF-*α*	Tumor necrosis factor-*α*
IL-6	Interleukin-6

ABBREVIATION AND SYMBOL (continued)

MCP-1	Monocyte chemotactic protein-1
hr	Hour
LDH	Lactate dehydrogenase
p	Probability value
Units/mL	Units per mililiter
NMDA	N-methyl-D-aspartate
mφ	Macrophages
iNOS	Induce nitric oxide synthase
SD	Standard deviation
ECM	Extracellular matrix
TGF-β	Transforming growth factor beta
ERS	Endoplasmic reticulum stress
MMPs	Role of Matrix Metalloproteinases
TIMPs	Tissue inhibitor of metalloproteinases
NF-κB	Nuclear factor kappa-B
JAK	Janus-associated kinases
STAT	Signal transducer and activator of transcription
β-MHC	β-Myosin heavy chain
SIRT1	Sirtuin 1
eNOS	Endothelial nitic oxide synthase
BHA	Beta hydroxy acid
CNS	Central nervous system
MIC	Minimum inhibitory concentration
DPPH	2,2–Diphenyl–1–picrylhydrazyl
nM	Nano molar
GLUT4	Glucose transporter type 4

ABBREVIATION AND SYMBOL (continued)

HCMV	Human cytomegalovirus
VZV	Varicella-zoster virus
PTP1B	Protein-tyrosine phosphatase 1B
M	Molar
APTT	Activated partial thromboplastin time
PTT	Partial thromboplastin time
FIB	Fibrinogen
ADP	Adenosine diphosphate
SEM	Standard error of mean
5-FU	5-Fluorouracil
EC_{50}	Half maximal effective concentration

CHAPTER 1

INTRODUCTION

1.1 Overview of the Publication

Leonurus japonicus (*L. japonicus*) is widely used in folk medicine to treat diabetes, menstrual irregularities, and bronchitis. This study evaluated the α-glucosidase inhibitory and anti-inflammatory activity of the crude extract, semi-purified fractions, and isolated compounds from the aerial parts of *L. japonicus* through bioassay-guided isolation. The crude ethanolic extract was partitioned with ethyl acetate. Bioassay-guided fractionation of an EtOAc-soluble extract led to the isolation of six known compounds (**1**-**6**). Their structures were elucidated based on data analysis, including ^{1}H NMR data, LC-QTOF-MS, ECD, UV, and FT-IR. Compounds **1**-**6** exhibited α-glucosidase inhibitory and anti-inflammatory activities in range IC_{50} values at 143.9 - 598.4 μM and 66.9 - 285.8 μM, respectively, when compared with the positive control.

1.2 Botanical Description and Literature Reviews

1.2.1 *Leonurus japonicus*

Leonurus japonicus or Chinese Motherwort is an herbaceous plant belonging to the Lamiaceae family. The character of the stem is an upright square along with fine hair. The plant grows to a height of 30 to 120 cm and 5 mm in diameter. The flowers are inflorescences, and the calyx shape is tubular-campanulate to long, 6-8 mm at the ends of branches or leaf prongs.

Distribution: The *L. japonicus* is a native plant to several regions, including Cambodia, Japan, Korea, Laos, Malaysia, Myanmar, Thailand, and Vietnam, as well as in some countries of Africa, North America, and South America.

Phenological periods: July through October is the growing season, and June through September is the blooming season. When it blooms, the plant will be died (Shang et al., 2014).

1.2.2 Constituents from *L. japonicus*

L. japonicus is well known to be a rich source of alkaloids, diterpenes, flavones, spirocyclic nortriterpenoids, phenylethanoid glycosides, and sesquiterpene glycosides (Shang et al., 2014). The information from the SciFinder scholar database reveals several types of compounds as presented in the plants of the *Lamiaceae* genus, as summarized in Table 1.1.

Alkaloids, diterpenes, flavones, spirocyclic nortriterpenoids, phenylethanoid glycosides, sesquiterpene glycosides, essential oils, and other chemicals are abundant in the *L. japonicus* (Shang et al., 2014). For a long time ago, the aerial parts of *L. japonicus* have been commonly used in Chinese herbal medicine for regulating menstrual disturbance, dysmenorrhea, amenorrhea, blood stasis, and postpartum bleeding, as well as activating blood circulation, diuretics, and dispelling edema. In promoting blood circulation and removing blood stasis. *L. japonicus* shows extraordinary clinical effects. According to literature reviews, *L. japonicus* has a pharmacological impact on the uterine smooth muscle, antibacterial activity, coagulant activity, cytotoxicity, angiogenic activity, and aggregative antiplatelet activity (Miao et al., 2019).

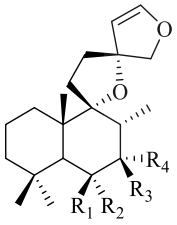

	R_1	R_2	R_3	R_4
Prehispanolone (**1**)	H	H	O	O
Preleoheterin (**3**)	O	O	OH	H

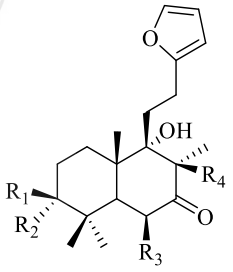

	R_1	R_2	R_3	R_4
Hispanolone (**2**)	H	H	H	H
Galeopsin (**5**)	H	H	H	OAc

Figure 1.1 Structure of compounds (**1-5**)

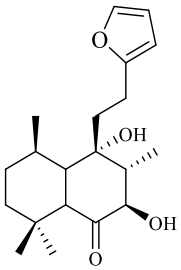

Leoheterin (**4**)

Figure 1.1 (continued)

In 1993, Hon et al. isolated five known diterpenes (**1**-**5**) from *L. japonicus*. Compound **1** demonstrated cytoprotective properties against glutamate-induced toxicity in rat cortical cells grown in primary culture (Table 1.1). Compound **2**, employing live macrophage (mφ) triggered by LPS in an iNOS inhibitory test, revealed a NO generation effect (Table 1.2). Furthermore, The anti-inflammatory effects of compounds **4** and **5** were demonstrated by their ability to inhibit the proinflammatory cytokines tumor necrosis factor-α (TNF-α), interleukin-6 (IL-6), and monocyte chemotactic protein-1 (MCP-1) (Table 1.3) and the cytotoxicity activity was demonstrated against five human cell lines, including the mouse mononuclear macrophage leukemia cell line, the human hepatoma cell line (HepG2), three lung adenocarcinoma cell lines (NCI-H1975, PC9, and XLA-07), and RAW264.7 (Table 1.4) (Moon et al., 2010; Nieto-Mendoza et al., 2005; Xiao et al., 2017).

Table 1.1 Cytoprotective effects against glutamate-induced toxicity in primary cultured rat cortical cells of compound **1**

Compound	**Cell viability[a,b] (%)**		
	0.1 µM	**1 µM**	**10 µM**
1	14.2± 0.3	11.3 ± 0.2	9.35 ± 0.2
Control[c]	-	100	-
Glutamate-treated[c,d]	-	0	-
APV[e]	11.5 ± 1.4	26.5 ± 2.3	42.5 ± 3.7
MK-80[f]	51.4 ± 4.6	63.5 ± 5.8	78.4 ± 2.0

Table 1.1 (continued)

Compound	Cell viability[a,b] (%)		
	0.1 µM	**1 µM**	**10 µM**
CNQX[g]	23.5 ± 3.7	44.8 ± 3.5	53.2 ± 4.6

Note [a] Rat cortical cell cultures were incubated with test compounds for 1 hr. The cultures were then exposed to 100 µM glutamate for 24 hr. After the incubation, the cultures were assessed for the extent of neuronal damage.

[b] Cell viability was calculated as 100 × (LDH released from glutamate-treated-LDH released from glutamate + test compound-treated) / (LDH released from glutamate-treated-LDH released from control). The values shown are the mean ± STD of three experiments (3-4 cultures per experiment). Results differ significantly from the glutamate-treated: * $p < 0.05$, ** $p < 0.01$, *** $p < 0.001$.

[c] LDH released from control and glutamate-treated cultures were 11.7 ± 1.3 and 47.9 ± 4.0 units/mL, respectively.

[d] Glutamate-treated value differed significantly from the untreated control at $p < 0.001$.

[e] APV, DL-2-amino-5-phosphonovaleric acid, a competitive NMDA receptor antagonist.

[f] MK-801, dizocilpine maleate, a noncompetitive NMDA receptor.

[g] CNQX, 6-cyano-7-nitroquinoxaline-2,3-dione, non-NMDA receptor antagonist.

Table 1.2 NO production effect in the iNOS inhibitory test using live macrophage (mφ) activated by LPS compound **2**

Compound	Concentrations (µM)	Production of NO_2^- (µM) ± SEM
2	10	83.20 ± 2.0* (a)
	31	71.51 ± 0.6* (a)
	100	52.63 ± 2.1* (a)
Aminoguanidin	10	97.82 ± 4.2* (a)
	31	80.01 ± 9.4* (a)
	100	66.16 ± 3.5* (a)

Note * $p < 0.05$; (% Cellular viability)

[a] Means 95-100% of the cells lived after the test

Table 1.3 Anti-inflammatory activity of compounds **4** and **5** on TNF-*α*, IL-6 and MCP-1) production

Compounds	IC_{50} Values (μM)[a]		
	TNF-*α*	**IL-6**	**MCP-1**
4	18.65 ± 0.43	> 40	> 40
5	17.01 ± 1.56	> 40	> 40
Dexamethasone ($x10^3$)[b]	1.17 ± 0.18	9.42 ± 0.75	2.91 ± 0.23

Note [a] Values of IC_{50} are presented as mean ± SD.

[b] Compound was used as a positive control.

Table 1.4 Cytotoxic activity of compounds **4** and **5**

Compounds	IC_{50} Values (μM)[a]			
	H1975	**XLA-07**	**PC9**	**HepG2**
4	71.42 ± 5.37	67.08 ± 3.50	> 80	> 80
5	68.73 ± 1.04	> 80	> 80	> 80
Taxol ($x10^3$)[b]	3.89 ± 0.50	80.18 ± 6.89	3.68 ± 0.80	10.28 ± 1.88

Note [a] Values of IC_{50} are presented as mean ± SD.

[b] Compound was used as a positive control.

In 1994, Horstmann et al. discovered two new monoterpenoids (**6-7**) with six known compounds (**8-13**) from *L. japonicus*. Compound **8** reported a wide range of biological activities, including strong antifibrotic properties (on various fibrosis types) by preventing the deposition of ECM (extracellular matrix) and lowering inflammatory and oxidative stress through several molecular mechanisms (including TGF-β, ERS-mediated apoptosis, MMPs/TIMPs, NF-κB, and JAK/STAT). Stachydrine exhibits cardioprotective and vasoprotective characteristics due to its reduction of β-MHC, excessive autophagy, SIRT1, eNOS uncoupling, and angiogenesis. In addition to its effects on the uterus, it has anticancer and neuroprotective qualities. Effects of compound **10** on antioxidative, anti-inflammatory, cancer-preventive, diabetes-reversing, antibacterial, and neuroprotective processes have been established (Cheng et al., 2020; Gullón et al., 2017).

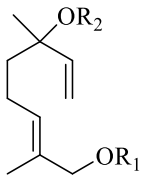

	R_1	R_2
9-Hydroxylinalool-6-O-glucoside (**6**)	H	Glc
9-Hydroxylinalool-9-O-glucoside (**7**)	Glc	H

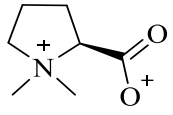

Stachydrine (**8**)

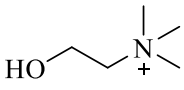

Choline (**9**)

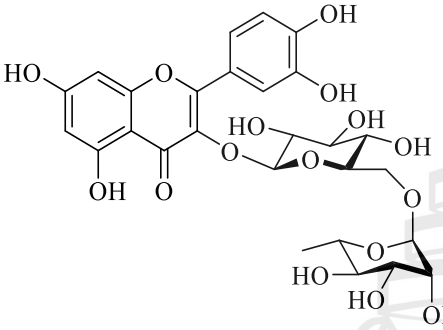

Rutin (**10**)

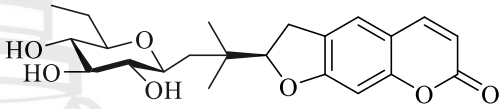

Nodakenin (**11**)

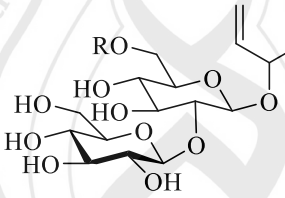

	R
Leonurenoside I (**12**)	Xyl
Leonurenoside II (**13**)	H

Figure 1.2 Structure of compounds (**6-13**)

In 1996, Morita et al. discovered three new cyclopeptides (**14-16**) from the fruit of *L. japonicus*. Compounds **15** and **16** showed growth-inhibitory effects on p-338 lymphocytic leukemia cells (IC_{50} values of 6.0 and 3.7 µg/mL, respectively) (Houshdar et al., 2021).

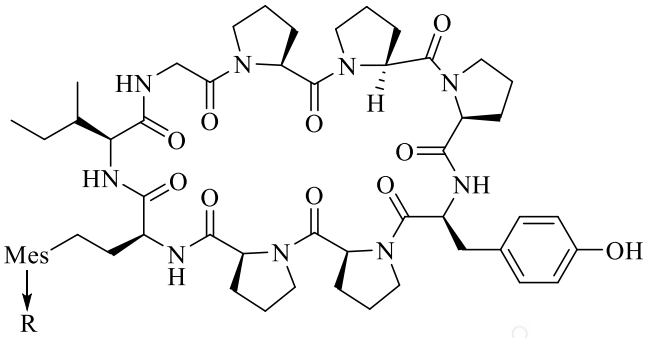

	R
Cycloleonuripeptide A (**14**)	Met
Cycloleonuripeptide B (**15**)	O [a]
Cycloleonuripeptide C (**16**)	O [a]

[a] Compound **15** and **16** are isomers with R=O

Figure 1.3 Structure of compounds (**14-16**)

In 1997, Morita et al. discovered a new cyclopeptide (**17**) from fruits of *L. japonicus*. Compound **17** demonstrated inhibition of cyclooxygenase activity.

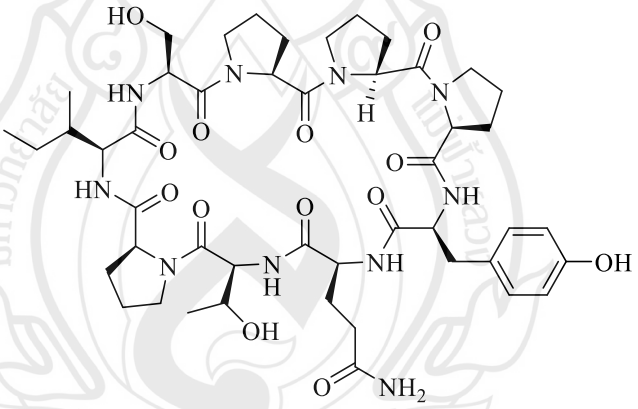

Cycloleonuripeptide D (**17**)

Figure 1.4 Structure of compound (**17**)

In 1998, Sugaya et al. discovered two new phenolic glycosides (**18-19**) and four known compounds (**20-23**) from whole part of *L. japonicus*. Compounds **18-23** showed more potent antioxidant properties than α-tocopherol and BHA. Compound **20** was reported to be beneficial in reducing eosinophilic inflammation. Compound **21** has been linked to several bioactivities, including antioxidant, anti-inflammatory,

hepatoprotective, allergic, antithrombotic, neuroprotective, osteogenic, anti-obesity, antidiabetic, antimicrobial, antiprotozoal, anti-aging, anticholinesterase, and antityrosinase (Rogerio et al., 2007; Grochowski et al., 2018).

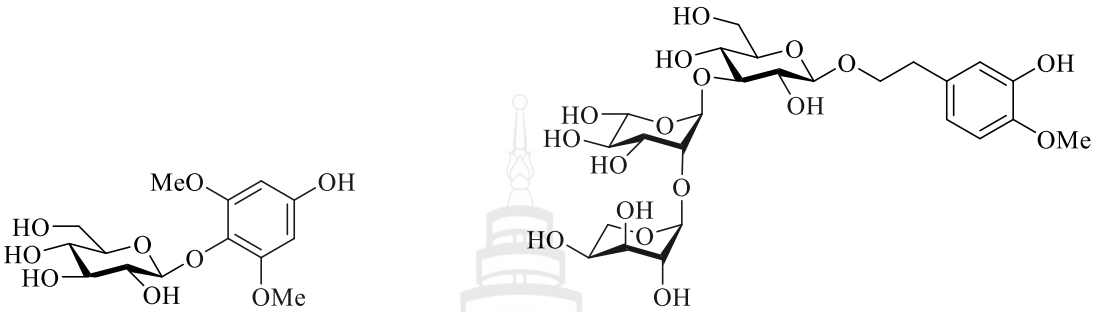

Leonuriside A (**18**)

Leonuriside B (**19**)

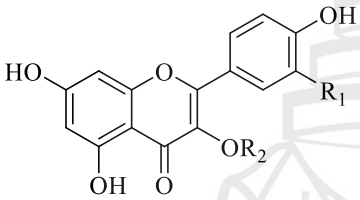

	R_1	R_2
Isoquercitrin (**20**)	OH	Glu
Tiliroside (**21**)	H	Glu (2’’-*p*-coum)
Isorhamnetin 3-*O*-Rutinoside (**22**)	OMe	Rut

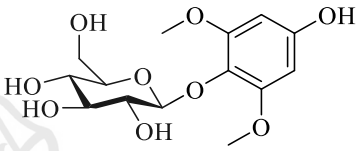

Leonuride (**23**)

Figure 1.5 Structure of compounds (**18-23**)

In 2003, Yue et al. isolated two known compounds (**24-25**) from *L. japonicus.* Compounds **25** demonstrated bio-activities such as antioxidative, anti-inflammation, anti-apoptosis, and cardioprotective properties on cardiomyocytes damaged by hypoxia and used pharmaceutically to treat uterine, neurological, and cardiovascular diseases.

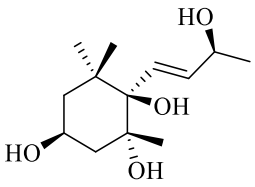

Megastigmane (**24**)

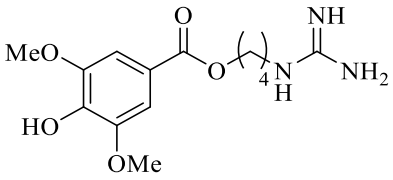

Leonurine (**25**)

Figure 1.6 Structure of compounds (**24-25**)

In 2005, Giang et al. discovered eight new spiro-labdane diterpenoids (**26-33**) along with four known compounds (**34-37**) from aerial parts of *L. japonicus*. Compound **26** showed cytotoxicity towards MCF-7 cells (Table 1.5) (Nguyen et al., 2021).

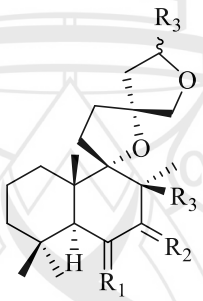

	R_1	R_2	R_3	R_3
Leoheteronone A (**26**)	H_2	O	OAc	*α*-OMe
Leoheteronone B (**27**)	H_2	O	H	*β*-OH
15-Epileoheteronone B (**28**)	H_2	O	H	*α*-OH
Leopersin B (**34**)	H_2	O	OAc	*β*-OH
15-Epileopersin B (**35**)	H_2	O	OAc	*α*-OH
Leopersin C (**36**)	O	*β*-OH, *α*-H	H	*β*-OH
15-Epileopersin C (**37**)	O	*β*-OH, *α*-H	H	*α*-OH

Figure 1.7 Structure of compounds (**26-37**)

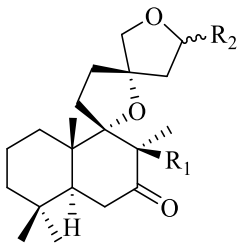

	R_1	R_2
Leoheteronone C (**29**)	OAc	α-OMe
Leoheteronone D (**30**)	H	β-OH
15-Epileoheteronone D (**31**)	H	α-OH
Leoheteronone E (**32**)	OAc	α-OH
15-Epileoheteronone E (**33**)	OAc	α-OH

Figure 1.7 (continued)

Table 1.5 Cytotoxic activity against MCF-7 cells of compounds **26**

Compounds	**IC_{50} Values (µM)**
	MCF-7
26	197.0 ± 5.7
Camptothecin	0.014 ± 0.002

In 2005, Giang et al. discovered five new labdane diterpenoids (**38-42**) and three known compounds (**43-45**) from aerial parts of *L. japonicus*. Compounds **38**, **39**, and **43** showed α-glucosidase inhibitory activity (Table 1.6) (Nguyen et al., 2017).

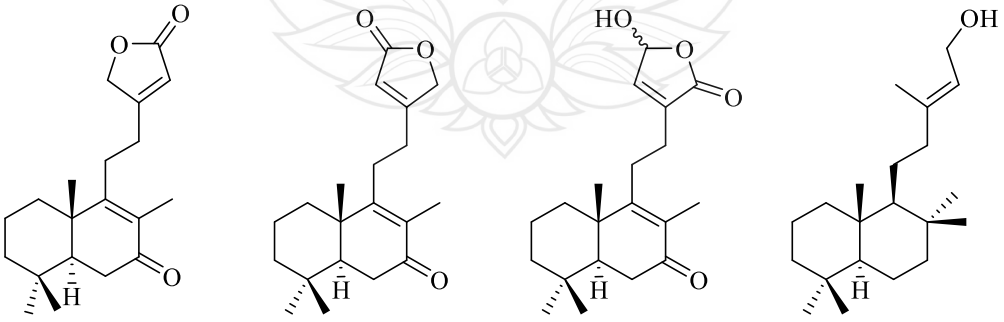

Leoheteronins A (**38**) Leoheteronins B (**39**) Leoheteronins C (**40**) Leoheteronins D (**41**)

Figure 1.8 Structure of compounds (**38-45**)

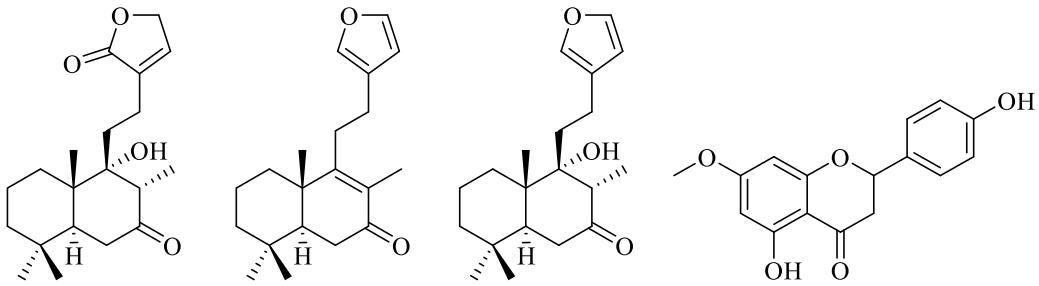

Leoheteronins E (**42**) Hispanone (**43**) Panolone (**44**) Genkwanin (**45**)

Figure 1.8 (continued)

Table 1.6 α-Glucosidase inhibitory activity of compounds **38**, **39** and **43**

Compounds	**IC_{50} Values (μM)**[a]
38	234.9
39	> 250.0
43	235.2
Acarbose[b]	214.5 ± 2.3

Note [a] Values of IC_{50} are presented as mean ± SD.

[b] Compound was used as a positive control.

In 2006, Morita et al. discovered two new cyclic nonapeptides (**46-47**) from the fruits of *L japonicus*. All compounds showed moderate vasorelaxant effects on rat aorta.

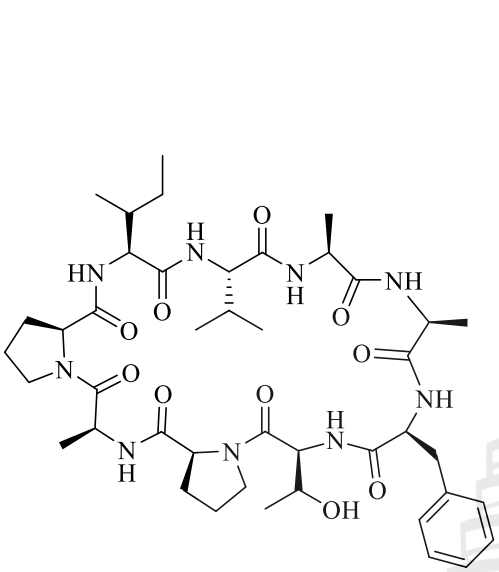

Cycloleonuripeptide E (**46**)

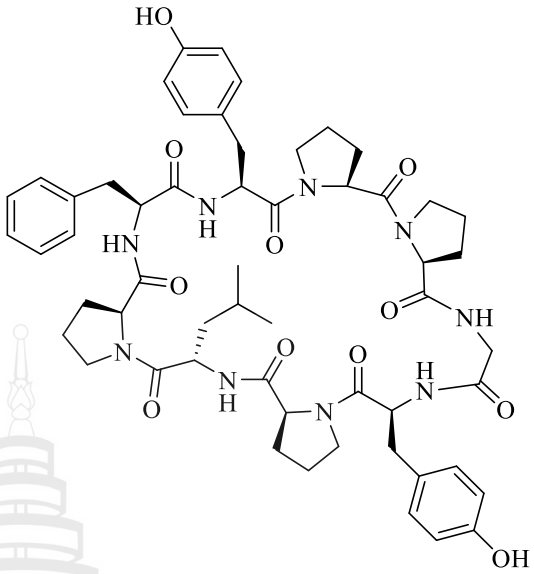

Cycloleonuripeptide F (**47**)

Figure 1.9 Structure of compounds (**46-47**)

In 2006, Qu et al. isolated seven known compounds (**48-54**) from aerial parts of *L. japonicus*. Compounds **48**, **51**, **52**, **53**, and **54** exhibited much higher antioxidant capacity than the controls, *α*-tocopherol, and BHT (Table 1.7). Compound **49**-**54** were reported bioactivities, including anti-microbial, anti-inflammatory, anti-bacterial, anti-oxidant, anti-cancer, anti-diabetic, anti-hypertensive properties, immunomodulatory, cardiovascular, anti-tumor and protection of the heart, liver, and brain/CNS. (Kashyap et al., 2018; Bangar et al., 2022; Dabeek et al., 2019; Taheri et al., 2020; Srinivasulu et al., 2018; Badhani et al., 2015).

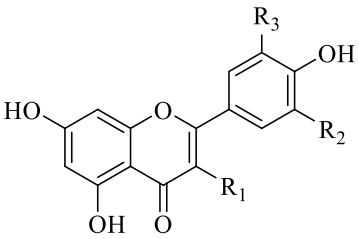

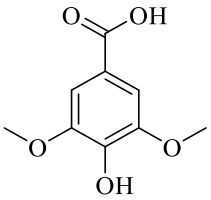

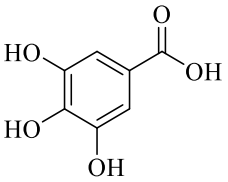

	R_1	R_2	R_3
Luteolin (**48**)	H	H	OH
Apigenin (**49**)	H	H	H
Kaempferol (**50**)	OH	H	H
Quercetin (**51**)	OH	H	OH
Myricetin (**52**)	OH	OH	OH

Syringic acid (**53**)

Gallic acid (**54**)

Figure 1.10 Structure of compounds (**48-54**)

Table 1.7 Antioxidant activities of compounds **48-54**

Compounds	**IC_{50} Values (μg/mL)**[a]
48	12
49	57
50	39
51	16
52	13
53	11
54	9
α-tocopherol[b]	26
Acarbose[b]	30

Note [a] Values of IC_{50} are presented as mean.

[b] Compounds were used as a positive control.

In 2006, Romero-González et al. isolated three known compounds (**55-57**) from the leaves of *L. japonicus*. Compounds **55** and **57** showed cytoprotective effects against glutamate-induced toxicity in primary cultured rat cortical cells (Table 1.8) (Moon et al., 2010).

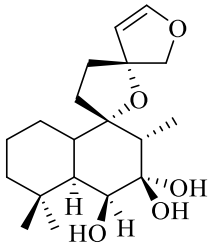

Iso-preleoheterin (**55**)

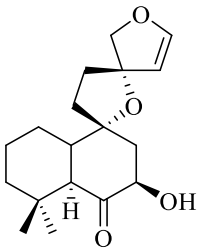

13-Epi- preleoheterin (**56**)

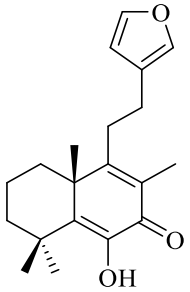

Leojaponin (**57**)

Figure 1.11 Structure of compounds (**55-57**)

Table 1.8 Cytoprotective effects against glutamate-induced toxicity in primary cultured rat cortical cells of compounds **55** and **57**

Compounds	**Cell viability[a,b] (%)**		
	0.1 μM	**1 μM**	**10 μM**
55	4.6 ± 0.8	7.2 ± 0.5	13.2 ± 0.4
57	10.3 ± 0.4	28.3 ± 0.4	68.9 ± 0.4
Control[c]	-	100	-
Glutamate-treated[c,d]	-	0	-
APV[e]	11.5 ± 1.4	26.5 ± 2.3	42.5 ± 3.7
MK-801[f]	51.4 ± 4.6	63.5 ± 5.8	78.4 ± 2.0
CNQX[g]	23.5 ± 3.7	44.8 ± 3.5	53.2 ± 4.6

Note [a] Rat cortical cell cultures were incubated with test compounds for 1 hr. The cultures were then exposed to 100 μM glutamate for 24 hr. After the incubation, the cultures were assessed for the extent of neuronal damage.

[b] Cell viability was calculated as 100 × (LDH released from glutamate-treated-LDH released from glutamate + test compound-treated) / (LDH released from glutamate-treated-LDH released from control). The values shown are the mean ± SD of three experiments (3-4 cultures per experiment). Results differ significantly from the glutamate-treated: * $p < 0.05$, ** $p < 0.01$, *** $p < 0.001$.

[c] LDH released from control and glutamate-treated cultures were 11.7 ± 1.3 and 47.9 ± 4.0 units/mL, respectively.

[d] Glutamate-treated value differed significantly from the untreated control at $p < 0.001$.

[e] APV, DL-2-amino-5-phosphonovaleric acid, a competitive NMDA receptor antagonist.

[f] MK-801, dizocilpine maleate, a noncompetitive NMDA receptor.

[g] APV, DL-2-amino-5-phosphonovaleric acid, a competitive NMDA receptor antagonist.

In 2006, Cai et al. discovered new diterpenes (**58**) together with four known compounds (**59**-**62**) from aerial parts of *L. japonicus*. Compound **58** demonstrated the viability of cancer cells (human and mouse) and fibroblasts (Table 1.9) (Yue et al., 2020).

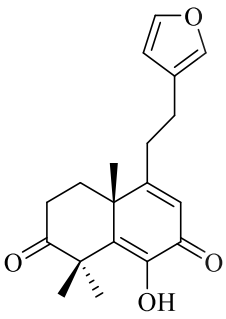

Heteronone B (**58**)

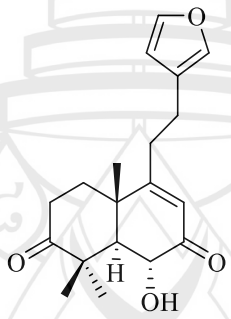

Heteronone A (**59**)

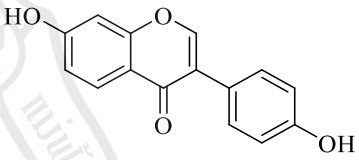

Daidzen (**60**)

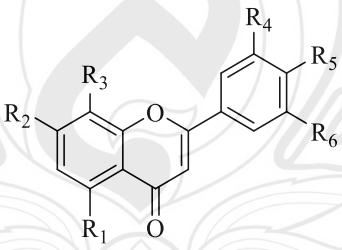

	R_1	R_2	R_3	R_4	R_5	R_6
Wogonin (**61**)	OH	OH	OMe	H	H	H
5,7,3',4',5'-Pentamethoxy flavone (**62**)	OMe	OMe	H	OMe	OMe	OMe

Figure 1.12 Structure of compounds (**58**-**62**)

Table 1.9 Effects of compound **58** on the cell viability of fibroblasts and cancer cells

Cell lines	IC_{50} Values (µg/mL)
Hs27	>500
MCF-7	97.5 ± 3.9
HT-29	282.5 ± 6.9
Panc-1	65.6 ± 2.4
HepG2	>500
DU145	128.8 ± 3.3
A427	105.2 ± 3.7
LLC	140.5 ± 3.8

In 2006, Cong et al. discovered a new compound (**63**) from aerial parts of *L. japonicus.*

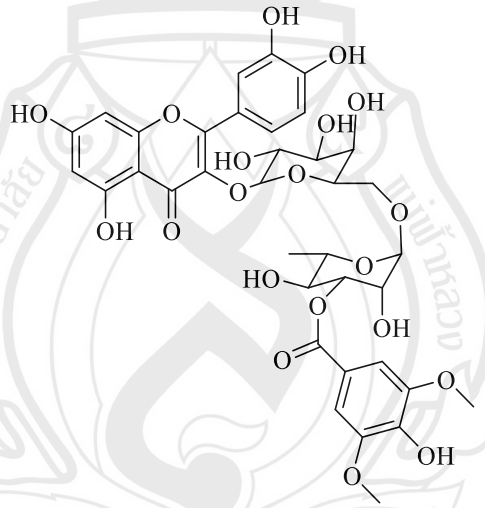

Heteronoside (**63**)

Figure 1.13 Structure of compound (**63**)

In 2009, Cong et al. isolated two known compounds (**64-65**) from the *L. japonicus*. Compound **64** inhibited tumor necrosis factor-*α*, interleukin-6, and NO production were all maximally at a rate of 32.31 ± 2.8%, 41.31 ± 3.1%, and 30.31 ± 4.1%, respectively, by using 5 µM hyperoside as a positive control (Kim et al., 2011).

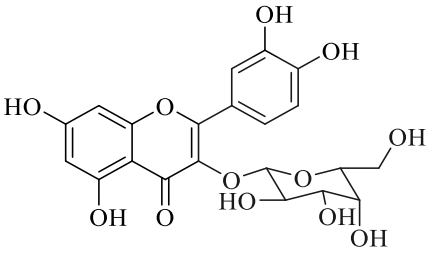

Hyperoside (**64**)

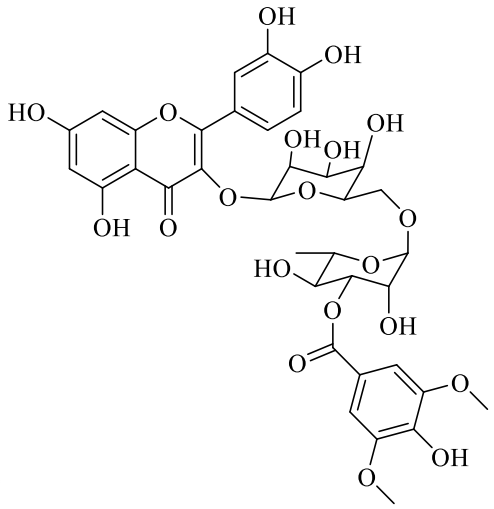

Quercetin-3-O-robinoside (**65**)

Figure 1.14 Structure of compounds (**64-65**)

In 2010, Chang et al. isolated two new compounds (**66-67**) from aerial parts of *L. japonicus*.

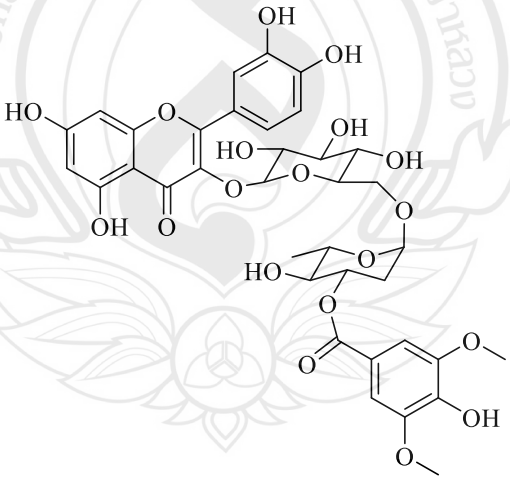

Quercetin-3-O-[(3-O-syringoyl-α-L-rhamnopyranosyl) -(1→6)-β-D-glucopyranoside] (**66**)

Figure 1.15 Structure of compounds (**66-67**)

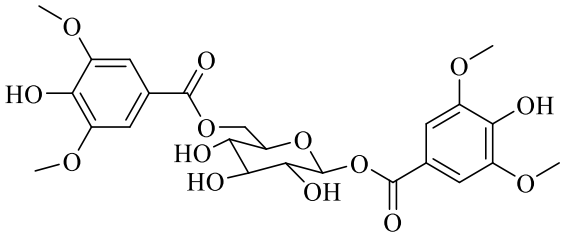

1,6-O-Syringoyl-β-D-glucopyranose (**67**)

Figure 1.15 (continued)

In 2010, Seo et al. discovered a new diterpene (**68**) together with six known compounds (**69-74**) from the aerial parts of *L. japonicus*. Compound **70** demonstrated both antibacterial activity against *Bacillus cereus* (MIC = 0.5 μg/mL) and anti-oxidant activity in the DPPH experiment (IC_{50} = 6.3 x 10^{-4} μmg/mL), respectively (Tables 1.10 and 1.11). Compound **71** was advantageous for diabetics at 20 μM. It showed a nearly similar response to that of 10 nM of insulin on the level of adiponectin secretion. It showed equal potential with 10 nM of insulin to increase the phosphorylation of insulin receptor-β, in addition to their favorable impact on GLUT4 translocation. Compound **72** showed potent antiviral activity against HCMV and VZV with no discernible cytotoxic side effects (Kumarasamy et al., 2006; Rao et al., 2011).

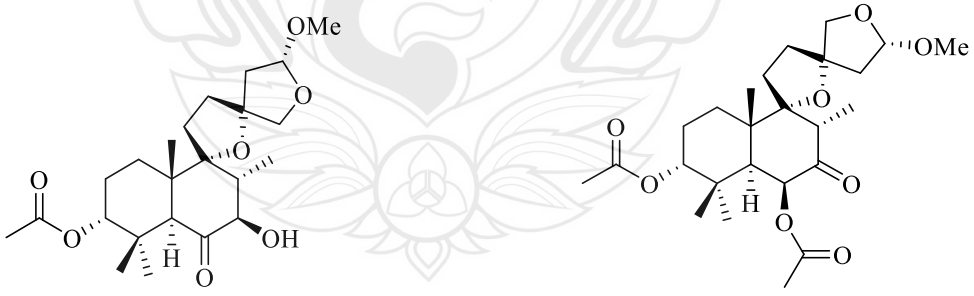

3α-Acetoxy-15-O-methylleopersin C (**68**)

Leosibirinone A (**69**)

Figure 1.16 Structure of compounds (**68-74**)

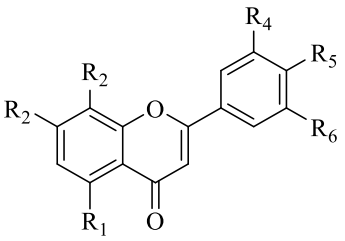

	R_1	R_2	R_3	R_4	R_5	R_6
Genkwanin (**70**)	OH	OMe	H	H	OH	H
Cosmosiin (**71**)	OH	OGlc	H	H	OH	H

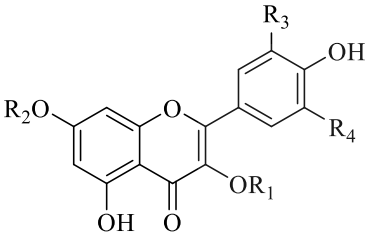

	R_1	R_2	R_3	R_4
Isoquercitrin (**72**)	H	Rha	H	H
Nicotiflorin (**73**)	Glc	Rha	H	H

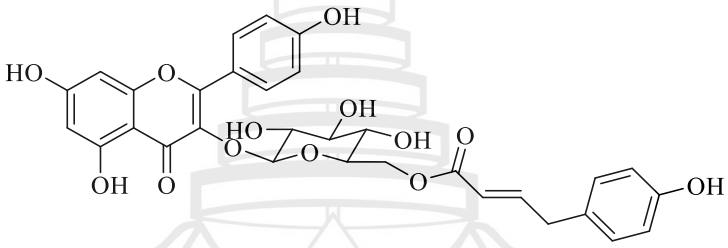

Tiliroside (**74**)

Figure 1.16 (continued)

Table 1.10 Antioxidant activity of compound **70**

Compound	DPPH assay (IC_{50} in mg/mL)
70	6.3×10^{-4}
Quercetin	2.88×10^{-4}

Table 1.11 Antibacterial activity of compound **70**

Bacterial strains	MIC (μg/mL)	
	Compound 70	Ciprofloxacin[a]
B. cereus	0.5	2.5×10^{-5}
C. freundii	25	2.5×10^{-4}

Table 1.11 (continued)

Bacterial strains	MIC (μg/mL)	
	Compound 70	**Ciprofloxacin[a]**
E. coli (penicillin resistant)	200	2.5×10^{-3}
K. aerogenes	200	2.5×10^{-4}
M. luteaus	200	2.5×10^{-4}
P. aerugenosa	100	2.5×10^{-5}

Note [a] Positive control for antibacterial

In 2010, Jun et al. isolated two known compounds (**75-76**) from aerial parts of *L. japonicus*. Compound **75** was a PTP1B enzyme model inhibitor of hypoglycemic effects.

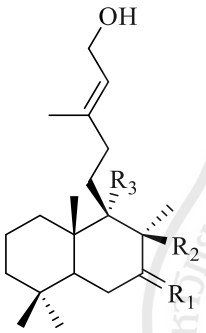

	R_1	R_2
Kaempferol-7-O-α-L-rhamnoside (**75**)	H	Rha
Kaempferol-3-O-β-D-glucopyranoside-7-O-α-L-Rhamnoside (**76**)	Glc	Rha

Figure 1.17 Structure of compounds (**75-76**)

In 2011, Huang et al. discovered a new diterpene (**77**) with three known compounds (**78-80**) from aerial parts of *L. japonicus*. The IC_{50} values for compounds **77** and **78** were 16.1 and 18.4 μM, respectively, indicating moderate inhibitory action, and the IC_{50} values for compounds **78** and **79** were 11.6 and 12.9 μM, respectively, demonstrating intense action in a dose-dependent manner.

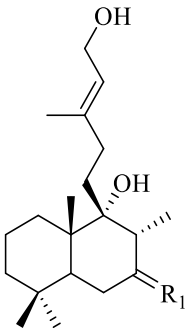

	R_1
Leoheteronin F (**77**)	O
Leoheteronin D (**78**)	H_2

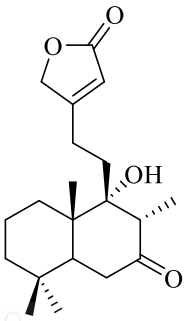

Leopersin G (**79**)

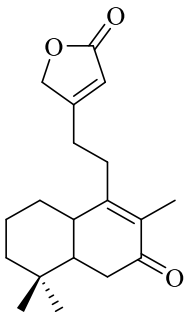

Leoheteronin A (**80**)

Figure 1.18 Structure of compounds (**77-80**)

In 2012, Gong et. isolated six new labdane-type diterpenes (**81-86**) from aerial parts of *L. japonicus*.

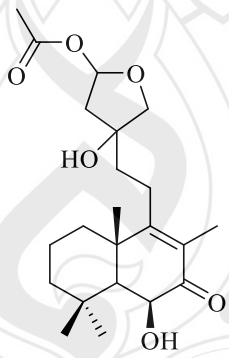

(6*β*)-15,16-Epoxy-15-ethoxy-6,13-dihydroxylabd-8-en-7-one (**81**)

Figure 1.19 Structure of compounds (**81-86**)

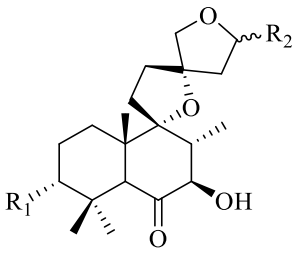

	R_1	R_2
(3*α*,7*β*,9*α*,15*β*)-3-(Acetyloxy)-9,13:15,16-diepoxy-15-ethoxy-7-hydroxylabdan-6-one) (**82**)	OAc	*β*-OEt
(3*α*,7*β*,9*α*,15*β*)-3-(Acetyloxy)-9*α*,13:15,16-diepoxy-15-ethoxy-7-hydroxylabdan-6-one) (**83**)	OAc	*α*-OEt
(3*α*,7*β*,9*α*,15*β*)-3-(Acetyloxy)-9,13:15,16-diepoxy-7-hydroxy-15-methoxylabdan-6-one) (**84**)	OAc	*α*-OMe
(3*α*,7*β*,9*α*,15*β*)-9,13:15,16-Diepoxy-15-ethoxy--3,7dihydroxylabdan6-one) (**85**)	OH	*β*-OEt
(3*α*,7*β*,9*α*,15*α*)-9,13:15,16-Diepoxy-15-ethoxy-3,7-dihydroxylabdan6-one) (**86**)	OH	*α*-OEt

Figure 1.19 (continued)

In 2012, Khan et al. isolated a known compound 15,16-epoxy-3*α*-hydroxylabda-8,13(16),14-trien-7-one (**87**) from aerial parts of *L. japonicus*. Compound **87** inhibited the degradation of inhibitory kappa B (I*κ*B*α*) and the nuclear translocation of p50 and p65 in LPS-stimulated RAW 264.7 macrophages.

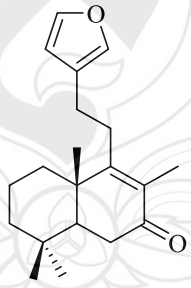

15,16-Epoxy-3*α*-hydroxylabda-8,13(16),14-trien-7-one (**87**)

Figure 1.20 Structure of compound (**87**)

In 2012, Li et al. discovered two new phenylethanoid glycosides (**88**-**89**) and a new sesquiterpene glycoside (**90**) with seven known compounds (**91**-**97**) from aerial parts of *L*. *japonicus*. At a 1x10^{-5} M concentration, compounds **88**, **89**, and **92** showed strong hepatoprotective efficacy against D-galactosamine-induced toxicity in HL-7702 cells (Table 1.12).

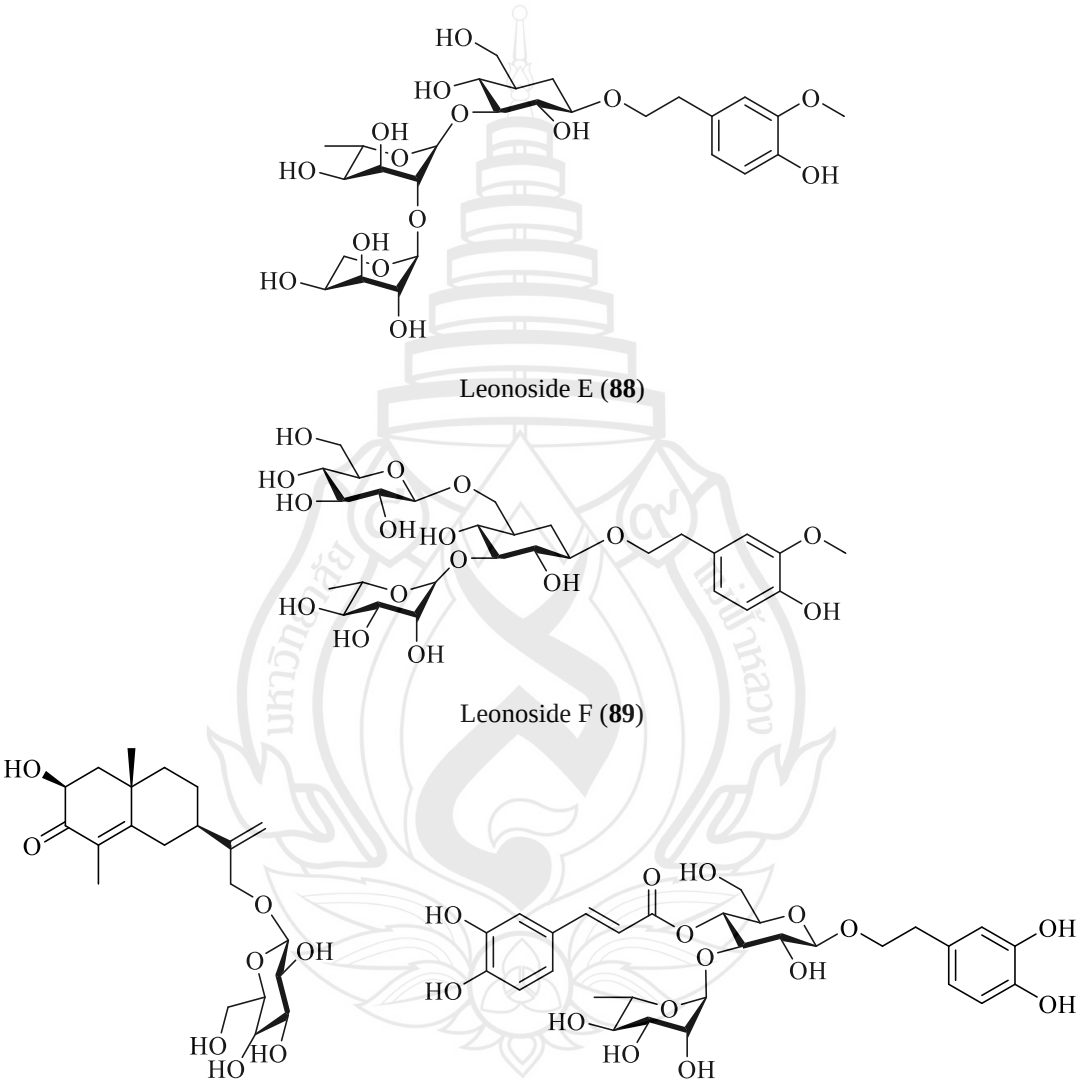

Leonoside E (**88**)

Leonoside F (**89**)

7*α*-(*H*)-Eudesmane-4,11 (12)-diene-3-one-2β-Hydroxy-13-β-D-glucopyranoside (**90**)

Verbascoside (**91**)

Figure 1.21 Structure of compounds (**88**-**97**)

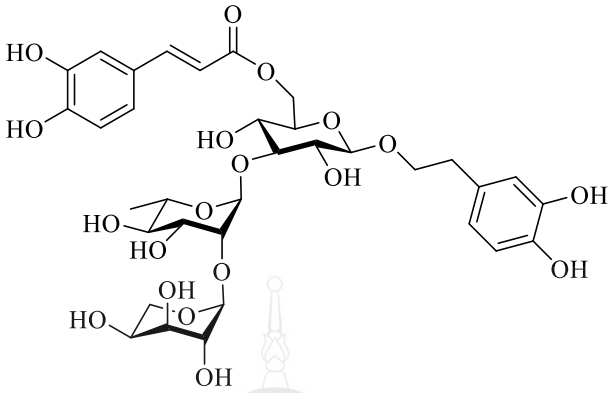

2-(3,4-Dihydroxyphenyl)-O-*α*-L-arabinopyranosy l- (1→2)-cistanoside E (**93**)

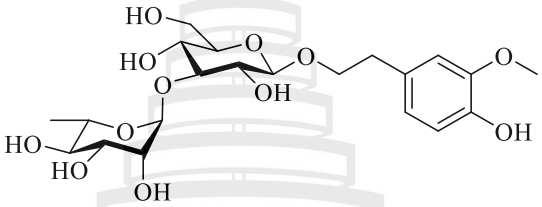

α-L-Rhamnopyranosyl - (1→3)-6-O-*β*-D-glucopyranoside (**92**)

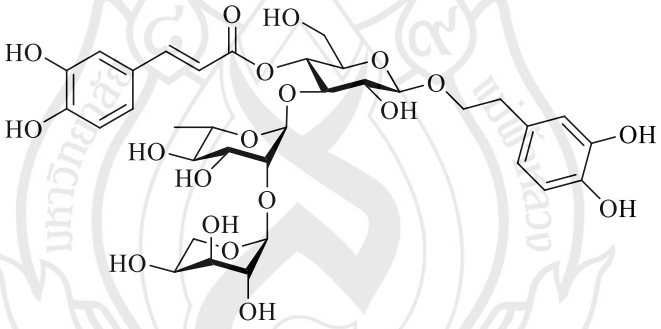

Lavandulifolioside (**94**)

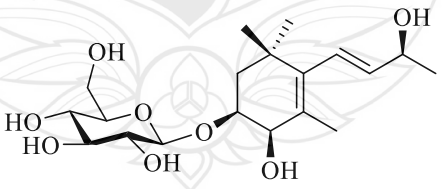

Staphylionoside E (**95**)

Figure 1.21 (continued)

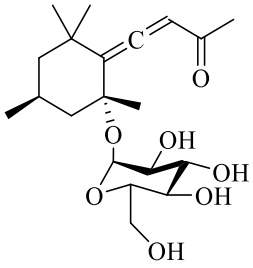

Citroside A (**96**)

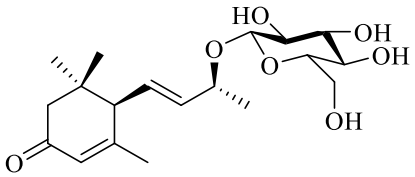

9-Hydroxy-megastigma4,7-dien-3 -one-9-O-glucopyranoside (**97**)

Figure 1.21 (continued)

Table 1.12 Hepatoprotective effects of compounds **88**, **89**, **91** and **93** against D-galactosamine-induced toxicity in HL-7702 cells[a]

Compounds	Cell survival (%)
Normal	100
Control	55 ***
Bicyclol[b]	66 **
88	68 **
89	69 **
91	66 *
93	69 **

Note [a] Results are expressed as mean ± SD (n = 3; for normal and control, n = 6)

[b] Positive control substance

* $p < 0.05$

** $p < 0.01$

*** $p < 0.001$

In 2012, Peng et al. discovered a new labdane diterpenoid (**98**) with seven known compounds (**99**-**103**) from *L. japonicus*. In the APTT, PTT, and FIB assays, compound **98** demonstrated in *vitro* coagulant activity.

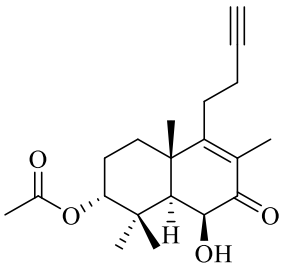

(−)-3*α*-Acetoxy-6*β*-hydroxy-15,16-dinorlabd-8(9)-ene-13-yne-7-one (**98**)

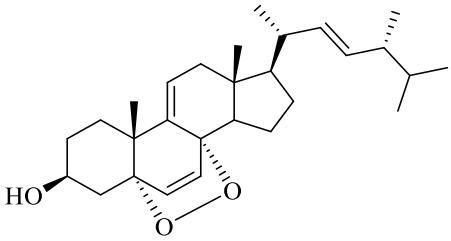

(22*E*,24*R*)-5*α*,8*α*-Epidioxyergosta-6,9(11),22-trien-*3β*-ol (**99**)

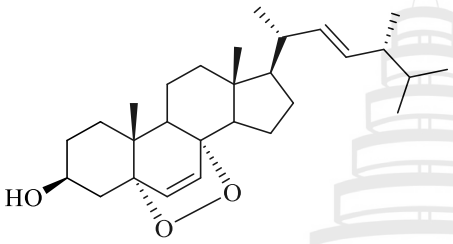

(22*E*,24*R*)-5*α*,8*α*-Epidioxyergosta-6,22-dien-3*β*-ol (**100**)

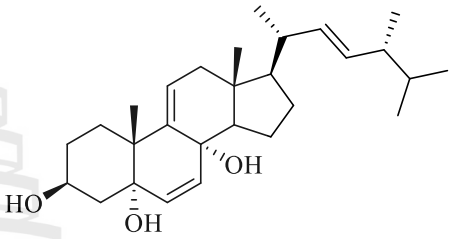

(22*E*)-Ergosta-6,9,22-triene-3*β*,5*α*,8*α*-triol (**101**)

Figure 1.22 Structure of compounds (**98**-**101**)

In 2012, Fuchino et al. discovered two new labdane diterpenes (**102**-**103**) from *L. japonicus*.

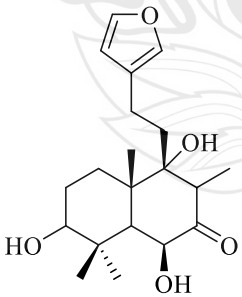

15,16-Epoxy-3α,6β,9α-trihydroxylabda-13(16),14-dien-7-one (**102**)

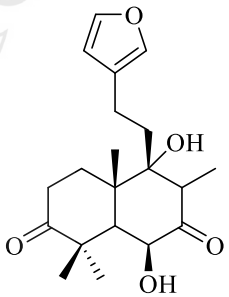

15,16-Epoxy-6β,9α-dihydroxylabda-13(16),14-dien-3,7-dione (**103**)

Figure 1.23 Structure of compounds (**102**-**103**)

In 2013, Xiong et al. discovered two new sesquiterpenoids (**104**-**105**) with six known compounds (**106**-**111**) from *L. japonicus*. Compound **106** significantly inhibited the abnormal increase of platelet aggregation induced by ADP, while compounds **110** and **111** showed obvious antibacterial activity against several bacteria strains.

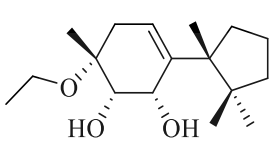

(−) - (1*S**,2*S**,3*R**)-3-Ethoxycupar-5-ene-1,2-diol (**104**)

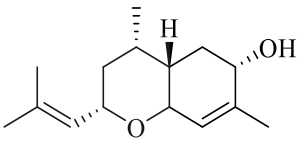

(−) - (1*S**,4*S**,9*S**)-1,9-Epoxybisabola-2,10-diene-4-ol (**105**)

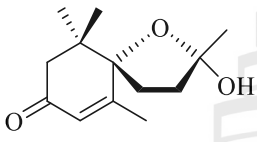

(2*S*,5*S*)-2-Hydroxy-2,6,10,10-tetramethyl-1-oxaspiro-dec-6-en-8-one (**106**)

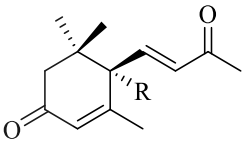

3-Oxo-*α*-ionone (**107**)	R = H
(+)-Dehydrovomifoliol (**108**)	R = OH

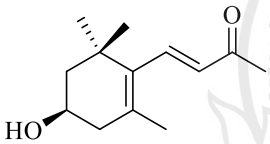

(+)-3-Hydroxy-*β*-ionone (**109**)

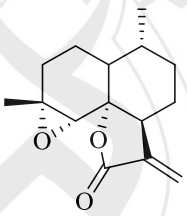

Arteannuin B (**110**)

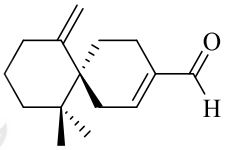

Chamigrenal (**111**)

Figure 1.24 Structure of compounds (**104**-**111**)

In 2013, Ye et al. discovered six new nortriterpenoids (**112**-**117**) with five known compounds (**118**-**122**) from fruits of *L. japonicus*. Compound **117** demonstrated the most potent cytotoxic activity, with IC_{50} values less than 10 μM (Table 1.13).

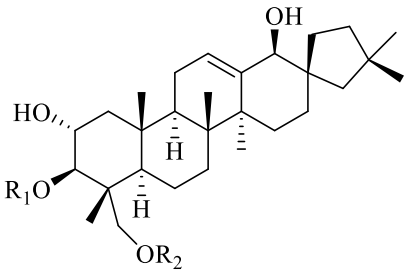

	R_1	R_2
Leonurusoleanolides E (**112**)	H	*trans*-feruloyl
Leonurusoleanolides F (**113**)	H	*cis*-feruloyl
Leonurusoleanolides G (**114**)	H	*trans*-*p*-coumaroyl
Leonurusoleanolides H (**115**)	H	*cis*-*p*-coumaroyl
Leonurusoleanolides I (**116**)	H	*trans*-caffeoyl
Leonurusoleanolides J (**117**)	*trans*-caffeoyl	H
Leonurusoleanolides A (**118**)	*trans*-*p*-coumaroyl	H
Leonurusoleanolides B (**119**)	*cis*-*p*-coumaroyl	H
Leonurusoleanolides C (**120**)	*trans*-feruloyl	H
Leonurusoleanolides D (**121**)	*cis*-feruloyl	H
Phlomistetraol B (**122**)	H	H

Figure 1.25 Structure of compounds (**112**-**122**)

Table 1.13 Cytotoxicity of compounds **116**, **117** and **122**

Compounds	**IC_{50} (mean ± SEM, µM)**				
	BGC-823	**KE-97**	**Huh-7**	**Jurkut**	**MCF-7**
116	>10	>10	9.7 ± 0.7	9.7 ± 5.7	43 ± 0.1
117	7.5 ± 1.3	3.0 ± 0.3	1.9 ± 0.5	3.9 ± 0.9	4.6 ± 0.08
118	>10	>10	>10	>10	8.5 ± 0.3
Staurosporine	0.38 ± 0.02	0.13 ± 0.01	0.23 > 0.07	0.14 ± 0.02	0.52 ± 0.1

In 2013, Zhou et al. discovered six new nortriterpenoids (**123**-**128**) from *L. japonicus*. Antioxidant and anti-inflammatory effects of compound **126** have been identified. Bioactivities for compound **128** include neuroprotection, anticarcinogenic, and antioxidant activity (Kong et al., 2016; Arya et al., 2021).

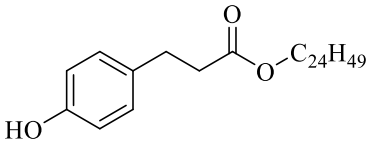

4’-Hydroxy-2,3-dihydrocinnamic acid tetracosyl ester (**123**)

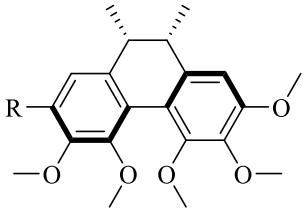

	R
Dimethylgomisin J (**124**)	OMe
(-)-Gomisin K_1 (**125**)	OH

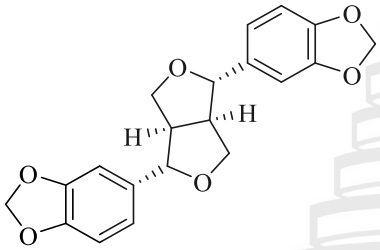

(+)-Sesamin (**126**)

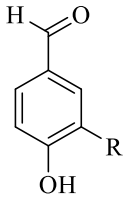

	R
4-Hydroxybenzaldehyde (**127**)	H
Vanillin (**128**)	OMe

Figure 1.26 Structure of compounds (**123**-**128**)

In 2013, Deng et al. isolated four known compounds (**129**-**132**) from *L. japonicus*.

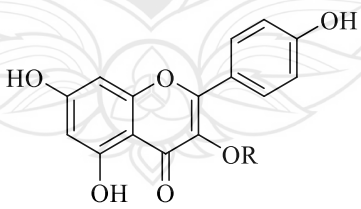

	R
Kaempferol-3-O-*β*-D-glucopyranoside (**129**)	Glc
Kaempferol-3-O-β-D-galactopyranoside (**130**)	Gal
Kaempferol-3-neohesperidoside (**131**)	Glc $\overset{2}{—}$ Rha
Kaempferol-3-neohesperidoside (**132**)	Glc $\overset{6}{—}$ Rha

Figure 1.27 Structure of compounds (**129**-**132**)

In 2013, Zhang et al. discovered five new flavanol glycosides (**133-137**) with four known compounds (**138-141**) from aerial parts of *L. japonicus*. The triglyceride accumulation in HepG2 cells driven by free fatty acid at 10 μM was prevented by compounds **133**, **134**, **136**, and **138**. Their reported inhibitory rates ranged 61.4, 10.0, 44.3, and 4.3%. According to research, compound **140** showed antioxidative activity and efficacy against diabetes, Alzheimer's, cancer, and cardiovascular disease. In addition, compound **141** was found to protect ex *vivo* bone marrow cells from the cell death and inflammatory response caused by the drug 5-fluorouracil (5-FU) by inhibiting the TNF signaling cascade, where II1b was the most regulatory gene (Zhao et al., 2008; Hong et al., 2021).

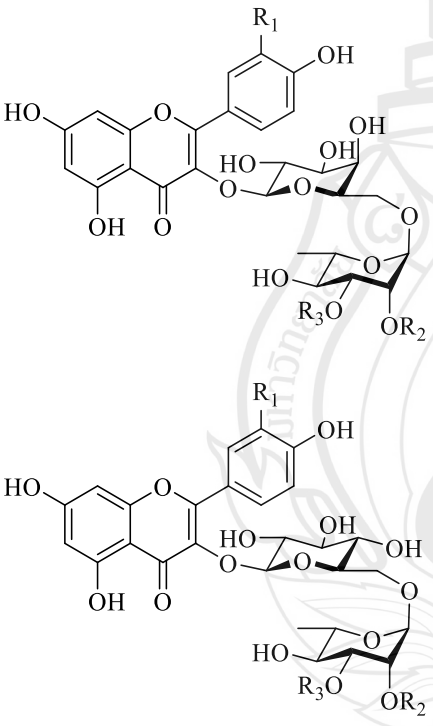

	R_1	R_2	R_3
Leonurusides A (**133**)	H	Syringoyl	H
Leonurusides C (**134**)	H	H	Syringoyl
Leonurusides E (**135**)	OH	Syringoyl	H

	R_1	R_2	R_3
Leonurusides D (**136**)	H	Syringoyl	H
Leonurusides B (**137**)	H	H	Syringoyl
2‴-Syringylrutin (**138**)	OH	Syringoyl	H

Figure 1.28 Structure of compounds (**133-141**)

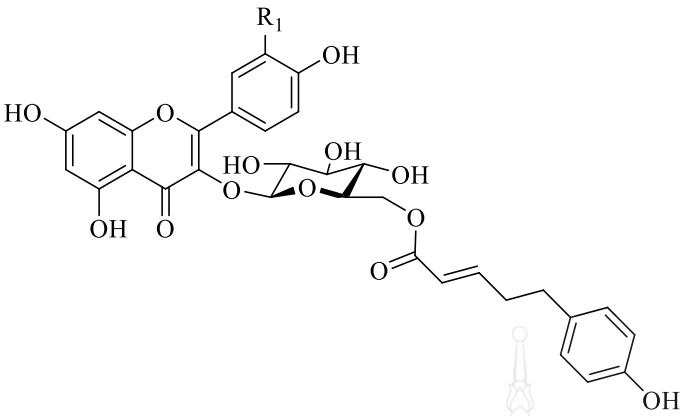

Kaempferol-3-O-(6″-O-cis-*p*-coumaroyl)-*β*-D-glucopyranoside (**139**)

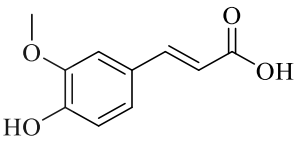

Ferulic acid (**140**)

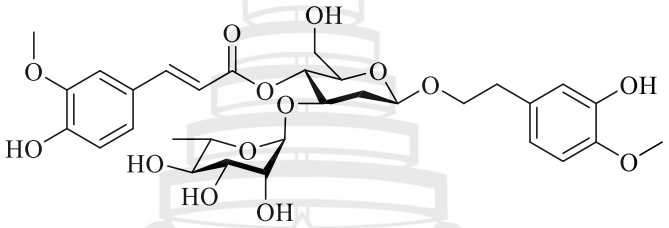

Martynoside (**141**)

Figure 1.28 (continued)

In 2014, He et al. isolated eleven known compounds (**142-151**) from *L. japonicus*. According to research, compound **142** was an anti-degranulation action against the emergence of allergy disorders. Compound **146** reported has antiviral and antitumor properties (Nugrahini et al., 2020; Pałasz et al., 2015).

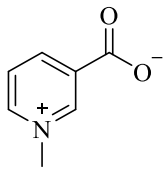

Trigonelline (**142**)

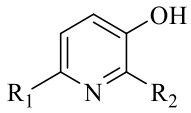

	R_1	R_2
3-Hydroxypyridine (**143**)	H	H
3-Hydroxy-2-methylpyridine (**144**)	H	Me
5-Hydroxy-2-hydroxymethylpyridine (**145**)	CH_2OH	H

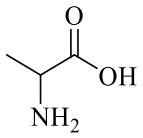

Alanine (**146**)

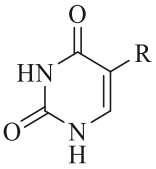

	R
Uracil (**147**)	H
5-Methyluracil (**148**)	Me

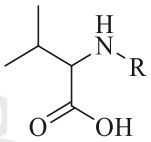

	R
Vanilin (**149**)	H
N-Isobutyl-L-valine (**150**)	Me

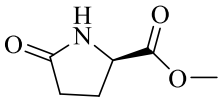

L-Pyroglutamate acid methyl ester (**151**)

Figure 1.29 Structure of compounds (**142-151**)

In 2014, Deng et al. isolated three known compounds (**152-154**) from *L. japonicus*. In *vitro* and in *vivo* studies on ischemic stroke, Alzheimer's disease, Parkinson's disease, spinal cord injury, nociception, and depression demonstrated the protective effects of compound **152** (Bettio et al., 2016).

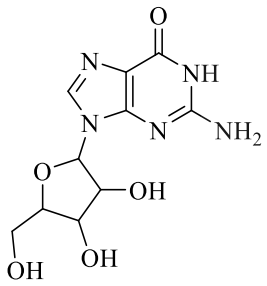

Guanosine (1**52**)

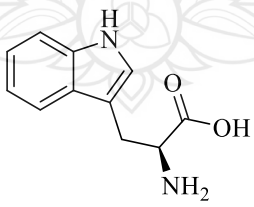

L-tryptophan (**153**)

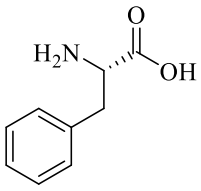

L-phenylalanine (**154**)

Figure 1.30 Structure of compounds (**152-154**)

In 2014, Yang et al. isolated ten known compounds (**155-164**) from *L. japonicus*. Compounds **159** and **160** significantly inhibited the abnormal increase of platelet aggregation induced by ADP.

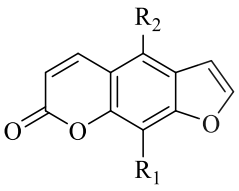

	R_1	R_2
Bergapten (**155**)	H	OMe
Xanthotoxin (**156**)	OMe	H
Isopimpinellin (**157**)	OMe	OMe

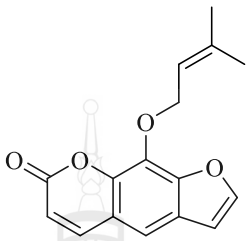

Imperatorin (**158**)

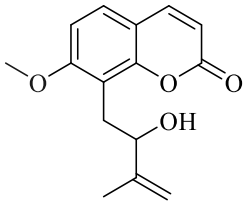

Isogosferal (**159**)

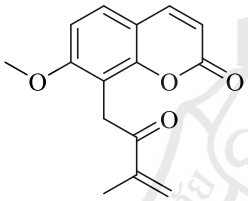

Murrayone (**160**)

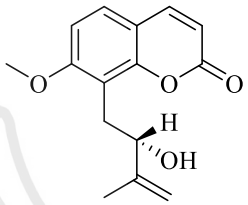

Auraptenol (**161**)

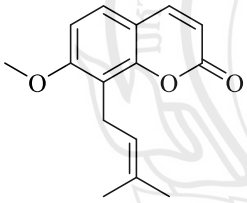

Osthol (**162**)

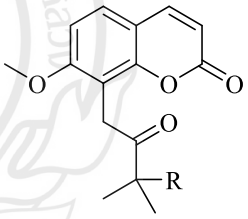

	R
Meransin hydrate (**163**)	OH
Isomeranzim (**164**)	H

Figure 1.31 Structure of compounds (**155-164**)

In 2014, Qin et al. discovered two new compounds (**165**-**166**) with known compound (**167**) from aerial parts of *L. japonicus*.

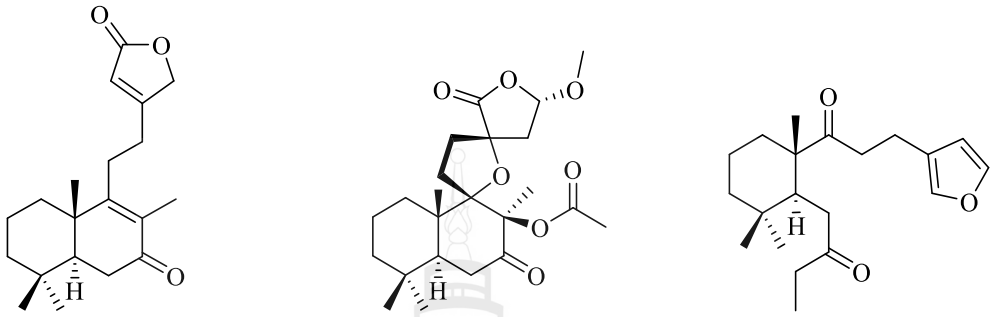

16-Oxo-leoheteronone A (**165**) 15-Methoxyleoheteronin B (**166**) 8,9-Secohispanolone (**167**)

Figure 1.32 Structure of compounds (**165**-**167**)

In 2014, Ye et al. discovered four new steroidal glycosides (**168**-**171**) from fruits of *L. japonicus*.

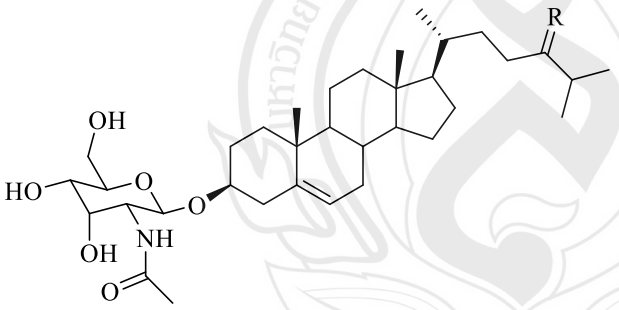

	R
Leonuroside A (**168**)	*β*-Et, *α*-H
Leonuroside B (**169**)	CH_2
Leonuroside C (**170**)	*β*-Me, *α*-H
Leonuroside D (**171**)	*α*-Et, *β*-H

Figure 1.33 Structure of compounds (**168**-**171**)

In 2015, Xiong et al. discovered six new bis-spirolabdane diterpenoids (**172**-**177**) with three known compounds (**178**-**180**) from aerial parts of *L. japonicus*.

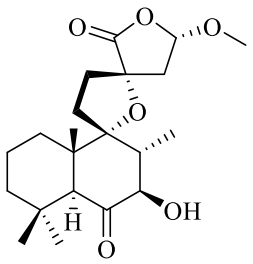

(+) - (5S,7R,8R,9R,10S,13S,15R)-7-Hydroxy-15-methoxy-9,13;15,16-diepoxylabdan-6,16-dione (**172**)

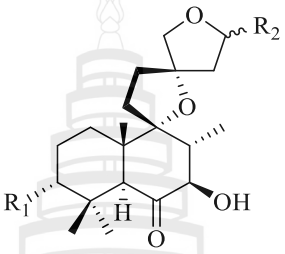

	R_1	R_2
(+)-(5*S*,7*R*,8*R*,9*R*,10*S*,13*S*,15*R*)-7-Hydroxy-15-ethoxy-9,13;15,16-diepoxylabdan-6-one (1**73**)	H	*α*-OEt
(-)-(5*S*,7*R*,8*R*,9*R*,10*S*,13*R*,15*R*)-7-Hydroxy-15-ethoxy-9,13;15,16-diepoxylabdan-6-one (**174**)	H	*β*-OMe
(-)-(3*R*,5*S*,7*R*,8*R*,9*R*,10*S*,13*S*,15*S*)-3-Acetoxy-7-hydroxy-15-methoxy-9,13;15,16-diepoxylabdan-6-one (**175**)	OAc	*β*-OMe
(3*α*,7*β*,9*α*,15*β*)-3-Acetyloxy-9,13:15,16-diepoxy-15-ethoxy-7-hydroxylabdan-6-one (**178**)	OAc	*β*-OEt
Leosibirone B (**179**)	OAc	*α*-OH
15-Epi-leosibirone B (**180**)	OAc	*β*-OH

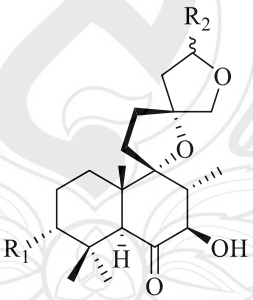

	R_1	R_2
(-)-(3*R*,5*S*,7*R*,8*R*,9*R*,10*S*,13*R*,15*R*)-3-Acetoxy-7-hydroxy-15-ethoxy-9,13;15,16-diepoxylabdan-6-one (**176**)	OAc	*α*-OEt
(-)-(5*S*,7*R*,8*R*,9*R*,10*S*,13*S*,15*S*)-7-Hydroxy-15-methoxy-9,13;15,16-diepoxylabdan-6-one (**177**)	H	*α*-OEt

Figure 1.34 Structure of compounds (**172**-**180**)

In 2015, Rauwald et al. reported a known compound (**181**) from aerial parts of *L. japonicus.*

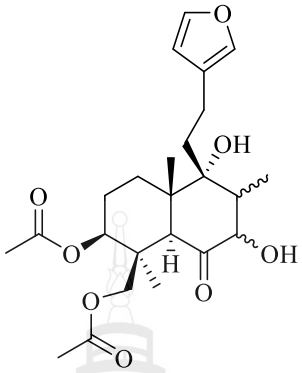

Isoleosibirin (**181**)

Figure 1.35 Structure of compound **181**

In 2015, Wu et al. discovered three new diterpenes (**182**-**184**) together with a known compound (**185**) from *L. japonicus*.

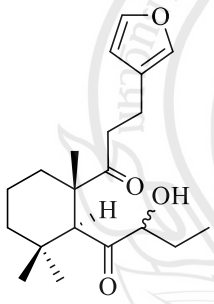

Secoleojaponol (**182**)

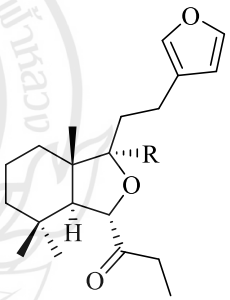

	R
Methoxy Isecolabdane (**183**)	OMe
seco-Labdane (**184**)	OH

Figure 1.36 Structure of compound (**182**-**185**)

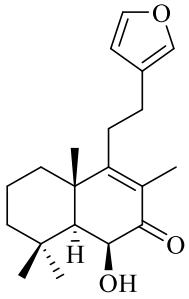

6*β*-Hydroxy-15,16-epoxy-labda- 8,13(16), 14-trien-7- one (**185**)

Figure 1.36 (continued)

In 2015, Xiong et al. isolated a known compound (**186**) from aerial parts of *L. japonicus*. Compound **186** demonstrated significant vasorelaxant activity against KCl-induced contraction of rat aorta, with the EC_{50} value of 2.32 μM.

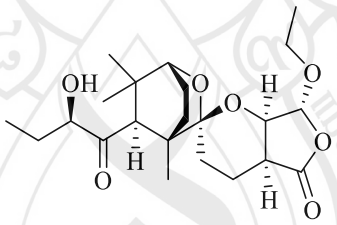

Leonuketal (**186**)

Figure 1.37 Structure of compound (**186**)

In 2015, Zhou et al. discovered two new steroids (**187**-**188**) and sixteen known compounds (**189**-**204**) from aerial parts of *L. japonicus*. Compounds **189**, **190**, and **195** demonstrated strong inhibitory effects against ADP-induced platelet aggregation.

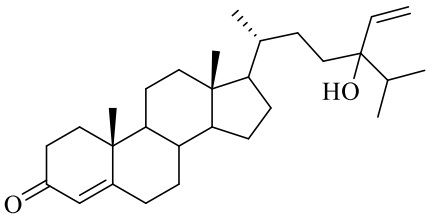

(24*S*)-Stigmast-4,28-diene-24-ol-3-one (**187**)

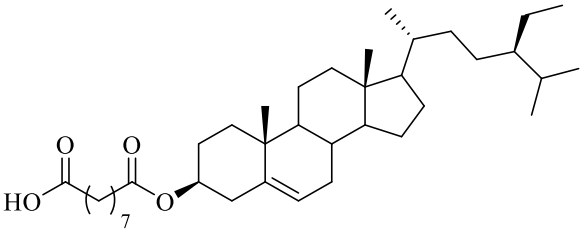

mono-*β*-Sitosteryl azelate (**188**)

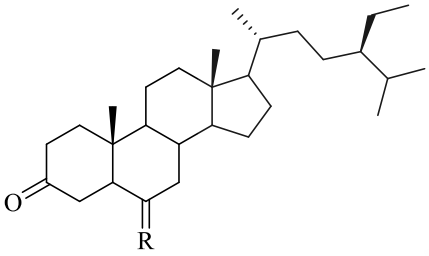

(24*R*)-5α-Stigmast-3,6-dione (**189**)

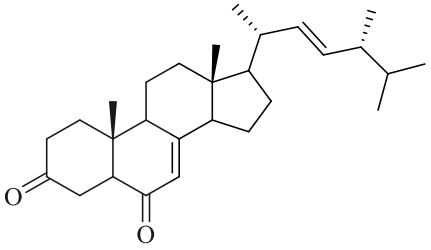

Cyathis-terone (**191**)

R
O
H_2, Δ^4

β-Sitosterone (**190**)

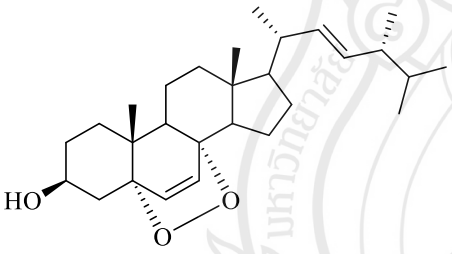

5*α*,8*α*-Epidioxy-23-methyl-(22*E*,24*R*)-ergosta-6,22-dien-3*β*-ol (**192**)

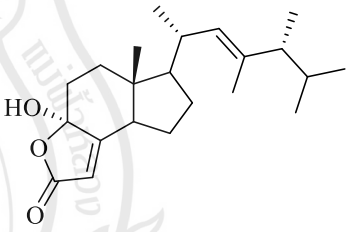

Demethylincisterol A_3 (**193**)

Figure 1.38 Structure of compounds (**187-204**)

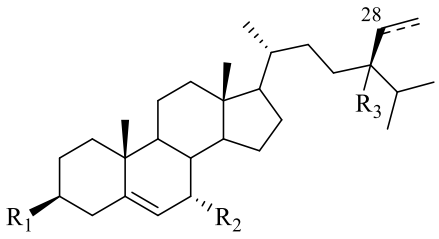

	R_1	R_2
β-Sitosterol (**194**)	H	H
(24*S*)-Saringosterol (**195**)	H	OH, Δ^{28}
(3*β*,7*α*)-Stigmast-5-ene-3,7-diol (**196**)	OH	H
(3*β*,7*α*)-7-Methoxystigmast-5-en-3-ol (**197**)	OMe	H
3*β*-Hydroxy-7*α*-ethoxy-24*β*-ethylcholest-5-ene (**198**)	OEt	H

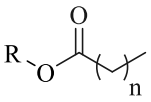

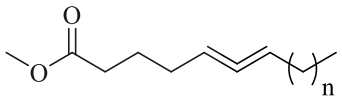

	n
(–)-Nonadeca-5,6-dienoic acid-methyl ester (**199**)	11
Methyl octadeca-5,6-dienoate (**200**)	10

	R	n
Arachidic acid (**201**)	H	18
Heneicosanoic acid (**202**)	H	19
Heptacosanoic acid (**203**)	H	25
Methyl myristate (**204**)	Me	11

Figure 1.38 (continued)

In 2015, Zhong et al. discovered a new labdane diterpenoid (**205**) and two new ionone derivatives (**206**-**207**) together with five known diterpenoids (**208**-**212**) from aerial parts of *L. japonicus*.

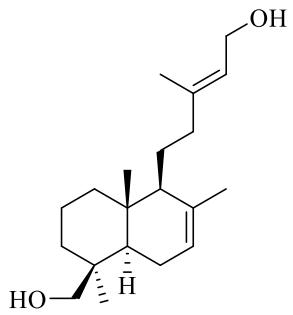

Leojaponin D (**205**)

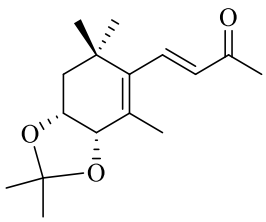

Leojapononones A (**206**)

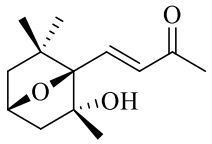

Leojapononones B (**207**)

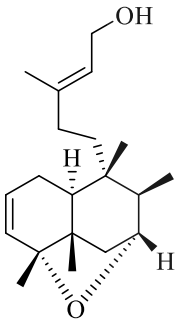

Leojaponin A (**208**)

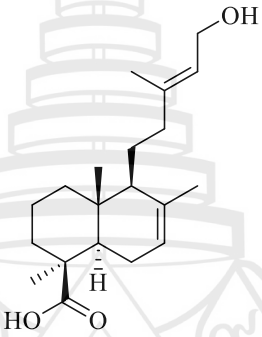

Leojaponin B (**209**)

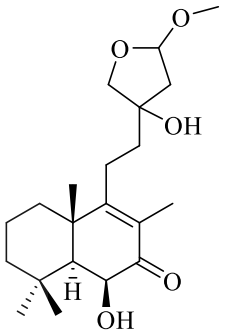

Leojaponin C (**210**)

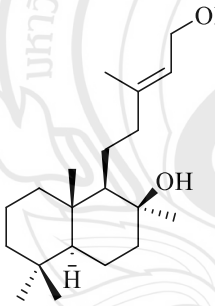

Leoheteronin D (**211**)

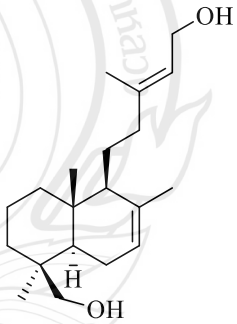

Villenol (**212**)

Figure 1.39 Structure of compounds (**205-212**)

In 2016, Han-Kui et al. discovered two new terpenoids (**213-214**) together with known terpenoids (**215**) from stems and leaves of *L. japonicus*.

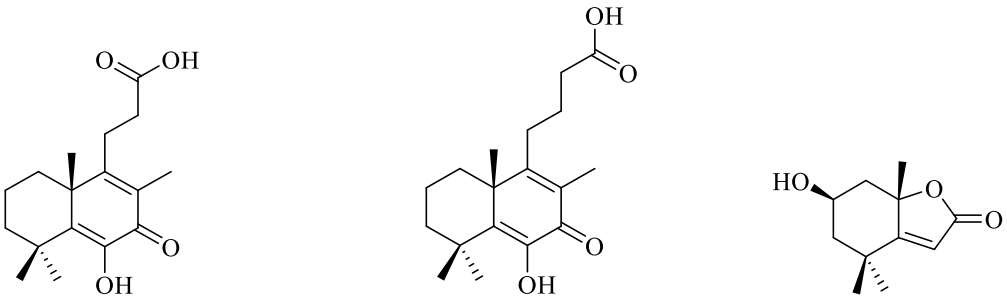

Leojaponic acid A (**213**) Leojaponic acid B (**214**) (−)-Loliolide (**215**)

Figure 1.40 Structure of compounds (**213-215**)

In 2017, Leem et al. discovered a new compound (**216**) together with a known compound (**217**) from *L. japonicus*.

10-Methoxy-leonurine (**216**) Hydroxygenkwanin (**217**)

Figure 1.41 Structure of compound (**216-217**)

In 2017, Peng et al. discovered three new diterpenes (**218-220**) with three known compounds (**221-223**) from aerial parts of *L. japonicus*. Compounds **218 - 220** promoted the contraction of uterine smooth muscle strips isolated from normal rats.

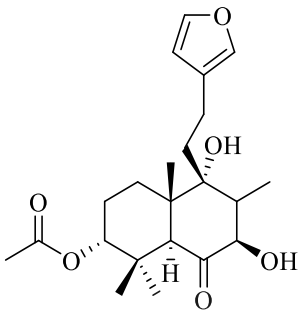

Leojapone A (**218**)

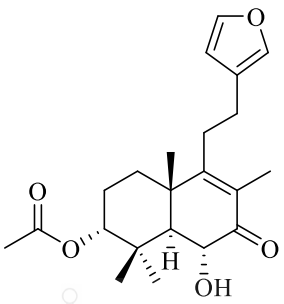

Leojapone B (**219**)

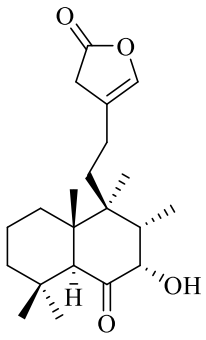

Leojapone B (**220**)

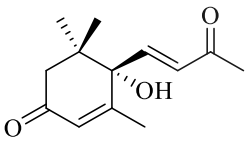

β-Chamigrenic acid (**221**)

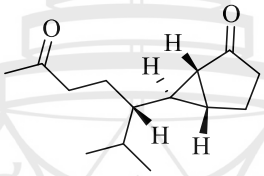

Saniculamoid D (**222**)

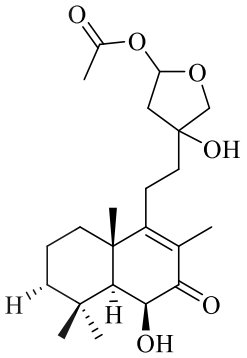

Leojapone D (**223**)

Figure 1.42 Structure of compound (**218-223**)

In 2017, Liu et al. discovered two new cyclopeptides (**224-225**) together with ten known compounds (**226-235**) from aerial parts of *L. japonicus.*

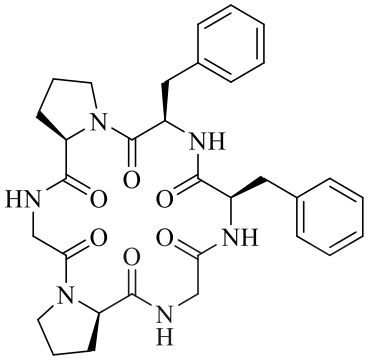

Cyclo-leonuripeptide G (**224**)

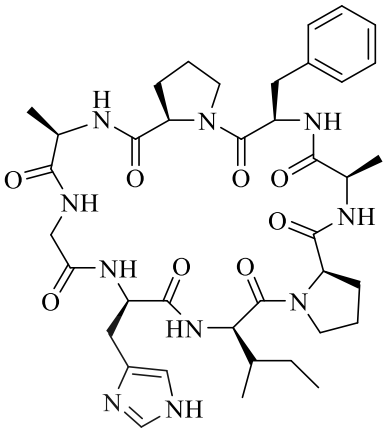

Cyclo-leonuripeptide H (**225**)

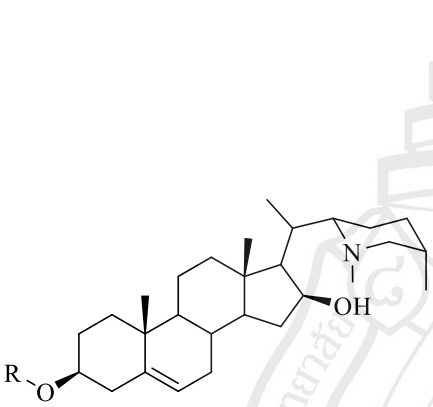

	R
Hapepunine 3-O-*α*-L-rhamnopyranosyl-(1→2)-*β*-D-glucopyranoside (**226**)	Glc-(1→2)-Rha
Hapepunine 3-O-*β*-cellobioside (**227**)	Glc-(1→2)-Glc

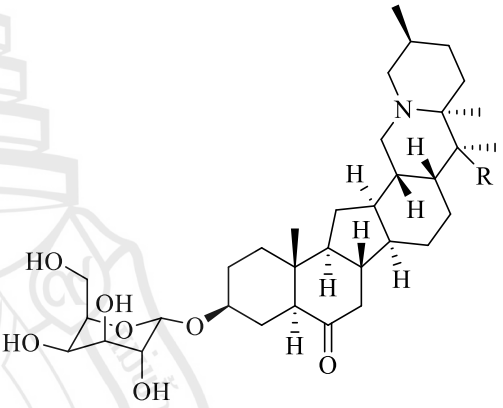

	R
Yibeinoside A (**228**)	Glc-(1→2)-Rha
Imperialine-3*β*-D-glucoside (**229**)	Glc-(1→2)-Glc

Figure 1.43 Structure of compounds (**224-237**)

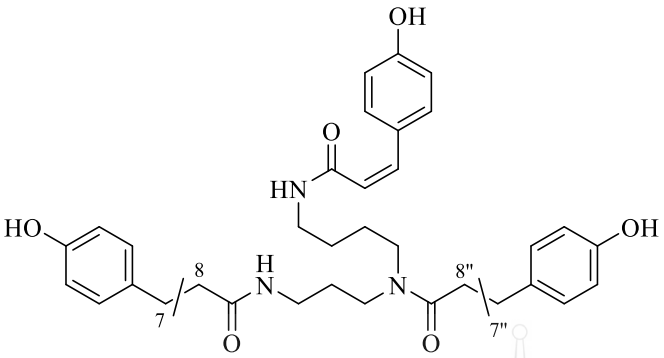

	R
N^1, N^5, N^{10}- tri-*p*-(*ZZZ*)-Coumaroylspermidine (**232**)	7’Z, 7’’Z
N^1, N^5, N^{10}- tri-*p*- (*EEZ*)-Coumaroylspermidine (**233**)	7’E, 7’’E

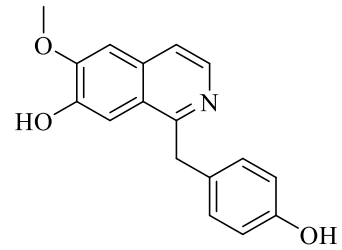

Juzirine (**234**)

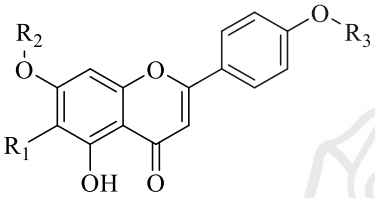

	R_1	R_2	R_3
Spinosyn (**235**)	Glc $\overset{2}{—}$ Glc	Me	H
Linarin (**236**)	H	Glc $\overset{6}{—}$ Rha	Me
Apigenin-7-O-β-D-glucopyranoside (**237**)	H	Glc	H

Figure 1.43 (continued)

In 2017, Han-Kui et al. discovered three new labdane diterpenoids (**238-240**) from stems and leaves of *L. japonicus*. Compared to huperzine A, compounds **238-240** have substantial inhibitory effects on acetylcholinesterase. However, low inhibitory effects on α-glucosidase when compared to acarbose (Table 1.14).

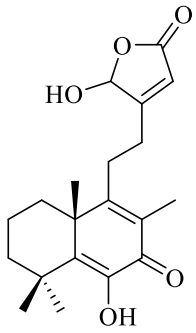

Leojaponicone A (**238**)

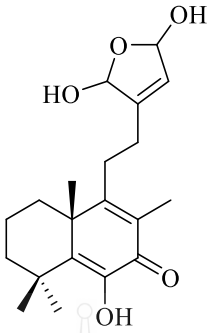

Isoleojaponicone A (**239**)

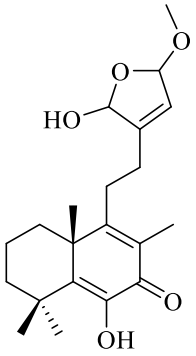

Methy-lisol-eojaponicone A (**240**)

Figure 1.44 Structure of compounds (**238-240**)

Table 1.14 Enzyme inhibitory activity of compounds **238 - 240**

Compounds	*α*-Glucosidase	Acetylcholinesterase
238	22.7	65.3
239	26.9	70.9
240	34.5	52.9
Staurosporine	98.4	NA
Huperzine A	NA	100

In 2018, Lai et al. discovered six new diterpenoids (**241**-**246**) together with nine known compounds (**247**-**255**) from aerial parts of *L. japonicus*. Compounds **242** and **246** enhanced melanin production at 13.5 and 10.6 %. In contrast, compounds **241**, **243**, and **244** inhibited melanin production at 10.4, 30.1, and 12.1 %, respectively.

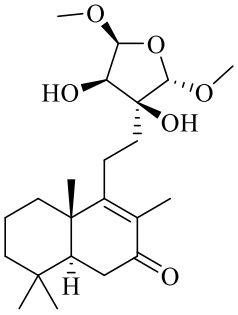

Leojaponicone G (**241**)

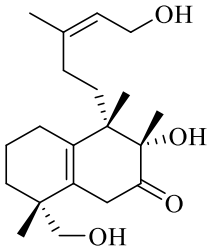

Leojaponicone H (**242**)

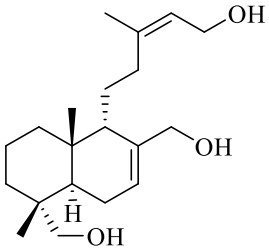

Leojaponicone I (**243**)

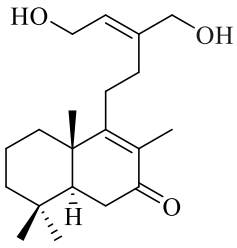

Leojaponicone J (**244**)

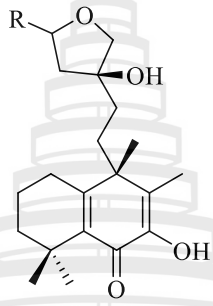

Leojaponicone K (**245**) *β*-OMe
Leojaponicone L (**246**) *α*-OMe

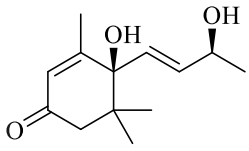

(6*S*,9*R*)-Vomifoliol (**247**)

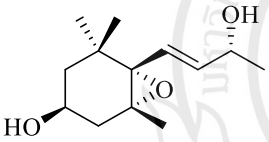

5, 6-Epoxy-3-hydroxy-7-5,7- megastigmen-9-one (**248**)

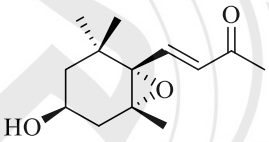

(3*S*,5*R*,6*S*,7*E*,9*R*)-5,6-Epoxy-3,9-dihydroxy-7-megastigmene (**249**)

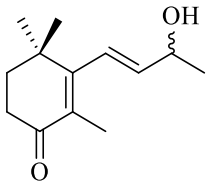

(7*E*,9*ξ*)-9-Hydroxy-megastigmadien-4-one (**250**)

Figure 1.45 Structure of compounds (**241-255**)

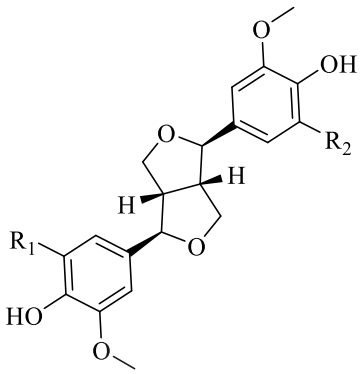

	R_1	R_2
(-)-Pinoresinol (**251**)	H	H
(-)-Syringaresinol (**252**)	OMe	OMe

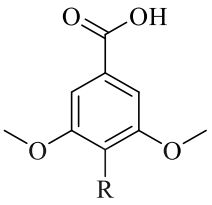

	R
Syringic acid (**253**)	OH
3,4,5-Trimethoxybenzoic acid (**254**)	OMe

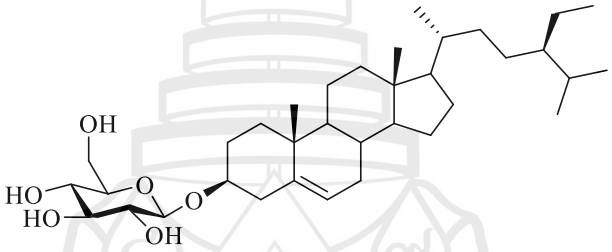

Sitosterol-3-β-D-glucose (**255**)

Figure 1.45 (continued)

In 2018, Hu et al. discovered two new labdane diterpenoids (**256**-**257**) from aerial parts of *L. japonicus*.

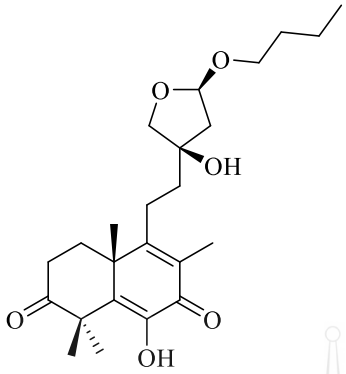

Leojaponn E (**256**)

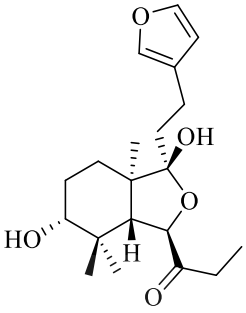

Leojaponicone F (**257**)

Figure 1.46 Structure of compounds (**256-257**)

In 2019, Zhou al. discovered three new triterpenoids (**258-260**) together with seventeen known compounds (**261-277**) from aerial parts of *L. japonicus*.

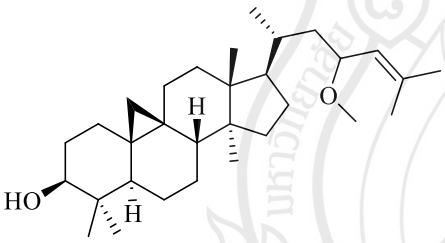

(23*S*)-23-Methoxy-cycloarta-24-en-3β-ol (**258**)

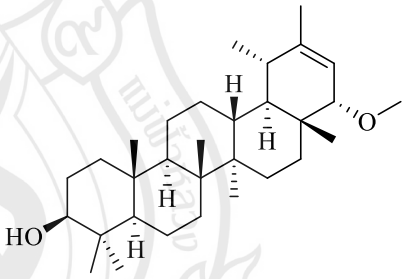

22α-Methoxy-20-tarax-astene-3β-ol (**259**)

Figure 1.47 Structure of compounds (**258-277**)

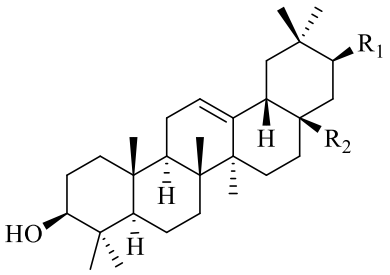

	R_1	R_2
2-Oleanene-3,21-diol (**260**)	OH	Me
Ursolic acid (**261**)	H	COOH

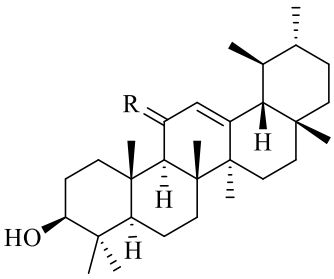

	R
12-en-3*β*-Hydroxy-urs-11-one (**262**)	H_2
α-Amyrin (**263**)	O

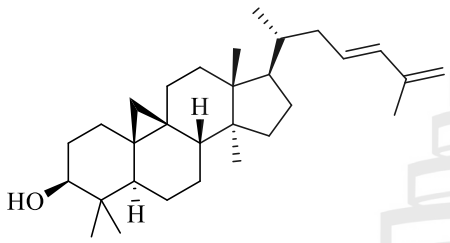

Cycloart-23,25(26)-dien-3*β*-ol (**264**)

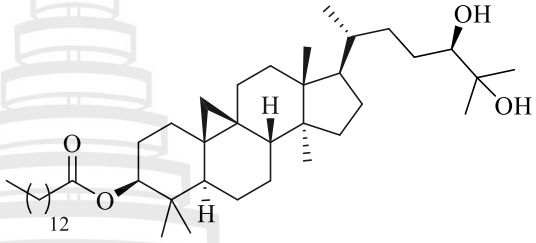

(24*R*)-Cycloartane-24,25-triol-3*β*-tetradecanoate (**265**)

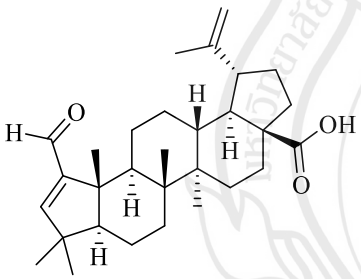

Zizyberenalic acid (**266**)

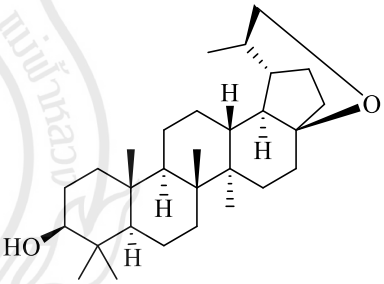

20*S*-17*β*,29-Epoxy-28-norlupan-3*β*-ol (**267**)

Figure 1.47 (continued)

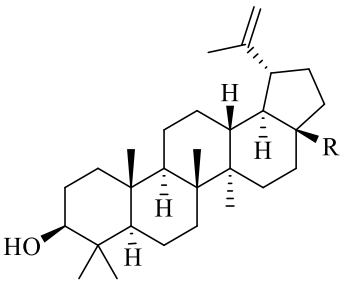

	R
28-Norlup-20(29)-ene-3β,17β-diol (**268**)	OH
28-Norlup-20(29)-en-3β-hydroxy-17β-Hydroperoxide (**269**)	COOH
Lupeol (**270**)	Me
Betulin (**271**)	CH_2OH
Betulinic acid (**272**)	COOH

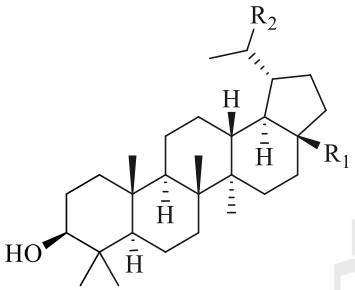

	R_1	R_2
Messagenic acid C (**273**)	COOH	CHO
Dihydrobetulin (**274**)	CH_2OH	Me

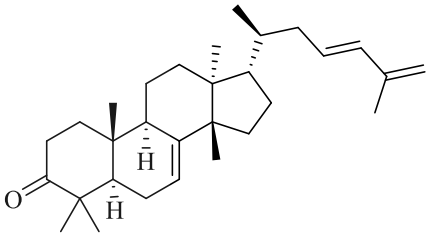

Cornusalterin D (**275**)

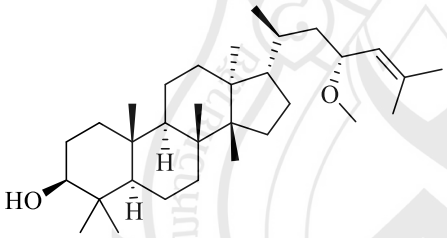

Cornusalterin J (**276**)

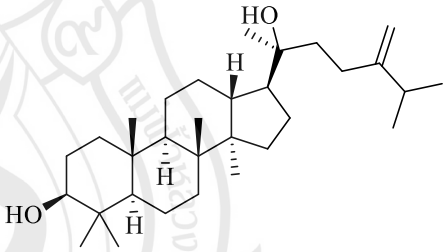

Foliasalacin A_4 (**277**)

Figure 1.47 (continued)

In 2019, Peng et al. discovered two new oleanane derivatives (**278**-**279**) together with three known compounds (**280**-**282**) from fruits of *L. japonicus*.

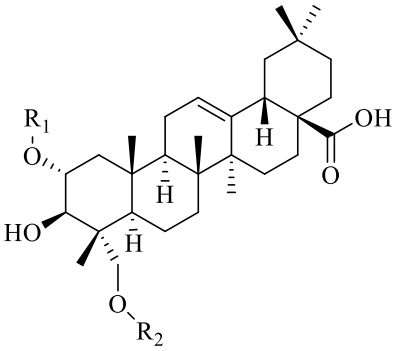

	R_1	R_2
Leonuronin A (**278**)	*trans-p*-coumaroyl	H
Leonuronin B (**279**)	H	*trans*-caffeoyl

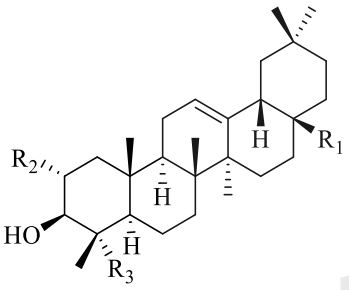

	R_1	R_2	R_3
Urjinolic acid (**280**)	COOH	OH	CH_2OH
Leonuronin B (**281**)	CH_3	H	CH_3

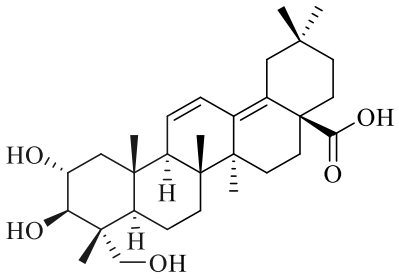

2α,3β,23-Trihydroxyoleana-11,13(18)-dien-28-oic-acid (**282**)

Figure 1.48 Structure of compounds (**278-282**)

1.3 Research Objective

This research aimed to extract, isolate, purify and identify the isolated structures of chemical constituents from aerial parts of *Leonurus japonicus* by bioassay-guided of *α*-glucosidase inhibitory and nitric oxide production inhibitory activities.

CHAPTER 2

BIOASSAY-GUIDED ISOLATION AND IDENTIFICATION OF BIOACTIVE COMPOUNDS FROM *LEONURUS JAPONICUS* HOUTT. EXTRACT

2.1 Introduction

The *Leonurus japonicus* Houtt. is a native plant in Asia, Europe, and Africa. It belongs to the Lamiaceae family and is known as Gun-Cha-Ted in Thailand. It is categorized as an herbaceous plant. The *L. japonicus* grows annually and twice a year, with a diameter of around 5 mm and ranges in height from 30 to 120 cm (Shang et al., 2014). A fine filament that resembles hair is found covering the main stem. The petal is white or reddish, and the flowering season lasts from June to September. The seed has a broad triangular form, measures 6 to 8 mm long, and the color is brown. *L. japonicus* was used extensively in Traditional Chinese Medicine (TCM) to treat blood disorders and diseases affecting women. This plant has many naturally occurring antioxidative, anticancer, cardioprotective, and neuroprotective properties. Approximately 282 substances have been isolated and identified from *L. japonicus* as of right now. Alkaloids, diterpenes, and flavones have been identified as major constituents in *L. japonicus* (Miao et al., 2019). So, *L. japonicus* has been the subject of numerous reviews over time, primarily concentrating on its chemical elements and pharmacological properties. Furthermore, the EtOAc extract of *L. japonicus* exhibited α-glucosidase and nitric oxide (NO) production activity with percent inhibition at 85% and 200%, respectively. During a preliminary screening of the biological activities of this plant, discovery urged an investigation of the chemical constituents from this extract. Therefore, isolation, structural elucidation, α-glucosidase inhibitory, and NO production inhibitor activities from *L. japonicus* are discussed.

2.2 Materials and Methods

2.2.1 Instrument and Chemical

The UV and ECD spectra were recorded with a JASCO J-1500 spectrophotometer. FT-IR spectra were recorded on a Thermo Scientific Nicolet IS50. 1H and 13C NMR spectra were obtained using Bruker AVANCE NEO, 500 MHz. LC-QTOF-MS were recorded with Agilent 1290 infinity II/G6545B QTOF/MS. Flash column chromatography (FCC) was recorded with a Pure C-815 Flash (BUCHI, Japan). High-Performance Liquid Chromatography (HPLC) was registered with Agilent 1260 Infinity II. Column chromatography (CC) and quick column chromatography (QCC) were performed on Merck silica gel 100 (0.063-0.200 mm), Merck silica gel 60 (40-63 mm), and Merck silica gel C_{18}, respectively. Thin layer chromatography (TLC) aluminum sheets of silica gel 60 F254 (20×20 cm) layer thickness 0.2 mm, (Merck), Germany, were used for analytical purposes. Organic solvents for extraction were hexane, dichloromethane (DCM), acetone, ethyl acetate (EtOAc), methanol (MeOH), ethanol (EtOH), and distilled water. Besides the normal phase silica gel, the reverse phase silica gel and Sephadex were also employed to isolate crude extract. In the reverse phase chromatography, distilled water and methanol were used as isolation solvents. The Sephadex technique is separation based on the difference in the size or shape of the interested analyte molecules using dichloromethane and methanol as the eluent.

2.2.2 Plant Material

The dried plants of *L. japonicus* Houtt. were received from Lanna herb, Chiang Mai, Thailand, in July 2018. To estimate the reliability of species identification using DNA barcoding regions. The sequence from ITS2 gene had 482 bp and was compared in the NCBI database. The result showed 92% query coverage and 100% identification of *L. japonicus*.

2.2.3 Extraction and Isolation

The aerial parts of *L. japonicus* Houtt. (1.20 kg) were soaked in EtOH at room temperature for three days. The solvent was evaporated using a rotary evaporator under reduced pressure. This extraction method was done in triplicate. The ethanolic extract

(TA10N 72.05 g) from plants of *L. japonicus* was partitioned with ethyl acetate (4x500 ml each) to obtain TA10N EtOAc crude extract (42.97 g). The aqueous phase was lyophilized and kept in the fridge for further studies. The ethyl acetate crude extract (TA10N EtOAc, 42.97 g) was subjected to quick column chromatography (QCC) (silica gel 60, 20:80 acetone/hexane) to give ten fractions (TA10N 01A-01J). Fraction TA10N 01H (696.6 mg) was subjected to flash column chromatography (FCC), using gradient elution with acetone/hexane (10-30%) to give eight fractions (TA10N 40A-40H). Fraction TA10N 40C (211.4 mg) was further subjected to FCC (80:20 MeOH/water) to give five fractions (TA10N 44A-44E). Fraction TA10N 44A (72.8 mg) was further subjected to Sephadex LH-20 (MeOH) to give five fractions (TA10N 47A-47E). Compound **T-1** (0.8 mg) was obtained from fraction TA10N 47D. Fraction TA10N 44D (30.8 mg) was further subjected to Sephadex LH-20 (MeOH) to give four fractions (TA10N 48A-48D). Compound **T-2** (1.8 mg) was obtained from fraction TA10N 48D. Fraction TA10N 48A.2 was precipitated from fraction TA10N 48A to afford compound **T-3** (4.9 mg). Fraction TA10N 40F (1.68 g) was further purified by RP C_{18} column chromatography (60:40 MeOH/water, R_t 6.2 min) to give six fractions (TA10N 52A-52F). Fraction TA10N 52B (203.6 mg) was further purified by RP C_{18} HPLC (50:50 MeOH/water, 1.5 mL/min) to afford compound **T-4** (3.6 mg, R_t 16.8 min). Fraction TA10N 52A (200.8 mg) was further purified by CC (5:95 MeOH/DCM) to give five fractions (TA10N 59A-59E). Fraction TA10N 59D (45.70 mg) was further purified by column chromatography (CC) (15:85 acetone/hexane) to give three fractions (TA10N 65A-65C). Fraction TA10N 65B (10.2 mg) was further purified by CC (30:70 EtOAc/Hexane) to afford compound **T-5** (1.0 mg). Fractions TA10N 59E (35.40 mg) was further purified by CC (10:90 MeOH/DCM) to give four fractions (TA10N 67A-67D). Fraction TA10N 67A (18.1 mg) was further purified by CC (10:90 acetone/hexane) to give six fractions (TA10N 70A-70F). Fraction TA10N 70F (3.3 mg) was further subjected to RP C_{18} HPLC (80:20 MeOH/water, 1.5 mL/min) to afford compound **T-6** (1.2 mg, R_t 8.1 min).

2.2.4 *α*-Glucosidase Inhibitory Assay

The enzyme *α*-glucosidase catalyzes the final step in the digestive process of carbohydrates, and hence *α*-glucosidase inhibitors could retard the absorption of dietary

carbohydrates to suppress postprandial hyperglycemia. A potent α-glucosidase inhibitor, acarbose, has been shown to effectively reduce the intestinal absorption of sugars in humans. Briefly, the tested samples were dissolved in DMSO. After that, the solutions were diluted with phosphate buffer (100 mM KH_2PO_4, pH 6.9) to the concentration of 10% DMSO. The 1.5 mM of the substrate, p-nitrophenyl α-D-glucoside, was prepared by dissolving with phosphate buffer. Fifty microliters of tasted sample were mixed with 100 µL of α-glucosidase enzyme solution then the mixture was pre-incubated at 37°C for 10 min. The enzymatic reaction was started by applying 100 µL of 1.5 mM substrate into the mix and incubating at 37°C for 20 min. Then, the response was terminated by adding 1 mL of 1 M Na_2CO_3. The absorption was immediately measured at 405 nm by measuring the quantity of *p*-nitrophenol released from the substrate. Acarbose was used as a positive control of α-glucosidase inhibitor with an IC_{50} value of 101.4 µg/mL (Thilagam et al., 2013; Suthiphasilp et al., 2020).

2.2.5 Nitric Oxide Production Inhibitory and Cell Viability Assays

The role of the free radical (NO) in inflammatory. So, inhibition of NO production in LPS-stimulated RAW 264.7 cells is one of the possible ways to screen various anti-inflammatory drugs. Briefly, RAW 264.7 cells were plated in 96-well plates at a 5.0×10^5 cells / mL density and incubated at 37 °C and 5% CO_2 for 24 hours. The culture supernatant of each well in the presence or absence of the compounds was discarded and stimulated with 1 µg/mL LPS. After 24 hr. incubation at 37°C, 50 µL of supernatant culture was incubated at room temperature for 10 min with 50 µL of a Griess reagent. The absorbance with sodium nitrite standards was measured at 570 nm against a calibration curve. Indomethacin was used as a positive control of NO production inhibitor with an IC_{50} value of 11.7 µg/mL. The MTT assay was carried out in cell viability tests (Suthiphasilp et al., 2020; Joo et al., 2014).

CHAPTER 3

RESULTS AND DISCUSSION

3.1 Structural Elucidation

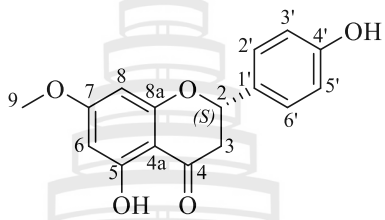

Figure 3.1 Structure of compound **T-1**

Compound **T-1** was isolated as white crystals (m.p. 181 °C). The molecular formula of compound **T-1** was $C_{16}H_{14}O_5$; the HRMS data displayed a molecular ion at *m/z* $[M+H]^+$ 287.2769 (calculated $[M+H]^+$ $C_{16}H_{14}O_5$, 287.2791). The UV (MeOH) spectrum showed two maxima absorbances at 358 and 287 nm. The FT-IR spectrum presented absorption in the broadband at 3379 cm^{-1}, indicating O-H stretching (hydroxy group), the narrow band at 2923 cm^{-1}, indicating aromatic rings, and the sharp band at 1639 cm^{-1}, indicating C=O stretching (ketone group). The ^1H NMR spectroscopic data of compound **T-1** showed chelated hydroxy protons [δ_H 12.03 (1H, *s*, 5-OH)], a set of AA'BB' aromatic protons [δ_H 7.33 (2H, *d*, *J* = 8.7 Hz, H-2' and H-6') and 6.88 (2H, *d*, *J* = 8.7 Hz, H-3' and H-5')], *meta*-coupled aromatic protons [δ_H 6.08 (1H, *d*, *J* = 2.3 Hz, H-8) and 6.06 (1H, *d*, *J* = 2.3 Hz, H-6)], one oxy-methine proton [δ_H 5.35 (1H, *dd*, *J* = 3.0 and 13.0 Hz, H-2)] coupled with nonequivalent methylene protons [δ_H 3.08 (1H, *dd*, *J* = 13.0 and 17.1 Hz, H-3a) and 2.80 (1H, *dd*, *J* = 3.0 and 17.1 Hz, H-3b)], and one methoxy group [δ_H 3.81 (3H, *s*, 7-OCH_3). The methoxy group was placed at C-7 due to the ^3J HMBC correlations of 7-OCH_3 (δ_H 3.81) with C-7 (δ_C 164.46) (Table 3.1). The absolute

configuration of the chiral center at position C-2 of compound **T-1** was identified by the specific rotation presented by levorotation ($[\alpha_D^{25}]$ -4.64°, *c* = 0.0028, MeOH). The ECD spectrum presented two maxima absorbance at 288 nm (Δε -5.6) and 330 nm (Δε +1.16). The ECD data showed a 2-aryl substituent in the equatorial position and exhibited a positive Cotton effect in the long-wavelength UV range (~330 nm, n→ π * transition; cinnamoyl system) and a negative effect at ~280 – 290 nm (π → π * transition; benzoyl system), which corresponded to the absolute *S*-configuration. Consequently, the structure of compound **T-1** was demonstrated to be (*S*)-sakuranetin, confirmed by a comparison of spectroscopic data with those reported in the literature reviews (Grecco et al., 2014; Takemoto et al., 2008; Yamashita et al., 2016; Bosabalidis et al., 1998). Detailed assignments of ^{1}H, ^{13}C, COSY, and HMBC NMR spectral data are shown in Table 3.1.

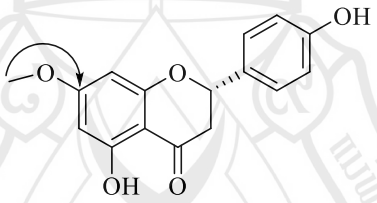

Figure 3.2 HMBC structure of compound **T-1**

Table 3.1 ^{1}H NMR (500 MHz), ^{13}C NMR (500 MHz), COSY, and HMBC Spectral Data of compound **T-1** in $CDCl_3$

Positions	**δ_H (mult., *J* in Hz)**	**δ_C**	**COSY ($^{1}H \rightarrow {}^{1}H$)**	**HMBC ($^{1}H \rightarrow {}^{13}C$)**
2	5.35 (*dd*, 3.0, 13.0)	78.9	H-3a, H-3b	C-2', C-6'
3	3.08 (*dd*, 13.0, 17.1)	43.0	H-2, H-3b	C-2, C-8a
	2.80 (*dd*, 3.0, 17.1)		H-2, H-3a	C8a
4	-	195.0	-	-
4a	-	103.0	-	-
5	-	162.9	-	C-4a, C-6, C-7

Table 3.1 (continued)

Positions	δ_H (mult., *J* in Hz)	δ_C	COSY ($^1H \rightarrow {}^1H$)	HMBC ($^1H \rightarrow {}^{13}C$)
6	6.06 (*d*, 2.3)	95.2	-	C-4a, C-8
7	-	164.46	-	-
8	6.08 (*d*, 2.3)	94.25	-	C-4a, C-5
8a	-	196.0	-	-
2'	7.33 (*d*, 8.7)	127.9	H-3'	C-2, C-4'
3'	6.88 (*d*, 8.7)	115.7	H-2'	C-4', C-5'
4'	-	156.0	-	-
5'	6.88 (*d*, 8.7)	115.7	H-6'	C-4', C-3'
6'	7.33 (*d*, 8.7)	127.9	H-5'	C-2, C-4'
7-OCH_3	3.81 (*s*)	55.3	-	C-7
5-OH	12.0 (*s*)	-	-	-

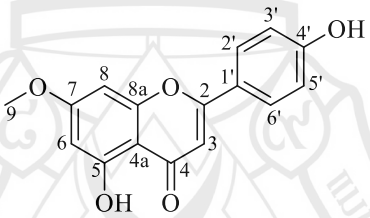

Figure 3.3 Structure of compound **T-2**

Compound **T-2** was isolated as white crystals (m.p. 318 °C). The molecular formula of compound **T-2** was $C_{16}H_{12}O_5$; the HRMS data displayed a molecular ion at *m/z* $[M+H]^+$ 285.0642 (calculated $[M+H]^+$ $C_{16}H_{12}O_5$, 285.0762). The UV (MeOH) spectrum showed three maxima absorbances at 267, 303 (sh), and 335 nm. The FT-IR spectrum presented absorption in the broadband at 3371 cm^{-1}, indicating O-H stretching (hydroxy group), the narrow band at 2919 cm^{-1}, indicating aromatic rings, and the sharp band at 1588 cm^{-1}, indicating C=O stretching (ketone group). The ^1H and ^{13}C NMR spectroscopic data of compound **T-2** were similar to those of compound **T-1**; however, the main differences were that the ^1H NMR spectrum of compound **T-2** showed one methine proton at δ_H 6.54 (1H, *s*, H-3) and one methoxy group at δ_H 3.58 (3H, 7-OCH_3). The HMBC showed correlations between the methine proton (δ_H 6.54) with C-2 (δ_C

163.86), C-4a (δ_C 104.37), and C-1' (δ_C 120.47). In addition, the methoxy group (δ_H 3.58) also showed ^3J HMBC correlation with C-7 (δ_C 164.84), respectively. The spectral data of compound **T-2** was demonstrated to be genkwanin, confirmed by a comparison with those reported in the literature reviews (Ray et al., 2014; Yang et al., 2013). Detailed assignments of ^{1}H, ^{13}C, COSY, and HMBC NMR spectral data are shown in Table 3.2.

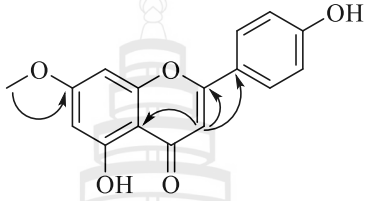

Figure 3.4 HMBC structure of compound **T-2**

Table 3.2 ^{1}H NMR (500 MHz), ^{13}C NMR (500 MHz), COSY, and HMBC Spectral data of compound **T-2** in DMSO

Position	**δ_H (mult., *J* in Hz)**	**δ_C**	**COSY (^{1}H → ^{1}H)**	**HMBC (^{1}H → ^{13}C)**
2	-	163.86	-	-
3	6.54 (*s*)	103.90	-	C-2, C-4a, C-1'
4	-	181.80	-	-
4a	-	104.37	-	-
5	-	157.2	-	-
6	6.09 (*d*, 2.3)	97.53	-	C-4a, C-7, C-8, C-8a
7	-	164.84	-	-
8	6.50 (*d*, 2.3)	92.45	-	C-3, C-5, C-6, C-7
2'	7.67 (*d*, 8.9)	129.07	C-3'	C-2, C-4', C-6'
3'	6.66 (*d*, 8.9)	116.40	C-2'	C-1', C-4', C-5'
4'	-	161.00	-	-
5'	6.66 (*d*, 8.9)	116.40	C-6'	C1', C-3', C-4'
6'	7.67 (*d*, 8.9)	129.07	C-5'	C-2, C-2', C-4'
-OCH_3	3.58 (*s*)	55.53	-	C-7
-OH	12.64 (*s*)	-	-	-

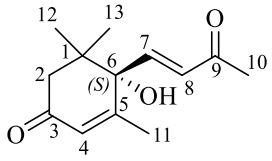

Figure 3.5 Structure of compound **T-3**

Compound **T-3** was isolated as a yellow viscous oil. The molecular formula of compound **T-3** was $C_{13}H_{18}O_3$; the HRMS data displayed a molecular ion at *m/z* $[M+H]^+$ 223.1329 (calculated $[M+H]^+$ $C_{13}H_{18}O_3$, 223.1256). The UV (MeOH) spectrum showed maxima absorbance at 233 nm. The FT-IR spectrum presented absorption in the broad band at 3430 cm^{-1}, indicating O-H stretching (hydroxy group), the narrow band at 2924 cm^{-1}, indicating aromatic rings, and the sharp band at 1662 cm^{-1}, indicating C=O stretching (conjugated ketone). The ^{1}H NMR spectroscopic data of compound **3** showed *trans* olefinic protons at δ_H 6.86 (1H, *d*, *J* = 15.6 Hz, H-8), and 6.49 (1H, *d*, *J* = 15.6 Hz, H-7), one olefinic proton of trisubstituted alkene [δ_H 5.96 (1H, *s*, H-4)], nonequivalent methylene protons [δ_H 2.53 (1H, *d*, *J* = 17.2 Hz, H-2a), and 2.36 (1H, *d*, *J* = 17.2 Hz, H-2b)], together with four methyl groups [δ_H 2.31 (3H, *s*, H-10), 1.89 (3H, *s*, H-11), 1.11 (3H, *s*, H-12), and 1.03 (3H, *s*, H-13)]. The locations of four methyl groups were supported by HMBC correlations (Table 3.3); from H-10 (δ_H 2.31) to C-9 (δ_C 197.41), from H-11 (δ_H 1.89) to C-4 (δ_C 127.93), C-5 (δ_C 41.25), and C-6 (δ_C 79.36), and from H-12 (δ_H 1.11) and H-13 (δ_H 1.03) to C-1 (δ_C 197.02), C-2 (δ_C 49.71), and C-6 (δ_C 79.36) (Table 2.3). The absolute configuration at C-6 of compound **T-3** was identified by the specific rotation presented by levorotation ($[\alpha_D^{25}]$ -1.81, *c* = 0.022, MeOH). The ECD spectrum presented maxima absorbance at 247 nm (Δε +22.7). The ECD data showed that position 6 exhibited a positive Cotton effect in the long-wavelength UV range (~250 nm, π→π* transition; enone system), which corresponded to the absolute *S*-configuration. Consequently, the structure of compound **T-3** was demonstrated to be (*6S*)-dehydrovomifoliol, confirmed by a comparison of spectroscopic data with those reported in the literature reviews (Aishan et al., 2010;

Circular Dichroism and Magnetic Circular Dichroism Spectroscopy for Organic Chemists, 2011; Gangadhar et al., 2020). Detailed assignments of ^{1}H, ^{13}C, COSY, and HMBC NMR spectral data are shown in Table 3.3.

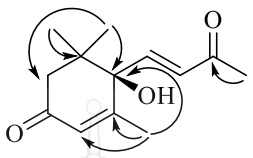

Figure 3.6 HMBC structure of compound **T-3**

Table 3.3 ^{1}H NMR (500 MHz), ^{13}C NMR (500 MHz), COSY, and HMBC Spectral data of compound **T-3** in $CDCl_3$

Position	**δ_H (mult., *J* in Hz)**	**δ_C**	**COSY ($^{1}H \rightarrow {}^{1}H$)**	**HMBC ($^{1}H \rightarrow {}^{13}C$)**
1	-	197.02	-	-
2	2.53 (*d*, 17.2)	49.71	H-11	C-1, C-3, C-6, C-12
	2.36 (*d*, 17.2)		H-11	C-1, C-3, C-4, C-6, C-12
3	-	160.3	-	
4	5.96 (*s*)	127.93	-	C-2, C-6, C-11
5	-	41.25	-	-
6	-	79.36	-	-
7	6.49 (*d*, 15.6)	144.91	H-8	C-6, C-9
8	6.86 (*d*, 15.6)	130.37	H-7	C-6, C-9
9	-	197.41	-	-
10	2.31 (*s*)	28.42	-	C-9
11	1.89 (*s*)	18.68	H-2a, H-2b	C-4, C-5, C-6
12	1.11 (*s*)	23.19	-	C-1, C-2, C-3, C-6, C-13
13	1.03 (*s*)	24.62	-	C-1, C-2, C-3, C-6, C-12

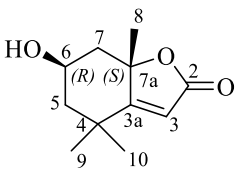

Figure 3.7 Structure of compound **T-4**

Compound **T-4** was isolated as a yellow viscous oil. The molecular formula of compound **T-4** was $C_{11}H_{16}O_3$; the HRMS data displayed a molecular ion at *m/z* $[M+H]^+$ 197.1169 (calculated $[M+H]^+$ $C_{11}H_{16}O_3$, 197.2364). The UV (MeOH) spectrum showed maxima absorbance at 206 nm. The FT-IR spectrum presented absorption in the broad band at 3360 cm^{-1}, indicating O-H stretching (hydroxy group), the narrow band at 2924 cm^{-1}, and the sharp band at 1726 cm^{-1} indicating C=O stretching (carbomethoxy group). The ^1H NMR spectroscopic data of compound **T-4** showed one olefinic proton of trisubstituted alkene [δ_H 5.70 (1H, *s*, H-3)], oxygenated methine proton [δ_H 4.34 (1H, *m*, H-6)], two sets of nonequivalent methylene protons [δ_H 2.46 (1H, *dd*, J = 14.1, and 4.0 Hz, H-7_a), and 1.80 (1H, *dd*, J = 14.1, and 4.0, H-7_b), and δ_H 1.98 (1H, *dt*, J = 14.1 and 2.7 Hz, H-5_a), and 1.52 (1H, *dt*, J = 14.1 and 2.7 Hz, H-5_b)], together with three methoxy groups [δ_H 1.79 (3H, *s*, H-9), 1.47 (3H, *s*, H-10), and 1.28 (3H, *s*, H-8)]. The locations of three methyl groups was supported by HMBC correlations (Table 2.4); from H-8 (δ_H 1.28) to C-3a (δ_C 182.47), C-4 (δ_C 35.60), and C-7 (δ_C 47.16), and from H-9 (δ_H 1.79) and H-10 (δ_H 1.47) to C-3a (δ_C 182.47), C-4 (δ_C 35.60), and C-5 (δ_C 47.79) (Table 3.3). The specific rotation of compound **T-4** presented the levorotation ($[\alpha_D^{25}]$ -3.57, *c* = 0.0028, MeOH). The ECD spectrum presented two Cotton effects at 227 nm ($\Delta\varepsilon$ -54.8) and 257 ($\Delta\varepsilon$ +5.8). A negative Cotton effect at ~230 nm ($\pi\rightarrow\pi^*$ transition; acyl system) and positive Cotton effect at 260-270 nm ($n\rightarrow\pi^*$ transition; C-C to C=C) established the 6*R*,7a*S* configuration. Consequently, the structure of compound **T-4** was demonstrated to be (–)-loliolide, confirmed by a comparison of spectroscopic data with those reported in the literature reviews (Bich et al., 2014; Chang et al., 2009). Detailed assignments of ^1H, ^{13}C, COSY, and HMBC NMR spectral data are shown in Table 3.4.

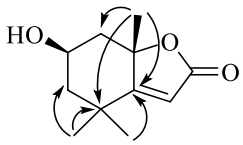

Figure 3.8 HMBC structure of compound **T-4**

Table 3.4 ^{1}H NMR (500 MHz), ^{13}C NMR (500 MHz), COSY, and HMBC Spectral data of compound **T-4** in $CDCl_3$

Position	δ_H (mult., *J* in Hz)	δ_C	COSY ($^{1}H \rightarrow {}^{1}H$)	HMBC ($^{1}H \rightarrow {}^{13}C$)
2	-	171.20	-	-
3	5.70 (*s*)	113.86	-	C-2, C-3a, C-4, C-7a
3a	-	182.47	-	-
4	-	35.60	-	-
5	1.98 (*dd*, 2.70,14.10)	47.79	H-5b	C-3a, C-6, C-7
	1.52 (*dd*, 2.70,14.10)		H-5a	C-4, C-8, C-10
6	4.34 (*m*)	66.22	-	C-4, C-7a
7	2.46 (*d*, 4.00)	47.16	H-7b	C-5
	1.80 (*d*, 4.00)		H-7a	C-7a
7a	-	86.45	-	-
8	1.28 (*s*)	30.60	-	C-3a, C-4, C-7
9	1.79 (*s*)	26.72	-	C-3a, C-4, C-5, C-6, C-7, C-7a, C-10
10	1.47 (*s*)	26.11	-	C-3a, C-4, C-5, C-6, C-7, C-8, C-9

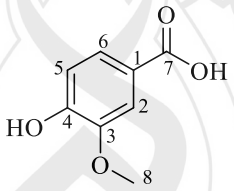

Figure 3.9 Structure of compound **T-5**

Compound **T-5** was isolated as a brown viscous oil. The molecular formula of compound **T-5** was $C_8H_8O_4$; the HRMS data displayed a molecular ion at *m/z* $[M-H]^-$ 167.0648 (calculated $[M+H]^-$ $C_8H_8O_4$, 167.0359). The UV (MeOH) spectrum showed two maxima absorbances at 292 and 259 nm. The FT-IR spectrum presented absorption in the broad band at 3479 cm^{-1}, indicating O-H stretching (hydroxy group), the narrow band at 2924 cm-1, indicating O-H stretching (carboxylic group), the medium band at 1680 cm^{-1}, indicating C=O stretch (carboxylic group), indicating aromatic rings, the narrow band at 1376 and 910 cm^{-1}, indicating O-H bending (hydroxy group), and the

narrow band at 1273 cm^{-1} indicating C–O stretch (carboxylic group). Compound **T-5** was also a phenol derivative based on ^{1}H NMR spectroscopic data, which showed a set of ABX aromatic protons [δ_H 7.72 (1H, *dd*, J = 8.3 and 2.0 Hz, H-5), 7.58 (1H, *d*, J = 2.0 Hz, H-2), and 6.97 (1H, *d*, J = 8.3 Hz, H-6)], together with one methoxy group [δ_H 3.97 (3H, *s*, -OCH_3)]. The methoxy group was placed at C-8 due to the ^{4}J HMBC correlations of 8-OCH_3 (δ_H 3.97) to C-4 (δ_C 146.03) (Table 3.5), confirmed by comparison of spectroscopic data with those reported in the literature (González-Baró et al., 2008; Maria et al., 2013). Compound **T-5** was thus identified as vanillic acid. Detailed assignments of ^{1}H, ^{13}C, COSY, and HMBC NMR spectral data are shown in Table 3.5.

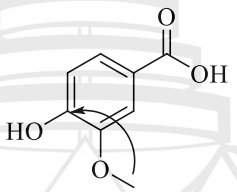

Figure 3.10 HMBC structure of compound **T-5**

Table 3.5 ^{1}H NMR (500 MHz), ^{13}C NMR (500 MHz), COSY, and HMBC Spectral data of compound **T-5** in $CDCl_3$

Position	δ_H (mult., *J* in Hz)	δ_C	COSY ($^{1}H \rightarrow {}^{1}H$)	HMBC ($^{1}H \rightarrow {}^{13}C$)
1	-	125.27	-	-
2	7.58 (*d*, 2.00)	112.26	-	C-1, C-3
3	-	150.92	-	-
4	-	146.03	-	-
5	7.72 (*dd*, 8.30, 2.00)	120.81	H-6	C-2, C-3
6	6.97 (*dd*, 8.30)	114.45	H-5	C-5, C-4
-COOH	-	168.69	-	-
-OCH_3	3.97 (*s*)	56.17	-	C-4

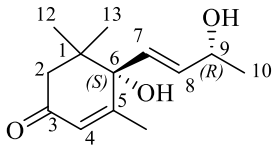

Figure 3.11 Structure of compound **T-6**

Compound **T-6** was isolated as a yellow viscous oil. The molecular formula of compound **T-6** was $C_{13}H_{20}O_3$; the HRMS data displayed a molecular ion at *m/z* $[M-H]^-$ 223.6024 (calculated [M+H]- $C_{13}H_{20}O_3$, 223.1412). The UV (MeOH) spectrum showed maxima absorbance at 235 nm. The FT-IR spectrum presented absorption in the broad band at 3417 cm^{-1}, indicating O-H stretching (hydroxy group), the narrow band at 2924 cm^{-1}, indicating aromatic rings, and the narrow band at 1655 cm^{-1}, indicating C=C stretching (alkene-cis). The ^1H and ^{13}C NMR spectroscopic data of compound **6** were similar to those of compound **T-3**. The main difference was that the ^1H NMR spectrum of compound **T-6** revealed one oxygenated methine proton at δ_H 5.91 (1H, *t*, J = 1.4 Hz, H-9). The HMBC data showedcorrelations between the oxygenated methine proton (δ_H 5.91) with C-7 (δ_C 129.05) and C-11 (δ_C 18.89) (Table 3.6). The absolute configuration at C-6 and C-9 of compound **T-6** was identified by the specific rotation presented by dextrorotation ($[\alpha_D^{25}]$ +7.17, c = 0.0053, MeOH). The ECD spectrum presented maxima absorbance at 242 nm (Δε +94.8) and 321 nm (Δε -9.36). The ECD data showed that position 6 exhibited a positive Cotton effect in the long-wavelength UV range (~250 nm, $\pi \rightarrow \pi^*$ transition; enone system), and position 9 exhibited a negative Cotton effect in the long-wavelength UV range (~320 nm, $n \rightarrow \pi^*$ transition; conjugated carbonyl system), which corresponded to the absolute *6S*-configuration, and *9R*-configuration. Consequently, the structure of compound **T-6** was demonstrated to be (*6S, 9R*)-vomifoliol, confirmed by a comparison of spectroscopic data with those reported in the literature reviews (Yamano et al., 2005; Grayer et al., 2008; Snatzke et al., 1979; Proença et al., 2017). Detailed assignments of ^1H, ^{13}C, COSY, and HMBC NMR spectral data are shown in Table 3.6.

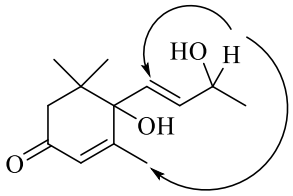

Figure 3.12 HMBC structure of compound **T-6**

Table 3.6 ^{1}H NMR (500 MHz), ^{13}C NMR (500 MHz), COSY, and HMBC Spectral data of compound **T-6** in $CDCl_3$

Position	δ_H (mult., *J* in Hz)	δ_C	COSY ($^1H \rightarrow {}^1H$)	HMBC ($^1H \rightarrow {}^{13}C$)
1	-	197.49	-	-
2	2.45 (*d*, 17.2)	49.75	H-2a	C-1, C-5, C-6, C-12
	2.25 (*d*, 17.2)		H-2b	C-1, C-4, C-5, C-6, C-12
3	-	162.08	-	-
4	5.91 (*t*, 1.40)	126.98	-	C-2, C-7
5	-	41.24	-	-
6	-	79.02	-	-
7	5.79 (*d*, 15.6)	129.05	H-8	C-6, C-8, C-9
8	5.86 (d, 15.6)	135.81	H-7	C-6, C-7, C-9
9	4.41 (*m*)	67.87	H-10	C-7
10	1.30 (*d*, 3.60)	24.06	H-9	C-7, C-9
11	1.90 (*s*)	18.89	-	C-3, C-4, C-6
12	1.08 (*s*)	22.95	-	C-2, C-5, C-6, C-10
13	1.01 (*s*)	24.20	-	C-1, C-2, C-5, C-6, C-10

3.2 Biological Activities

3.2.1 *α*-Glucosidase and Nitric Oxide Production Inhibitory Activity-guided Fractionation of the Extract of *L. japonicus*

α-Glucosidase and nitric oxide (NO) production inhibitory activity of the EtOAc-soluble and its different polar fractions of *L. japonicus* were summarized in Table 3.1. Fractions E, F, and H, exhibited stronger *α*-glucosidase and NO production inhibitory activities than EtOAc-soluble and positive control, as showed in Table 3.7.

Table 3.7 *α*-Glucosidase inhibitory and NO production inhibitory activites of fractions isolated from *L. japonicus*

Fractions	*α*-Glucosidase inhibitory		NO production inhibitory	
	Percentage inhibition (%)	**IC_{50} Values (μg/mL)**	**Percentage inhibition (%)**	**IC_{50} Values (μg/mL)**
Crude	85.9 ± 0.1	72.2 ± 1.9	87.8 ± 2.1	20.7 ± 2.2
A	Inactive[c]	-	69.2 ± 0.6	64.0 ± 4.0
B	Inactive[c]	-	78.1 ± 1.3	51.2 ± 3.4
C	Inactive[c]	-	78.5 ± 2.0	39.8 ± 4.6
D	Inactive[c]	-	82.5 ± 1.8	49.4 ± 2.9
E	98.9 ± 0.1	49.4 ± 1.5	52.2 ± 1.9	29.0 ± 3.2
F	96.7 ± 0.9	72.8 ± 1.0	76.8 ± 1.9	59.8 ± 3.8
G	Inactive[c]	-	Inactive[d]	-
H	99.7 ± 0.6	27.9 ± 0.1	55.9 ± 4.2	34.3 ± 3.5
I	Inactive[c]	-	Inactive[d]	-
J	Inactive[c]	-	74.0 ± 0.6	54.4 ± 5.2
Acarbose[a]	-	120.3 ± 0.5	-	-
Indomethacin[b]	-	-	-	-

Note [a] Positive control (anti-diabetic drug).

[b] Positive control (anti-inflammatory drug).

[c] Inactive at >200 μM.

[d] Fractions lead to cell death.

3.2.2 *α*-Glucosidase and NO Production Inhibitory of Isolated Compounds from *L. japonicus*

Compounds **T-1** to **T-6** were tested for α-glucosidase and NO production inhibitory activity (Table 3.2). Many flavonoid compounds have antidiabetic properties, according to in vitro studies (Şöhretoğlu et al., 2018). Compound **T-1** showed stronger against α-glucosidase inhibitory activity than other compounds and positive control. Compound **T-1** exhibited effective α-glucosidase inhibitory activity, with an IC_{50} value of 143.9 μM, and compound **T-2** showed a lower activity with an IC_{50} value of 367.5 μM. The main flavonoids subclasses as flavones, flavonols, flavanones, and isoflavones, are the numerous members that have been proved to be effective α-glucosidase inhibitors in many studies (Kumar et al., 2011; Proença et

al., 2017; Şöhretoğlu et al., 2018). The results agreed with the previously reported that flavanone showed stronger α-glucosidase inhibitory activity than flavone skeleton. The above data shows that the main components responsible for the α-glucosidase inhibitory activities of *L. japonicus* were flavonoid derivatives.

However, compounds **T-2** and **T-3** showed the strongest NO production inhibitory activity with IC_{50} values of 66.9 and 70.6 μM, respectively. According to in vitro studies, flavonoid and terpenoid derivatives that have been proved to be against NO production in LPS-activated macrophages (Matsuda et al., 2003; Morikawa et al., 2017). These data demonstrated with the previously reported that the flavone and terpenoid derivatives were the main components responsible for the NO production inhibitory activity of *L. japonicus*.

Table 3.8 *α*-Glucosidase and NO production inhibitory activity of compounds isolated from *L. japonicus*

Compounds	*α*-Glucosidase inhibitory		NO production inhibitory	
	Percentage inhibition (%)	**IC_{50} Values (μM)**	**Percentage inhibition (%)**	**IC_{50} Values (μM)**
T-1	100.0 ± 1.3	143.9 ± 0.6	77.9 ± 2.2	214.8 ± 3.3
T-2	89.5 ± 0.1	367.5 ± 0.6	84.6 ± 1.2	66.9 ± 3.7
T-3	73.9 ± 0.4	408.5 ± 1.9	79.5 ± 5.6	70.6 ± 3.8
T-4	89.8 ± 0.1	434.7 ± 1.1	74.6 ± 4.2	187.5 ± 3.7
T-5	99.8 ± 0.1	598.4 ± 0.6	73.6 ± 0.9	285.8 ± 2.5
T-6	99.3 ± 0.3	192.2 ± 0.5	Inactive[c]	Inactive[c]
Acarbose[a]	-	157.1 ± 0.1	-	-
Indomethacin[b]	-	-	-	32.7 ± 3.9

Note [a] Positive control (anti-diabetic drug).

[b] Positive control (anti-inflammatory drug).

[c] Fractions lead to cell death.

CHAPTER 4

CONCLUSION

In conclusion, the bioassay-guided chemical investigation of *L. japonicus* led to the isolation and identification of six known compounds including of two flavonoid derivatives (**T-1** and **T-2**), two sesquiterpene derivatives (**T-3** and **T-6**), one benzofuran derivative (**T-4**), and phenol derivative (**T-5**) (Figure 4.1).

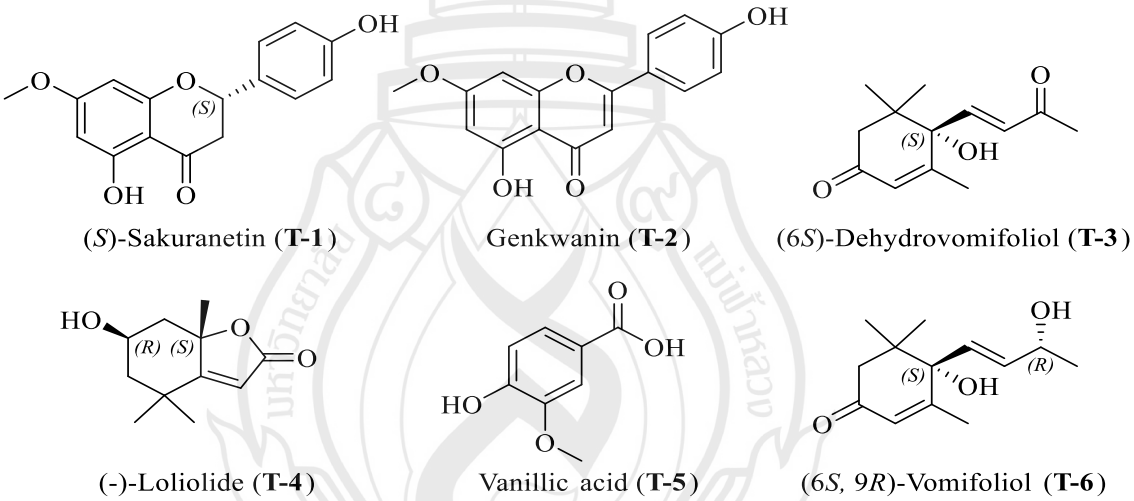

Figure 4.1 Structure of compounds (**T-1** to **T-6**)

During our ongoing research project on bioactive natural products from the aerial parts of *L. japonicus*, an EtOAc-soluble partition of the EtOH extract of the aerial of *L. japonicus* displayed α-glucosidase and NO production inhibitory activities. This prompted us to perform detailed bioassay-guided isolation from this plant, which led to the isolation of six known compounds. (*S*)-sakuranetin (**T-1**) showed the highest efficacy in inhibiting α-glucosidase enzyme with IC_{50} values of 143.9 μM. However, genkwanin (**T-2**) and (6*S*)-dehydrovomifoliol (**T-3**) also showed moderate anti-inflammatory with

IC_{50} values of 66.9 and 70.6 μM, respectively. These findings support that *L. japonicus* are a good source of bioactive compounds.

Acknowledgments

This work was supported by Medicinal Plants Innovation Center (MPIC), and Mae Fah Luang University was acknowledged for its laboratory facilities. My parents and Center of Chemical Innovation for Sustainability (CIS) partially financially support me.

REFERENCES

REFERENCES

Aishan, H., Baba, M., Iwasaki, N., Kuang, H., & Okuyama, T. (2010). The constituents of *Urtica cannabina* used in Uighur medicine. *Pharmaceutical Biology*, *48*(5), 577-583.

Arya, S. S., Rookes, J. E., Cahill, D. M., & Lenka, S. K. (2021). Vanillin: A review on the therapeutic prospects of a popular flavouring molecule. *Advances in Traditional Medicine*, *21*(3), 1-17.

Badhani, B., Sharma, N., & Kakkar, R. (2015). Gallic acid: A versatile antioxidant with promising therapeutic and industrial applications. *Rsc Advances*, *5*(35), 27540-27557.

Bangar, S. P., Chaudhary, V., Sharma, N., Bansal, V., Ozogul, F., & Lorenzo, J. M. (2022). Kaempferol: A flavonoid with wider biological activities and its applications. *Critical Reviews in Food Science and Nutrition*, *15*, 1-25.

Bettio, L. E., Gil-Mohapel, J., & Rodrigues, A. L. S. (2016). Guanosine and its role in neuropathologies. *Purinergic Signalling*, *12*(3), 411-426.

Bich, T. T. N., & Kato-Noguchi, H. (2014). Isolation and identification of a phytotoxic substance from the emergent macrophyte *Centrostachys aquatica*. *Botanical Studies*, *55*(1), 1-5.

Bosabalidis, A., Gabrieli, C., & Niopas, I. (1998). Flavone aglycones in glandular hairs of *Origanum x intercedens*. *Phytochemistry*, *49*(6), 1549-1553.

Cai, X. H., Che, C. T., Lam, C. K., Mak, T. C., & Wu, L. J. (2006). A new labdane diterpene from *Leonurus heterophyllus*. *Journal of Asian Natural Products Research*, *8*(7), 599-603.

Cai, X., Che, Z., Wu, B., Gao, H., & Wu, L. (2006). Studies on chemical constituents of *Leonurus japonicus*. *Shenyang Yaoke Daxue Xuebao*, *23*, 13-21.

Chang, J. M., Shen, C. C., Huang, Y. L., Shieh, B. J., & Chen, C. C. (2010). Two new glycosides from *Leonurus japonicus*. *Journal of Asian Natural Products Research*, *12*(9), 740-744.

Chang, S. W., Kim, K. H., Lee, I. K., Choi, S. U., Ryu, S. Y., & Lee, K. R. (2009). Phytochemical constituents of *Bistorta manshuriensis*. *Natural Product Sciences*, *15*(4), 234-240.

Cheng, F., Zhou, Y., Wang, M., Guo, C., Cao, Z., Zhang, R., & Peng, C. (2020). A review of pharmacological and pharmacokinetic properties of stachydrine. *Pharmacological Research*, *155*, 104755.

Circular dichroism and magnetic circular dichroism spectroscopy for organic chemists (1st ed.). (2011). *Royal Society of Chemistry*.

Cong, Y., Guo, J., Wang, T., Li, M., Li, K., Wang, J., & Li, Q. (2009). Chemical constituents and antitumor activity on leukemia K562 cell of *Leonurus heterophyllus*. *China Journal of Chinese Materia Medica*, *34*(14), 1816-1818.

Cong, Y., Wang, J. H., & Li, X. (2005). Note: A new flavonoside from *Leonurus heterophyllus*. *Journal of Asian Natural Products Research*, *7*(3), 273-277.

Dabeek, W. M., & Marra, M. V. (2019). Dietary quercetin and kaempferol: Bioavailability and potential cardiovascular-related bioactivity in humans. *Nutrients*, *11*(10), 2288.

Deng, S., Liu, L. L., Chen, Y., Li, X. X., Wang, T., & Zhang, Y. (2014). Study on chemical constituents of *Leonurus japonicas* Houtt. III. J Tianjin Univ *Tradit Chin Med*, *33*(6), 362-364.

Deng, S., Wang, T., Wu, C. H., Qu, L., Han, L. F., & Zhang, Y. (2013). Isolation and identification of constituents from *Leonurus japonicus*. *Chin J Med Chem*, *23*, 209-212.

Fuchino, H., Daikonya, A., Kumagai, T., Goda, Y., Takahashi, Y., & Kawahara, N. (2013). Two new labdane diterpenes from fresh leaves of *Leonurus japonicus* and their degradation during drying. *Chemical and Pharmaceutical Bulletin*, *61*(5), 497-503.

Gangadhar, K. N., Rodrigues, M. J., Pereira, H., Gaspar, H., Malcata, F. X., Barreira, L., . . . Varela, J. (2020). Anti-hepatocellular carcinoma (HepG2) activities of monoterpene hydroxy lactones isolated from the marine microalga *Tisochrysis Lutea*. *Marine Drugs*, *18*(11), 567.

Giang, P. M., Son, P. T., Matsunami, K., & Otsuka, H. (2005). New Labdane-Type Diterpenoids from *Leonurus heterophyllus* S W. *Chemical and Pharmaceutical Bulletin*, *53*(8), 938-941.

Giang, P. M., Son, P. T., Matsunami, K., & Otsuka, H. (2005). New Bis-spirolabdane-Type Diterpenoids from *Leonurus heterophyllus* SW. *Chemical and Pharmaceutical Bulletin*, *53*(11), 1475-1479.

Gong, H. Q., Wang, R., & Shi, Y. P. (2012). New Labdane-Type Diterpenoids from *Leonurus heterophyllus*. *Helvetica Chimica Acta*, *95*(4), 618-625.

González-Baró, A.C, Parajón-Costa, B. S., Franca C. A., & Pis-Diez R. (2008). Theoretical and spectroscopic study of vanillic acid. *Journal of Molecular Structure*, *889*(1-3), 204-210.

Grayer, R. J., Thabrew, M. I., Hughes, R. D., Bretherton, S., Lever, A., Veitch, N. C., . . . Simmonds, M. S. (2008). Phenolic and Terpenoid Constituents from the Sri Lankan Medicinal Plant *Osbeckia aspera*. *Pharmaceutical Biology*, *46*(3), 154-161.

Grecco, S. D. S., Dorigueto, A. C., Landre, I. M., Soares, M. G., Martho, K., Lima, R., . . . Lago, J. H. G. (2014). Structural crystalline characterization of sakuranetin-An antimicrobial flavanone from twigs of *Baccharis retusa* (Asteraceae). *Molecules*, *19*(6), 7528-7542.

Grochowski, D. M., Locatelli, M., Granica, S., Cacciagrano, F., & Tomczyk, M. (2018). A review on the dietary flavonoid tiliroside. *Comprehensive Reviews in Food Science and Food Safety*, *17*(5), 1395-1421.

Gullón, B., Lú-Chau, T. A., Moreira, M. T., Lema, J. M., & Eibes, G. (2017). Rutin: A review on extraction, identification and purification methods, biological activities and approaches to enhance its bioavailability. *Trends in Food Science & Technology*, *67*, 220-235.

Han-Kui, W. U., Ting, S. U. N., Feng, Z. H. A. O., Zhang, L. P., Gang, L. I., & Zhang, J. (2017). New diterpenoids isolated from *Leonurus japonicus* and their acetylcholinesterase inhibitory activity. *Chinese Journal of Natural Medicines*, *15*(11), 860-864.

Han-Kui, W. U., Yan-Jun, M. A. O., Shan-Shan, S. U. N., Zhi-Yong, X. U., Ya, M. A., Jin-Xia, C. A. O., . . . Wei-Hua, Y. A. N. G. (2016). Leojaponic acids A and B, two new homologous terpenoids, isolated from *Leonurus japonicus*. *Chinese Journal of Natural Medicines*, *14*(4), 303-307.

HE, C. J. (2014). Chemical constituents from Leonurus japonicus Injection. *Chinese Traditional and Herbal Drugs*, *24*, 3048-3052.

Hon, P. M., Wang, E. S., Lam, S. K., Choy, Y. M., Lee, C. M., & Wong, H. N. (1993). Preleoheterin and leoheterin, two labdane diterpenes from *Leonurus heterophyllus*. *Phytochemistry*, *33*(3), 639-641.

Hong, M., Chen, D., Hong, Z., Tang, K., Yao, Y., Chen, L., . . . Sun, R. (2021). Ex vivo and in vivo chemoprotective activity and potential mechanism of Martynoside against 5-fluorouracil-induced bone marrow cytotoxicity. *Biomedicine & Pharmacotherapy*, *138*, 111501.

Horstmann, U., Pachaly, P., & Sin, K. S. (1994). P6 Leonurenosid I and II, two new glycosides from *Leonurus japonicus* houtt. *European Journal of Pharmaceutical Sciences*, *2*(1-2), 120.

Houshdar Tehrani, M. H., Gholibeikian, M., Bamoniri, A., & Mirjalili, B. B. F. (2021). Cancer treatment by Caryophyllaceae-type cyclopeptides. *Frontiers in Endocrinology*, *11*, 600856.

Hu, Y. M., Liu, W. J., Li, M. X., Li, H. B., Jiang, T., Cheng, N. B., & Xiao, W. (2019). Two new labdane diterpenoids from aerial parts of *Leonurus japonicus* and their anti-inflammatory activity. *Natural Product Research*, *33*(17), 2490-2497.

Hung, T. M., Luan, T. C., Vinh, B. T., Cuong, T. D., & Min, B. S. (2011). Labdane-type diterpenoids from *Leonurus heterophyllus* and their cholinesterase inhibitory activity. *Phytotherapy Research*, *25*(4), 611-614.

Joo, T., Sowndhararajan, K., Hong, S., Lee, J., Park, S. Y., Kim, S., . . . Jhoo, J. W. (2014). Inhibition of nitric oxide production in LPS-stimulated RAW 264.7 cells by stem bark of *Ulmus pumila* L. *Saudi Journal of Biological Sciences*, *21*(5), 427-435.

Jun, Y., Jing, Y. L., Xiao, Q. C., Yue, L. G., Ping, L., Ze, W. Z., & Wen, J. Y. (2010). *Leonurus heterophyllus* sweet extract improves hemorheology and inhibits thrombosis in rat with induced myocardial ischemia. *Journal of Medicinal Plants Research*, *4*(9), 732-740.

Kashyap, D., Sharma, A., Tuli, H. S., Sak, K., Garg, V. K., Buttar, H. S., . . . Sethi, G. (2018). Apigenin: A natural bioactive flavone-type molecule with promising therapeutic function. *Journal of Functional Foods*, *48*, 457-471.

Khan, S., Shehzad, O., Jin, H. G., Woo, E. R., Kang, S. S., Baek, S. W., . . . Kim, Y. S. (2012). Anti-inflammatory mechanism of 15, 16-epoxy-3α-hydroxylabda-8, 13 (16), 14-trien-7-one via inhibition of LPS-induced multicellular signaling pathways. *Journal of Natural Products*, *75*(1), 67-71.

Kim, S. J., Um, J. Y., Hong, S. H., & Lee, J. Y. (2011). Anti-inflammatory activity of hyperoside through the suppression of nuclear factor-κB activation in mouse peritoneal macrophages. *The American journal of Chinese Medicine*, *39*(01), 171-181.

Kong, P., Chen, G., Jiang, A., Wang, Y., Song, C., Zhuang, J., & Yan, J. (2016). Sesamin inhibits IL-1β-stimulated inflammatory response in human osteoarthritis chondrocytes by activating Nrf2 signaling pathway. *Oncotarget*, *7*(50), 83720.

Kumar, S., Narwal, S., Kumar, V., & Prakash, O. (2011). *α*-glucosidase inhibitors from plants: A natural approach to treat diabetes. *Pharmacognosy reviews*, *5*(9), 19.

Kumarasamy, Y., Cox, P. J., Jaspars, M., Nahar, L., & Sarker, S. D. (2006). Bioactivity of hirsutanolol, oregonin and genkwanin, isolated from the seeds of *Alnus glutinosa* (Betulaceae). *Natural Product Communications*, *1*(8), 641-644.

Lai, K. Y., Hu, H. C., Chiang, H. M., Liu, Y. J., Yang, J. C., Lin, Y. A., . . . Lee, C. L. (2018). New diterpenes leojaponins G–L from *Leonurus japonicus*. *Fitoterapia*, *130*, 125-133.

Leem, H. H., Lee, G. Y., Lee, J. S., Lee, H., Kim, J. H., & Kim, Y. H. (2017). Soluble epoxide hydrolase inhibitory activity of components from *Leonurus japonicus*. *International Journal of Biological Macromolecules*, *103*, 451-457.

Li, Y., Chen, Z., Feng, Z., Yang, Y., Jiang, J., & Zhang, P. (2012). Hepatoprotective glycosides from *Leonurus japonicus* Houtt. *Carbohydrate Research*, *348*, 42-46.

Liu, J., Peng, C., Zhou, Q. M., Guo, L., Liu, Z. H., & Xiong, L. (2018). Alkaloids and flavonoid glycosides from the aerial parts of *Leonurus japonicus* and their opposite effects on uterine smooth muscle. *Phytochemistry*, *145*, 128-136.

Ma, Q. G., Wen, R. R., Liu, W. M., Sang, Z. P., Zhang, S., Wang, Q. Q., . . . Li, Y. P. (2016). Studies on flavonoids from *Cirsium setosum*. *China Journal of Chinese Materia Medica*, *41*(5), 868-873.

Maria, S., Islam, F., Qais, N., & Hasan, C. M. (2013). Isolation of vomifoliol: A megastigmane from leaves of *Antidesma ghaesembilla*. *Asian Journal of Chemistry*, *25*(6), 3533.

Matsuda, H., Morikawa, T., Ando, S., Toguchida, I., & Yoshikawa, M. (2003). Structural requirements of flavonoids for nitric oxide production inhibitory activity and mechanism of action. *Bioorganic & medicinal chemistry*, *11*(9), 1995-2000.

Miao, L. L., Zhou, Q. M., Peng, C., Liu, Z. H., & Xiong, L. (2019). *Leonurus japonicus* (Chinese motherwort), an excellent traditional medicine for obstetrical and gynecological diseases: A comprehensive overview. *Biomedicine & Pharmacotherapy*, *117*, 109060.

Moon, H. I. (2010). Three diterpenes from *Leonurus japonicus* houtt protect primary cultured rat cortical cells from glutamate-induced toxicity. *Phytotherapy Research*, *24*(8), 1256-1259.

Morikawa, T., Matsuda, H., & Yoshikawa, M. (2017). A review of anti-inflammatory terpenoids from the incense gum resins frankincense and myrrh. *Journal of oleo science*, ess16149.

Morita, H., Gonda, A., Takeya, K., & Itokawa, H. (1996). Cycloleonuripeptides A, B and C, three new proline-rich cyclic nonapeptides from *Leonurus heterophyllus*. *Bioorganic & Medicinal Chemistry Letters*, *6*(7), 767-770.

Morita, H., Gonda, A., Takeya, K., Itokawa, H., & Iitaka, Y. (1997). Cycloleonuripeptide D, a new proline-rich cyclic decapeptide from *Leonurus heterophyllus*. *Tetrahedron*, *53*(5), 1617-1626.

Morita, H., Iizuka, T., Gonda, A., Itokawa, H., & Takeya, K. (2006). Cycloleonuripeptides E and F, Cyclic Nonapeptides from *Leonurus heterophyllus*. *Journal of Natural Products*, *69*(5), 839-841.

Nguyen, L. T., Tran, P. T., Bui, D. N., Nguyen, H. T., Trinh, B. T., Ngo, N. T., . . . Nguyen, L. H. D. (2021). Three labdane diterpenoids from the aerial parts of *Leonurus japonicus*. *Phytochemistry Letters*, *44*, 82-86.

Nguyen, L. T., Vo, H. K., Dang, S. V., Le, T. H., Ha, L. D., Nguyen, L. T. T., . . . Nguyen, L. H. D. (2017). Labdane and norlabdane diterpenoids from the aerial parts of *Leonurus japonicus*. *Phytochemistry Letters*, *22*, 174-178.

Nieto-Mendoza, E., Guevara-Salazar, J. A., Ramírez-Apan, M. T., Frontana-Uribe, B. A., Cogordan, J. A., & Cárdenas, J. (2005). Electro-oxidation of hispanolone and anti-inflammatory properties of the obtained derivatives. *The Journal of Organic Chemistry*, *70*(11), 4538-4541.

Nugrahini, A. D., Ishida, M., Nakagawa, T., Nishi, K., & Sugahara, T. (2020). Trigonelline: An alkaloid with anti-degranulation properties. *Molecular Immunology*, *118*, 201-209.

Pałasz, A., & Cież, D. (2015). In search of uracil derivatives as bioactive agents. Uracils and fused uracils: Synthesis, biological activity and applications. *European Journal of Medicinal Chemistry*, *97*, 582-611.

Peng, F., Xiong, L., & Zhao, X. M. (2013). A bicyclic diterpenoid with a new 15, 16-dinorlabdane carbon skeleton from *Leonurus japonicus* and its coagulant bioactivity. *Molecules*, *18*(11), 13904-13909.

Peng, W., Huo, G., Zheng, L., Xiong, Z., Shi, X., & Peng, D. (2019). Two new oleanane derivatives from the fruits of *Leonurus japonicus* and their cytotoxic activities. *Journal of Natural Medicines*, *73*(1), 252-256.

Peng, Y., Zheng, C., Wang, Y. N., & Dai, O. (2017). Novel labdane diterpenoids from the aerial parts of *Leonurus japonicus*. *Phytochemistry Letters*, *20*, 45-48.

Proença, C., Freitas, M., Ribeiro, D., Oliveira, E. F., Sousa, J. L., Tome, S. M., . . . Fernandes, E. (2017). *α*-Glucosidase inhibition by flavonoids: An in vitro and in silico structure–activity relationship study. *Journal of Enzyme Inhibition and Medicinal Chemistry, 32*(1), 1216-1228.

Qin, J., Li, H. M., Gao, L. H., Liu, D., Li, R. T., & Lee, K. H. (2014). New labdane diterpenoids from *Leonurus japonicus* and their anti-inflammatory activity. *Phytochemistry Letters, 10*, 313-317.

Qu, G. Z., Si, C. L., & Wang, M. H. (2006). Antioxidant constituents from *Leonurus japonicus*. *Natural Product Sciences, 12*(4), 197-200.

Rao, Y. K., Lee, M. J., Chen, K., Lee, Y. C., Wu, W. S., & Tzeng, Y. M. (2011). Insulin-mimetic action of rhoifolin and cosmosiin isolated from *Citrus grandis* (L.) Osbeck leaves: Enhanced adiponectin secretion and insulin receptor phosphorylation in 3T3-L1 cells. *Evidence-Based Complementary and Alternative Medicine*, 2011.

Rauwald, H. W., Savtschenko, A., Merten, A., Rusch, C., Appel, K., & Kuchta, K. (2015). GABAA receptor binding assays of standardized *Leonurus cardiaca* and *Leonurus japonicus* extracts as well as their isolated constituents. *Planta Medica, 81*(12/13), 1103-1110.

Ray, G., Leelamanit, W., Sithisarn, P., & Jiratchariyakul, W. (2014). Antioxidative compounds from *Aquilaria crassna* leaf. *Journal of Pharmaceutical Sciences, 41*(4), 54-58.

Rogerio, A. P., Kanashiro, A., Fontanari, C., Da Silva, E. V. G., Lucisano-Valim, Y. M., Soares, E. G., . . . Faccioli, L. H. (2007). Anti-inflammatory activity of quercetin and isoquercitrin in experimental murine allergic asthma. *Inflammation Research*, *56*(10), 402-408.

Romero-González, R. R., Ávila-Núñez, J. L., Aubert, L., & Alonso-Amelot, M. E. (2006). Labdane diterpenes from *Leonurus japonicus* leaves. *Phytochemistry, 67*(10), 965-970.

Seo, H. K., Kim, J. S., & Kang, S. S. (2010). Labdane diterpenes and flavonoids from *Leonurus japonicus*. *Helvetica Chimica Acta, 93*(10), 2045-2051.

Shang, X., Pan, H., Wang, X., He, H., & Li, M. (2014). *Leonurus japonicus* Houtt.: Ethnopharmacology, phytochemistry and pharmacology of an important traditional Chinese medicine. *Journal of Ethnopharmacology, 152*(1), 14-32.

Snatzke, G. (1979). Circular dichroism and absolute conformation: Application of qualitative MO theory to chiroptical phenomena. *Angewandte Chemie International Edition in English, 18*(5), 363-377.

Şöhretoğlu, D., Sari, S., Barut, B., & Özel, A. (2018). Discovery of potent *α*-glucosidase inhibitor flavonols: Insights into mechanism of action through inhibition kinetics and docking simulations. *Bioorganic Chemistry, 79*, 257-264.

Srinivasulu, C., Ramgopal, M., Ramanjaneyulu, G., Anuradha, C. M., & Kumar, C. S. (2018). Syringic acid (SA)–a review of its occurrence, biosynthesis, pharmacological and industrial importance. *Biomedicine & Pharmacotherapy, 108*, 547-557.

Sugaya, K., Hashimoto, F., Ono, M., Ito, Y., Masuoka, C., & Nohara, T. (1998). Antioxidative constituents from *Leonurii Herba* (*Leonurus japonicus*). *Food Science and Technology International, Tokyo, 4*(4), 278-281.

Suthiphasilp, V., Maneerat, W., Rujanapun, N., Duangyod, T., Charoensup, R., Deachathai, S., . . . Laphookhieo, S. (2020). *α*-Glucosidase inhibitory and nitric oxide production inhibitory activities of alkaloids isolated from a twig extract of *Polyalthia cinnamomea*. *Bioorganic & Medicinal Chemistry, 28*(10), 115462.

Taheri, Y., Suleria, H. A. R., Martins, N., Sytar, O., Beyatli, A., Yeskaliyeva, B., . . . Sharifi-Rad, J. (2020). Myricetin bioactive effects: Moving from preclinical evidence to potential clinical applications. *BMC Complementary Medicine and Therapies, 20*(1), 1-14.

Takemoto, J. K., Remsberg, C. M., Yáñez, J. A., Vega-Villa, K. R., & Davies, N. M. (2008). Stereospecific analysis of sakuranetin by high-performance liquid chromatography: pharmacokinetic and botanical applications. *Journal of Chromatography B, 875*(1), 136-141.

Thilagam, E., Parimaladevi, B., Kumarappan, C., & Mandal, S. C. (2013). *α*-Glucosidase and α-amylase inhibitory activity of *Senna surattensis*. *Journal of Acupuncture and Meridian Studies*, *6*(1), 24-30.

Wu, H., Wang, S., Liu, H., Yan, E., Wang, J., Wang, X., . . . Shi, Y. (2015). Diterpenoids from *Leonurus japonicus*. *Journal of the Korean Chemical Society*, *59*(2), 179-182.

Xiao, C. J., Liu, Y. C., Luo, S. H., Hua, J., Liu, Y., & Li, S. H. (2017). Localisation of two bioactive labdane diterpenoids in the peltate glandular trichomes of *Leonurus japonicus* by laser microdissection coupled with UPLC-MS/MS. *Phytochemical Analysis*, *28*(5), 404-409.

Xiong, L., Zhou, Q. M., Peng, C., Xie, X. F., Guo, L., Li, X. H., & Dai, O. (2013). Sesquiterpenoids from the herb of *Leonurus japonicus*. *Molecules*, *18*(5), 5051-5058.

Xiong, L., Zhou, Q. M., Peng, C., Xie, X. F., Liu, L. S., Guo, L., . . . Liu, Z. H. (2015). Bis-spirolabdane diterpenoids from *Leonurus japonicus* and their antiplatelet aggregative activity. *Fitoterapia*, *100*, 1-6.

Xiong, L., Zhou, Q. M., Zou, Y., Chen, M. H., Guo, L., Hu, G. Y., . . . Peng, C. (2015). Leonuketal, a spiroketal diterpenoid from *Leonurus japonicus*. *Organic letters*, *17*(24), 6238-6241.

Yamano, Y., & Ito, M. (2005). Synthesis of optically active vomifoliol and roseoside stereoisomers. *Chemical and Pharmaceutical Bulletin*, *53*(5), 541-546.

Yamashita, Y., Hanaya, K., Shoji, M., & Sugai, T. (2016). Simple synthesis of sakuranetin and selinone via a common intermediate, utilizing complementary regioselectivity in the deacetylation of *Naringenin triacetate*. *Chemical and Pharmaceutical Bulletin*, *64*(7), 961-965.

Yang, H., Zhou, Q. M., Peng, C., Liu, L. S., Xie, X. F., Xiong, L., . . . Liu, Z. H. (2014). Coumarins from *Leonurus japonicus* and their antiplatelet aggregative activity. *Journal of Chinese Materia Medica*, *39*(22), 4356-4359.

Yang, Y., Bakri, M., Gu, D., & Aisa, H. A. (2013). Separation of (*S*)-dehydrovomifoliol from leaves of *Nitraria sibirica* Pall. by high-speed counter-current chromatography. *Journal of Liquid Chromatography & Related Technologies*, *36*(5), 573-582.

Ye, M., Ma, G. L., Su, J. J., Xiong, J., & Hu, J. F. (2014). Leonurosides A–D: Steroid N-acetylglucosaminides from the fruits of *Leonurus japonicus*. *Phytochemistry Letters*, *10*, 287-290.

Ye, M., Xiong, J., Zhu, J. J., Hong, J. L., Zhao, Y., Fan, H., & Hu, J. F. (2014). Leonurusoleanolides E–J, minor spirocyclic triterpenoids from *Leonurus japonicus* fruits. *Journal of Natural Products*, *77*(1), 178-182.

Yue, C., Jinhui, W., Hongren, G., & Xian, L. (2003). Isolation and identification of the chemical constituents of *Leonurus japonicus* Houtt. II. *Chinese Journal of Medicinal Chemistry*, *13*(6), 349-352.

Yue, G. G. L., Liang, X. X., Li, X. L., Lee, J. K. M., Gao, S., Kwok, H. F., . . . Xiao, W. L. (2020). Immunomodulatory and antitumour bioactive labdane diterpenoids from *Leonurus japonicus*. *Journal of Pharmacy and Pharmacology*, *72*(11), 1657-1665.

Zhang, Y., Deng, S., Qu, L., An, Y. T., Wu, C. H., Han, L. F., . . . Wang, T. (2013). Rare syringyl acylated flavonol glycosides from the aerial parts of *Leonurus japonicus* Houtt. *Molecules*, *18*(3), 2967-2977.

Zhao, Z., & Moghadasian, M. H. (2008). Chemistry, natural sources, dietary intake and pharmacokinetic properties of ferulic acid: A review. *Food Chemistry*, *109*(4), 691-702.

Zhong, W. M., Cui, Z. M., Liu, Z. K., Yang, Y., Wu, D. R., Liu, S. H., . . . Xiao, W. L. (2015). Three minor new compounds from the aerial parts of *Leonurus japonicus*. *Chinese Chemical Letters*, *26*(8), 1000-1003.

Zhou, Q. M., Peng, C., Li, X. H., Xiong, L., He, C. J., Guo, L., . . . Liu, Z. H. (2013). Aromatic compounds from *Leonurus japonicus* Houtt. *Biochemical Systematics and Ecology*, *51*, 101-103.

Zhou, Q. M., Peng, C., Yang, H., Liu, L. S., Yang, Y. T., Xie, X. F., . . . Xiong, L. (2015). Steroids from the aerial parts of *Leonurus japonicus*. *Phytochemistry Letters*, *12*, 287-290.

Zhou, Q. M., Zhu, H., Feng, R., Peng, C., Yang, H., Liu, F., . . . Xiong, L. (2019). New triterpenoids from *Leonurus japonicus* (Lamiaceae). *Biochemical Systematics and Ecology*, *82*, 27-30.

APPENDIX

APPENDIX

NMR SPECTRUM OF COMPOUNDS FROM *L. JAPONICUS*

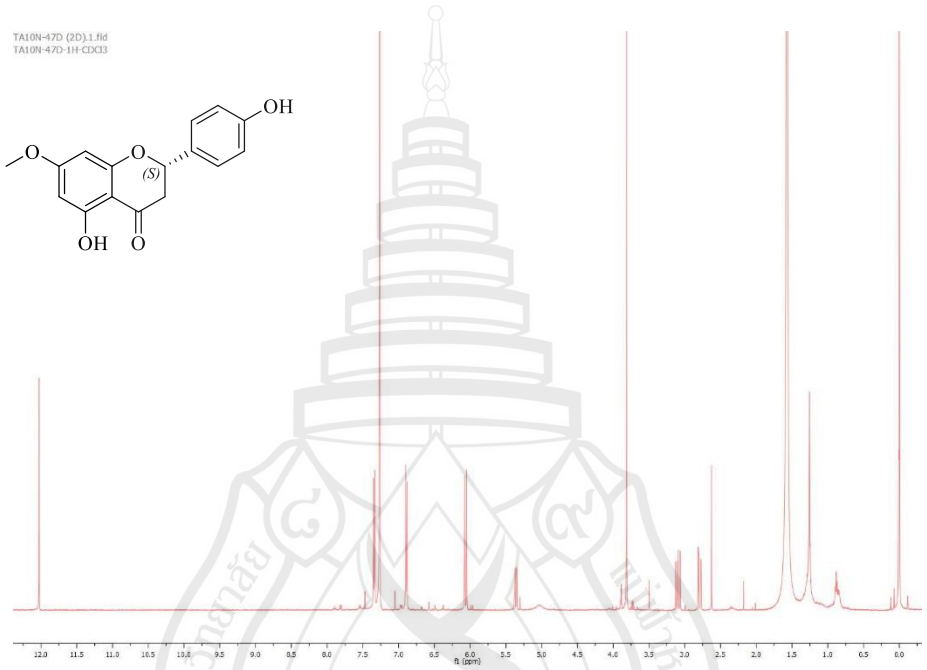

Figure A1 ^{1}H NMR Spectrum of Compound **T-1** in $CDCl_3$ (500 MHZ)

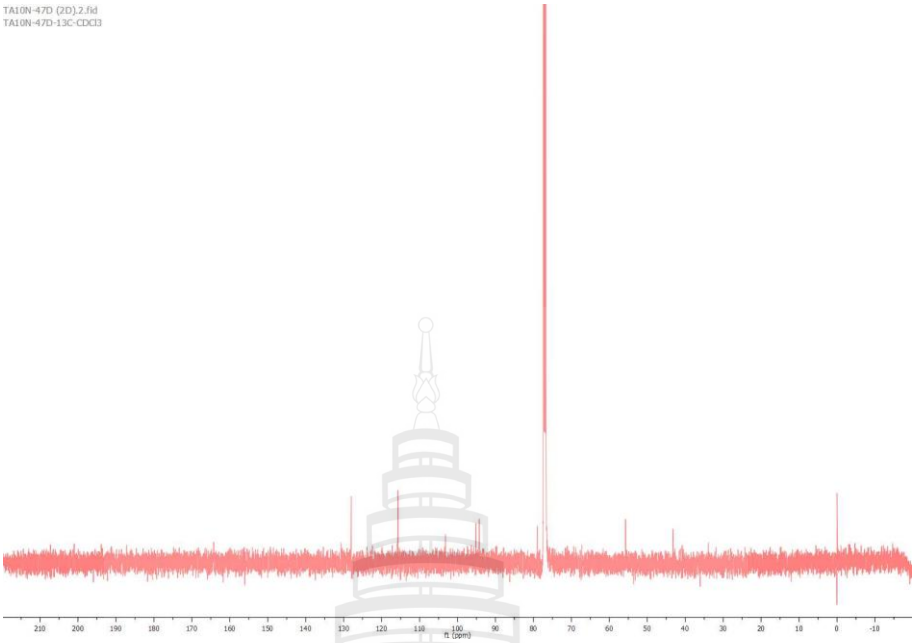

Figure A2 ^{13}C NMR Spectrum of Compound **T-1** in $CDCl_3$ (500 MHZ)

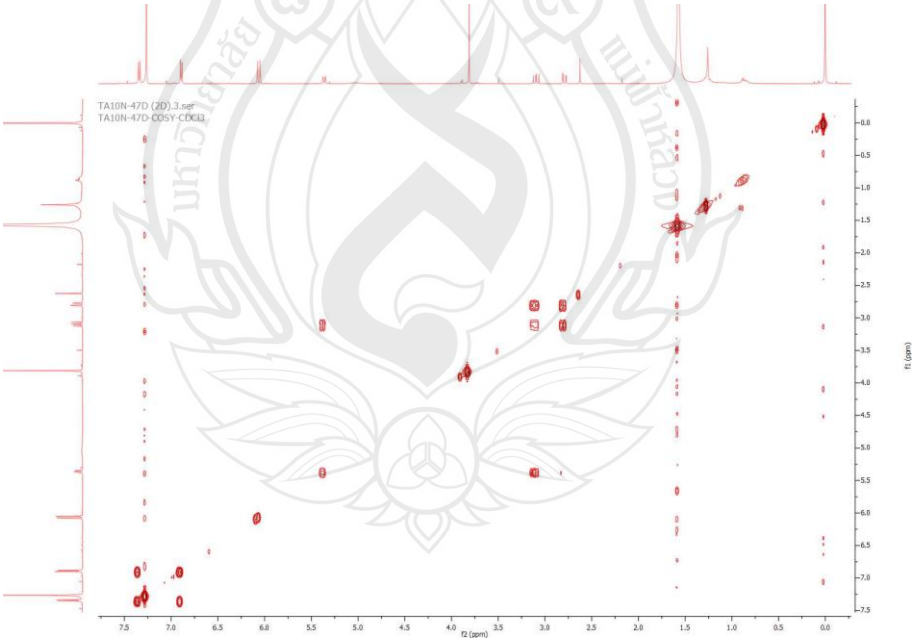

Figure A3 COSY NMR Spectrum of Compound **T-1** in $CDCl_3$

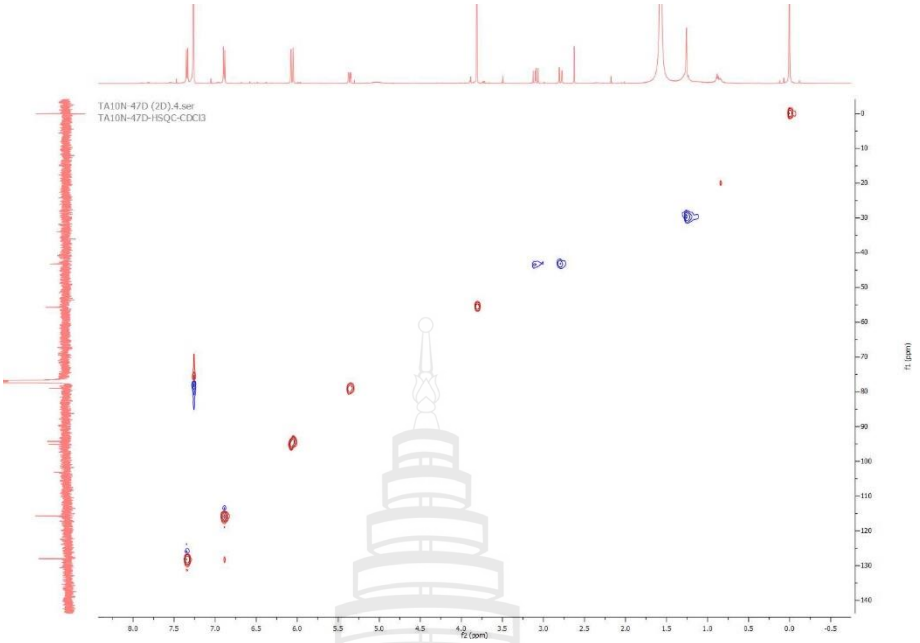

Figure A4 HSQC NMR Spectrum of Compound **T-1** in $CDCl_3$

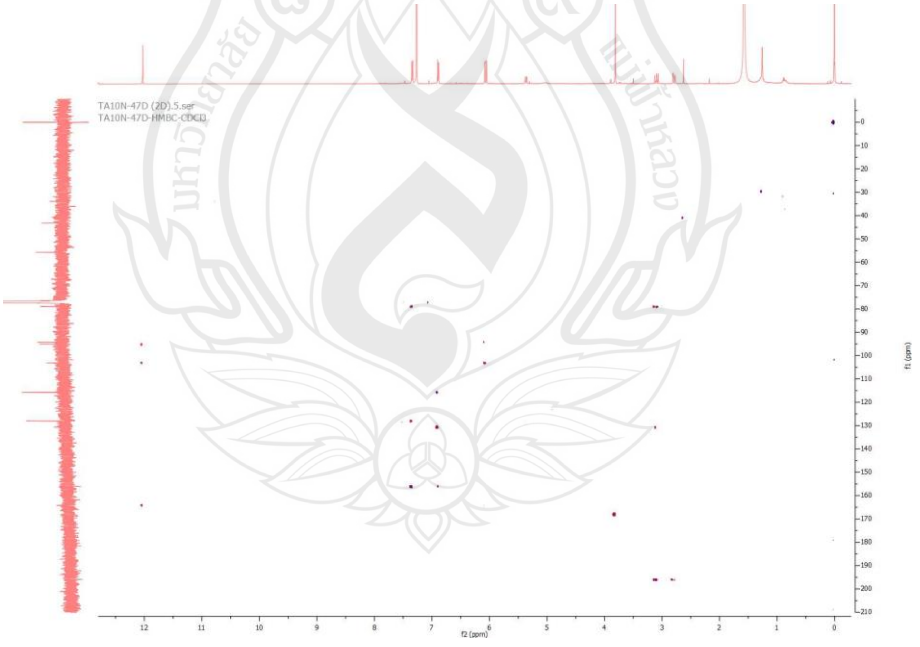

Figure A5 HMBC NMR Spectrum of Compound **1** in $CDCl_3$

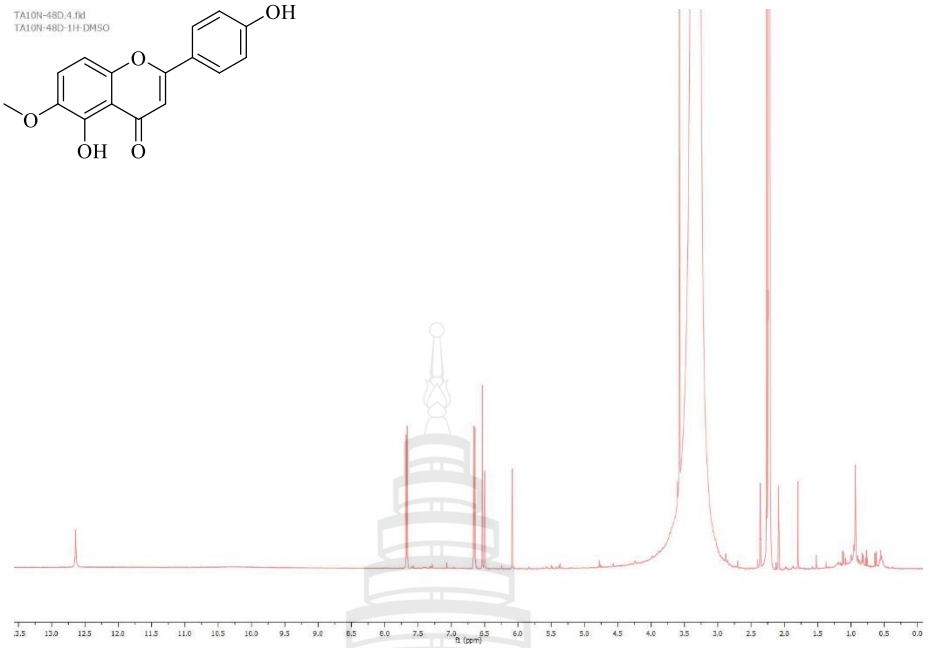

Figure A6 ^{1}H NMR Spectrum of Compound **T-2** in DMSO (500 MHZ)

Figure A7 ^{13}C NMR Spectrum of Compound **T-2** in DMSO (500 MHZ)

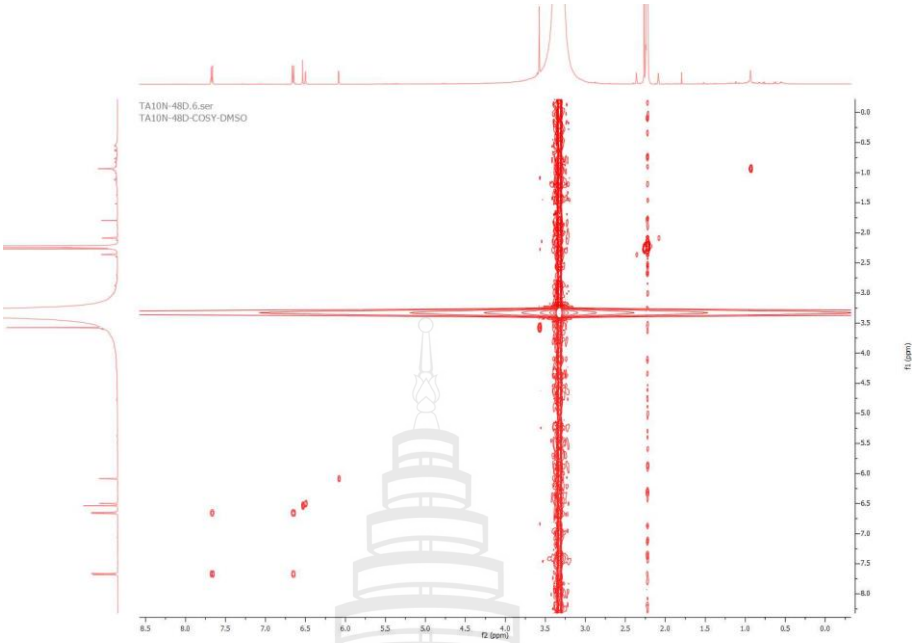

Figure A8 COSY NMR Spectrum of Compound **T-2** in DMSO

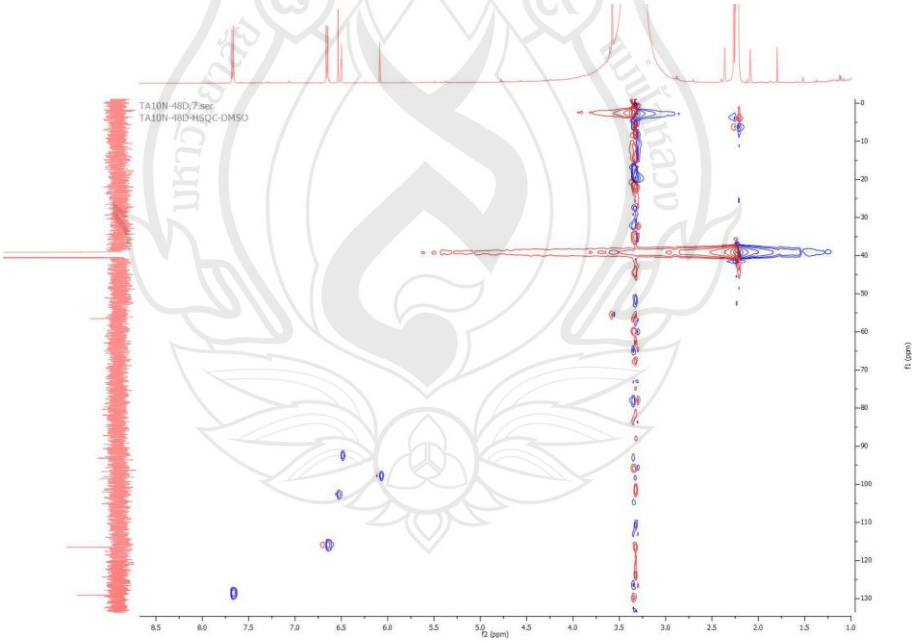

Figure A9 HSQC NMR Spectrum of Compound **T-2** in DMSO

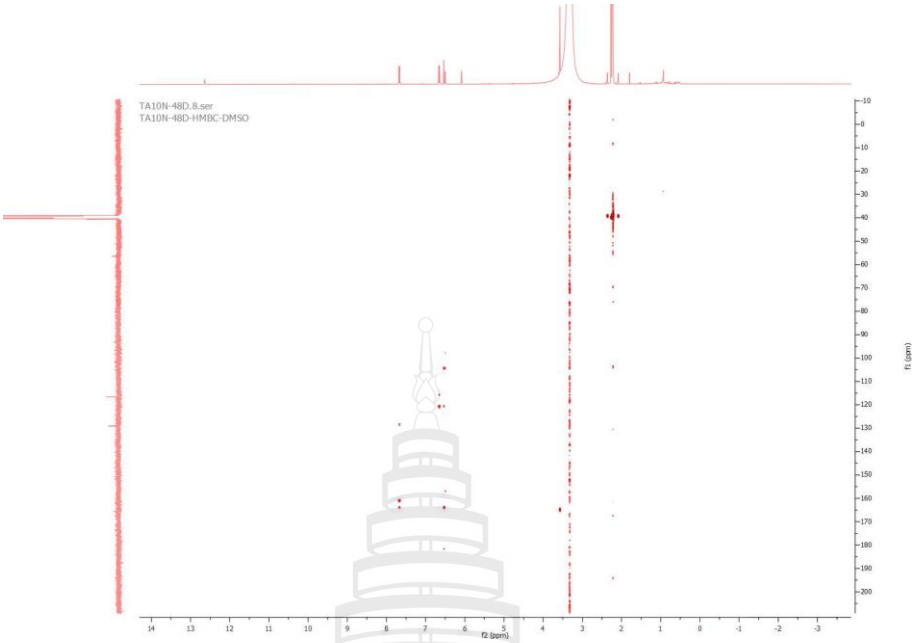

Figure A10 HMBC NMR Spectrum of Compound **T-2** in DMSO

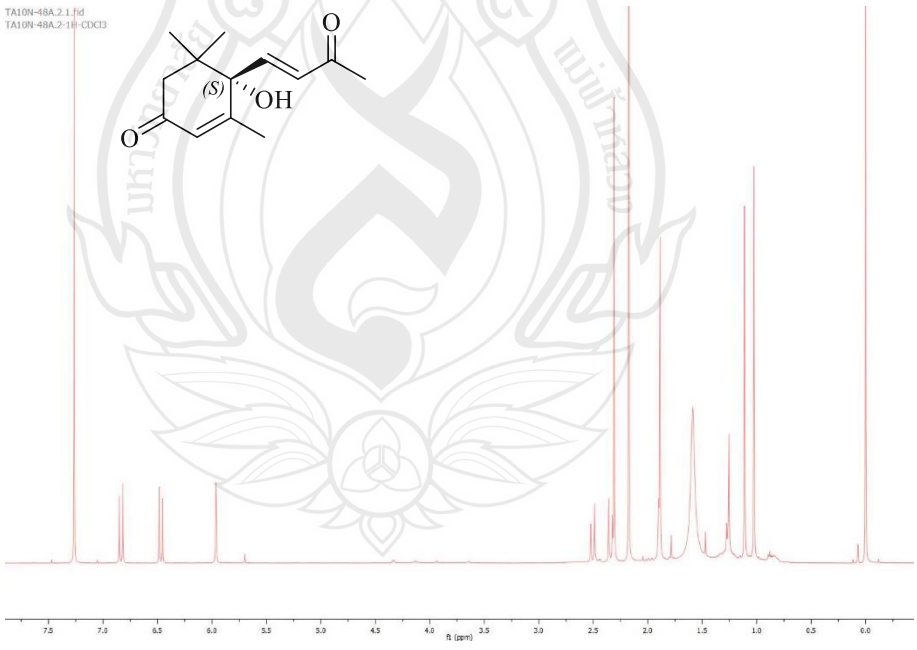

Figure A11 ^{1}H NMR Spectrum of Compound **T-3** in $CDCl_3$ (500 MHZ)

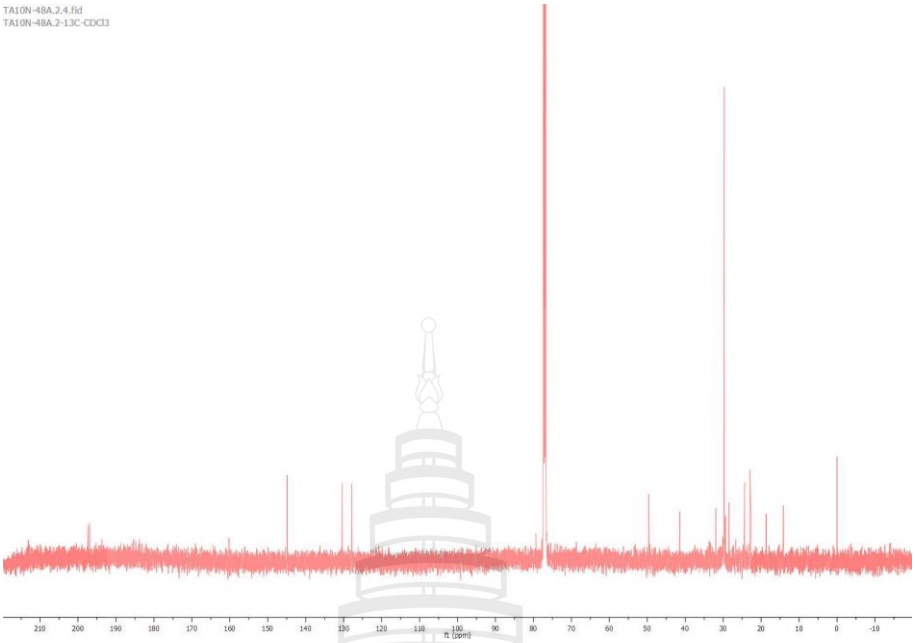

Figure A12 ^{13}C NMR Spectrum of Compound **T-3** in $CDCl_3$ (500 MHZ)

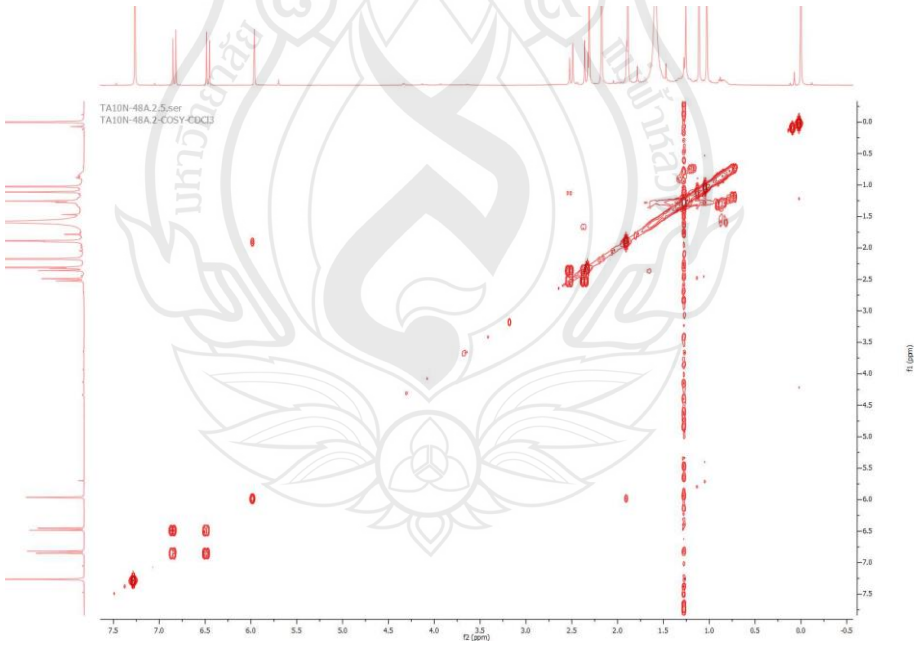

Figure A13 COSY NMR Spectrum of Compound **T-3** in $CDCl_3$

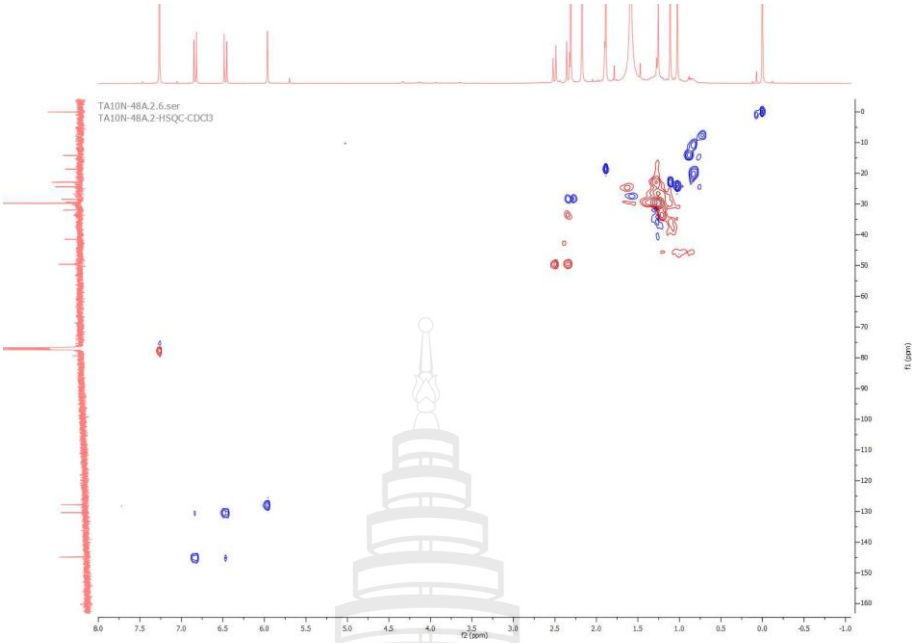

Figure A14 HSQC NMR Spectrum of Compound **T-3** in $CDCl_3$

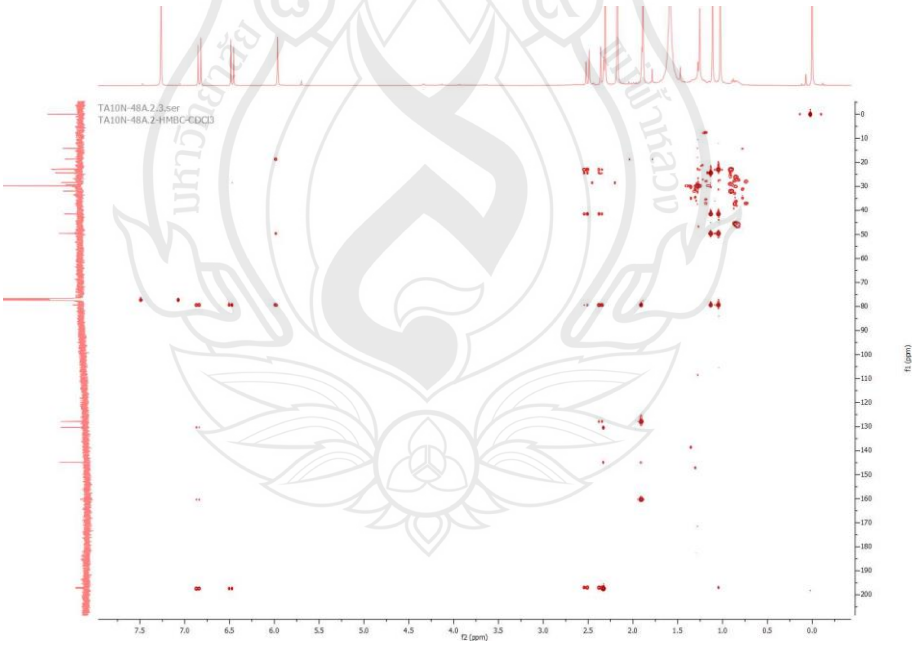

Figure A15 HMBC NMR Spectrum of Compound **T-3** in $CDCl_3$

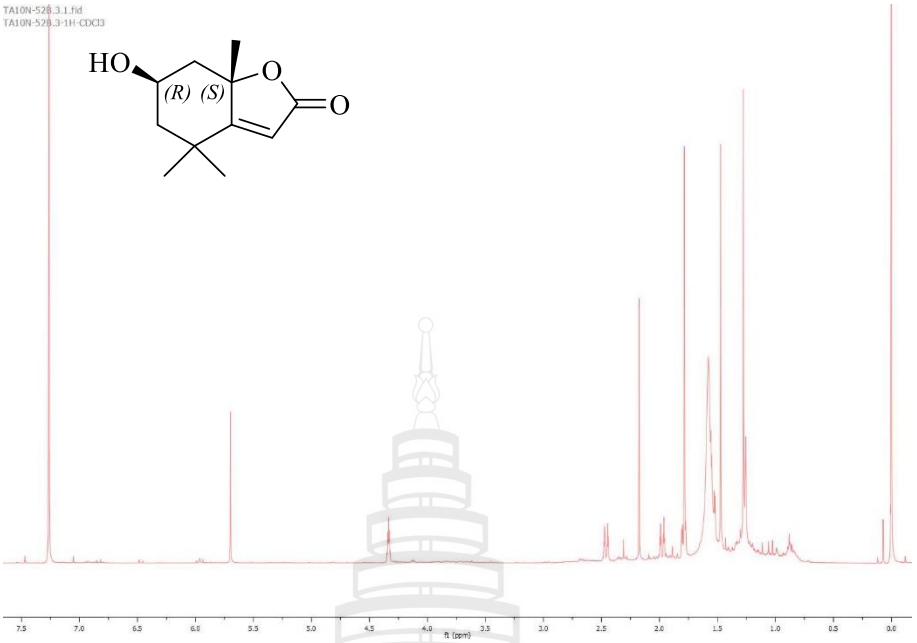

Figure A16 ^{1}H NMR Spectrum of Compound **T-4** in $CDCl_3$ (500 MHZ)

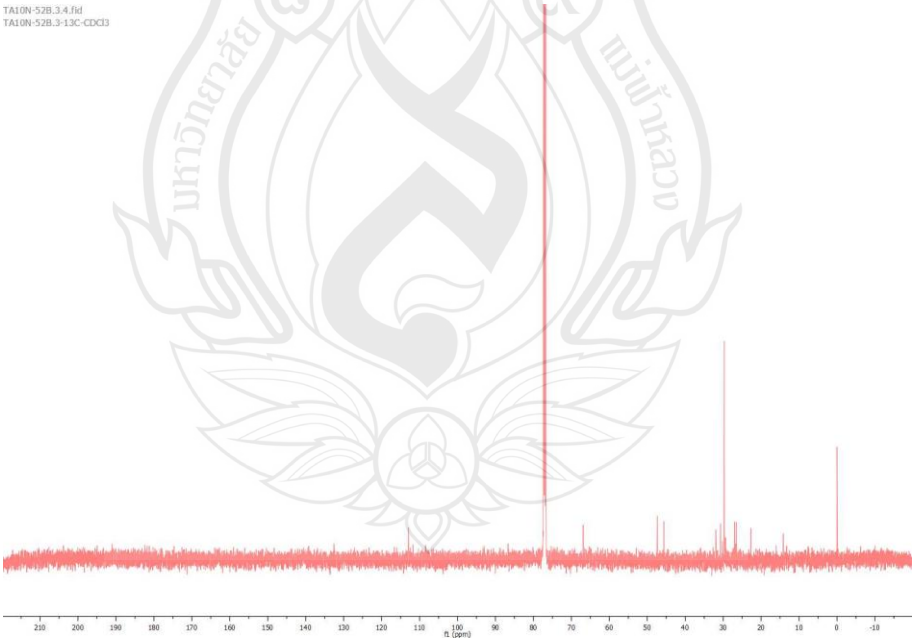

Figure A17 ^{13}C NMR Spectrum of Compound **T-4** in $CDCl_3$ (500 MHZ)

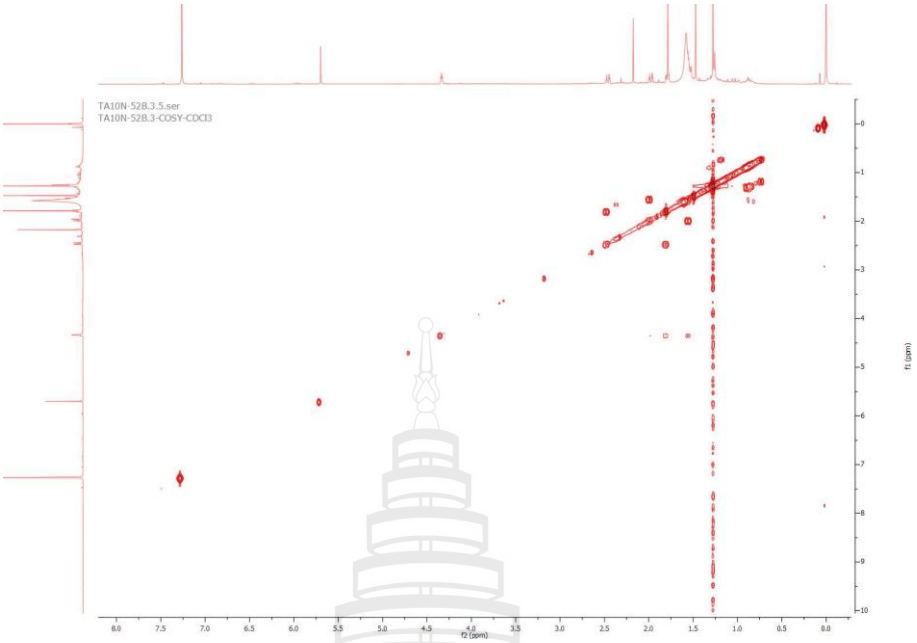

Figure A18 COSY NMR Spectrum of Compound **T-4** in $CDCl_3$

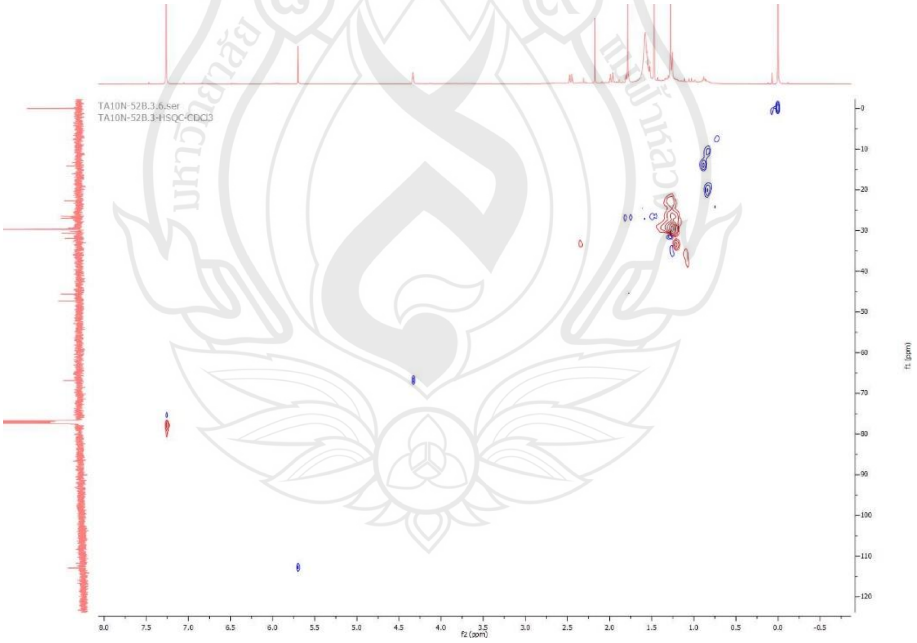

Figure A19 HSQC NMR Spectrum of Compound **T-4** in $CDCl_3$

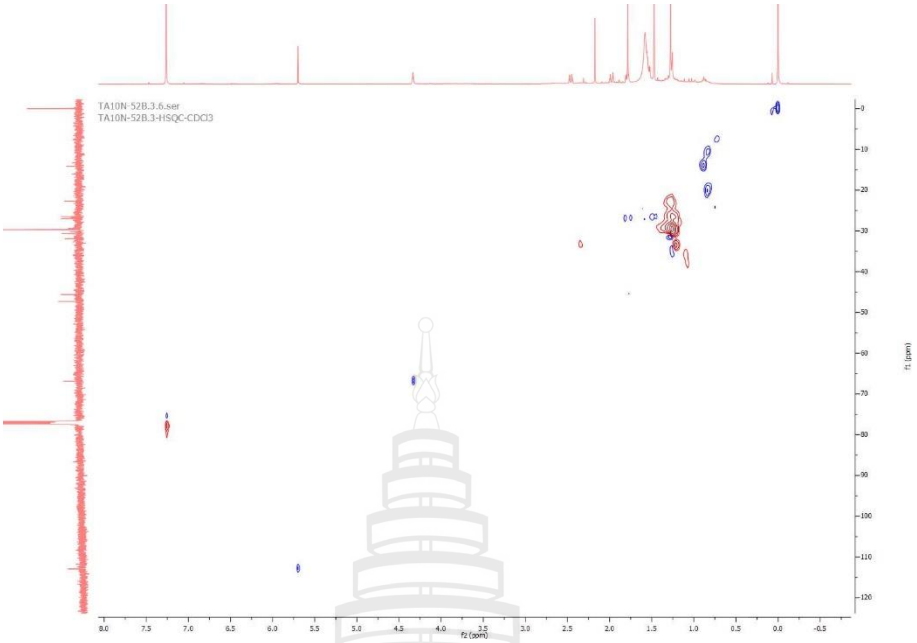

Figure A20 HMBC NMR Spectrum of Compound **T-4** in $CDCl_3$

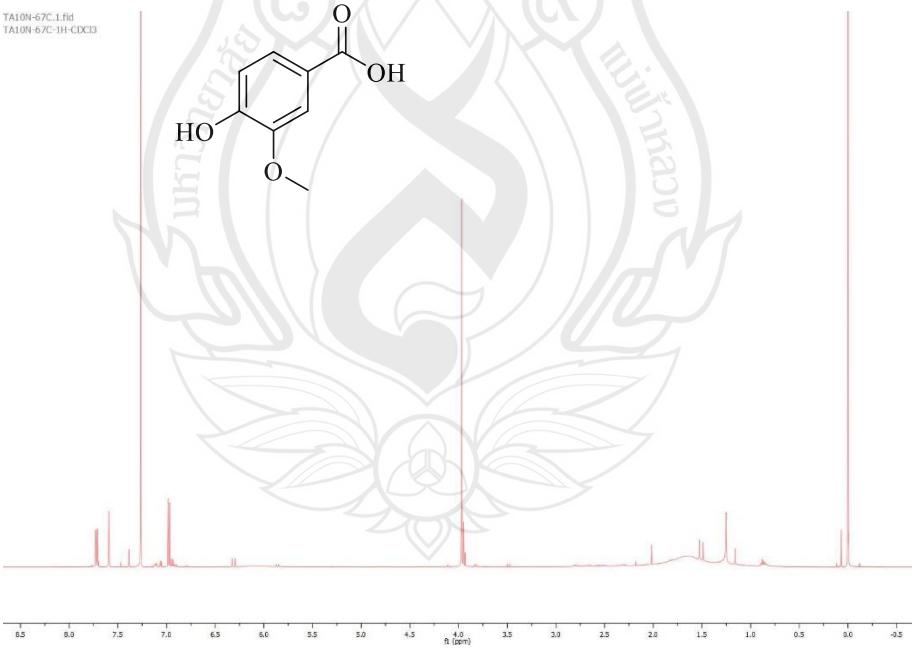

Figure A21 ^{1}H NMR Spectrum of Compound **T-5** in $CDCl_3$ (500 MHZ)

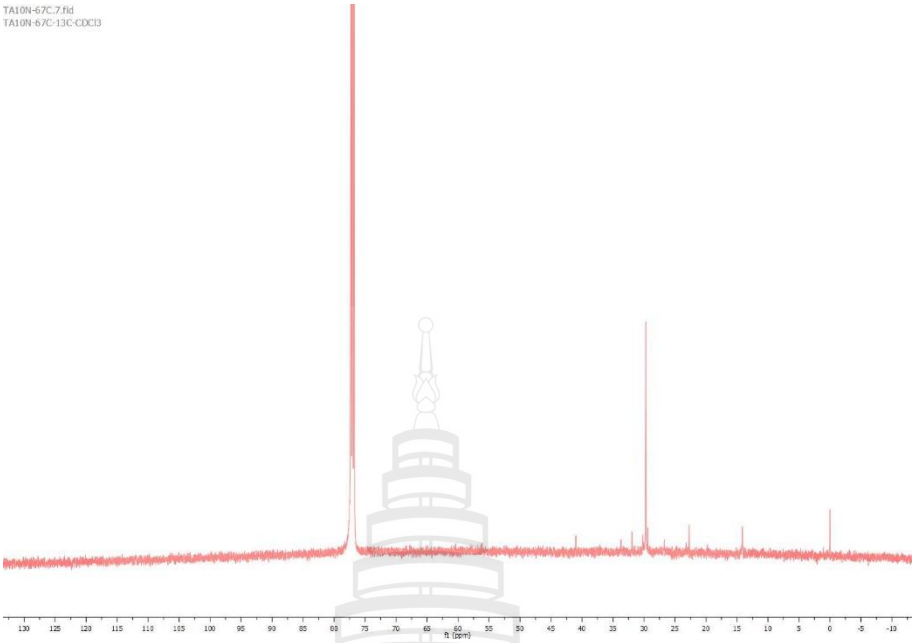

Figure A22 ^{13}C NMR Spectrum of Compound **T-5** in $CDCl_3$ (500 MHZ)

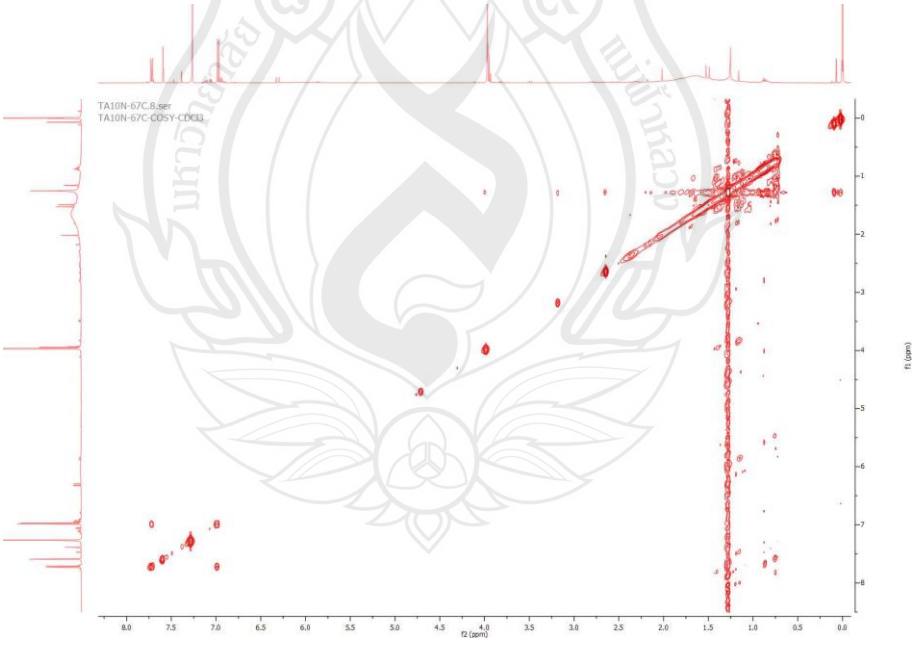

Figure A23 COSY NMR Spectrum of Compound **T-5** in $CDCl_3$

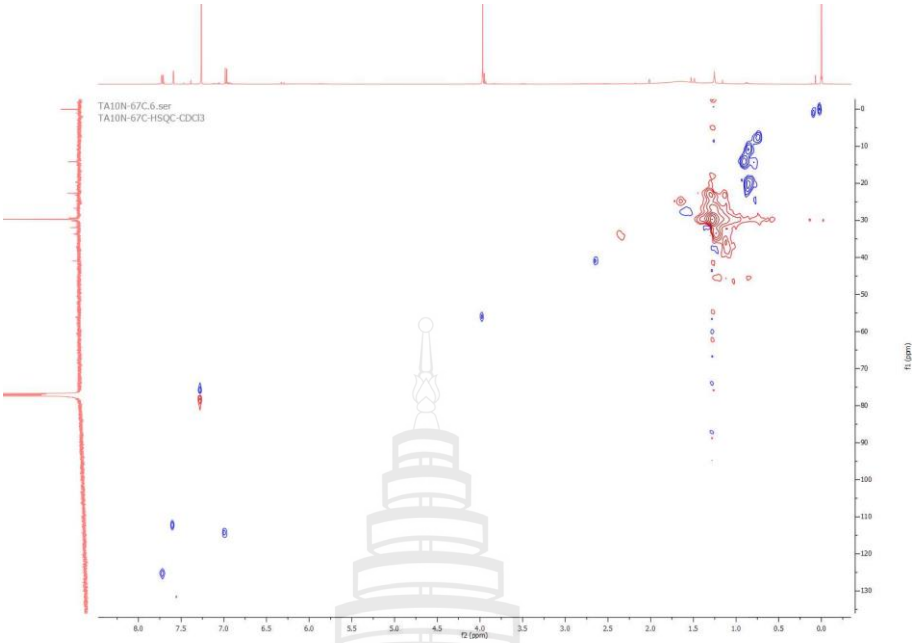

Figure A24 HSQC NMR Spectrum of Compound **T-5** in $CDCl_3$

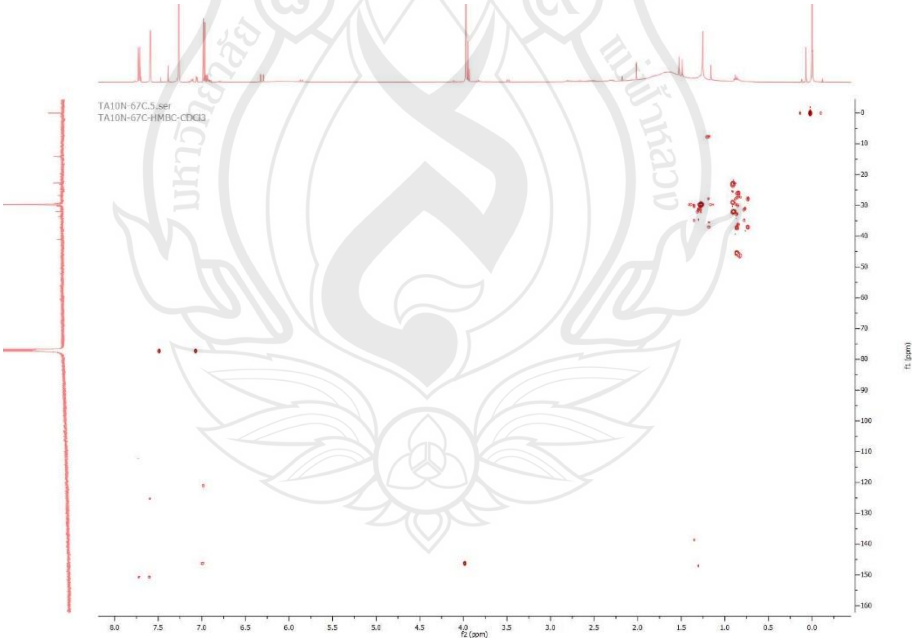

Figure A25 HMBC NMR Spectrum of Compound **T-5** in $CDCl_3$

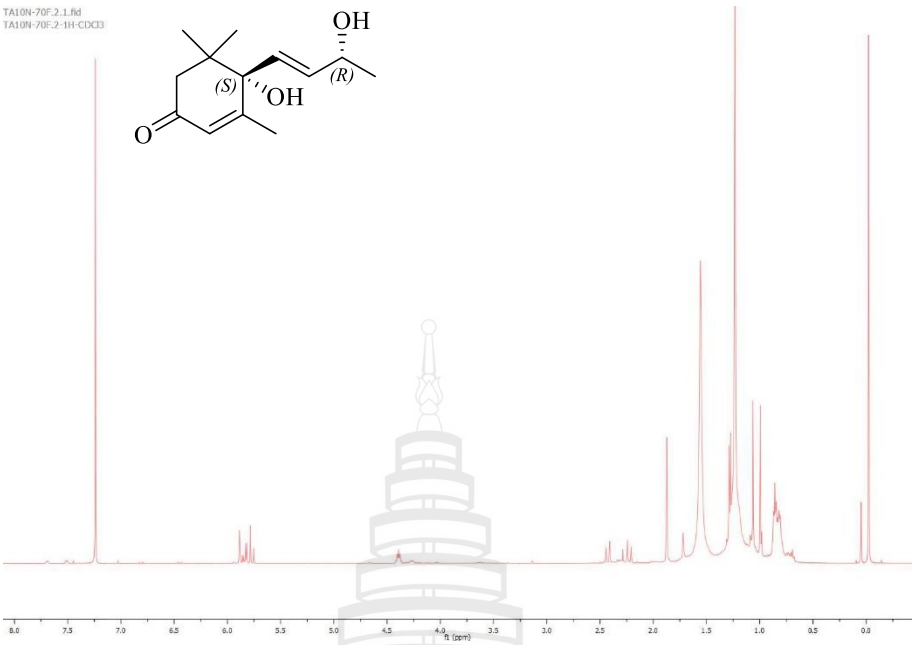

Figure A26 ^{1}H NMR Spectrum of Compound **T-6** in $CDCl_3$ (500 MHZ)

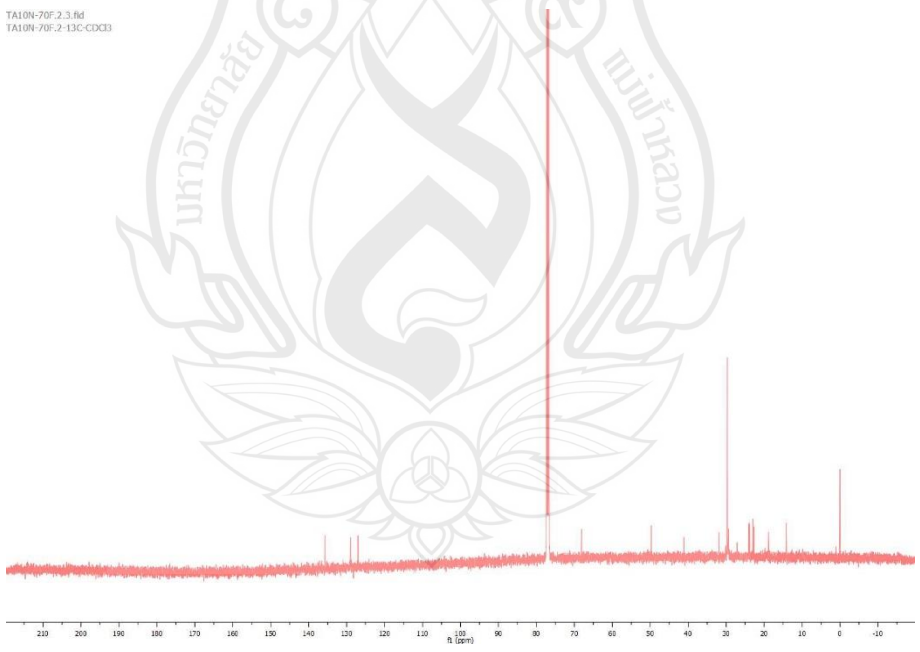

Figure A27 ^{13}C NMR Spectrum of Compound **T-6** in $CDCl_3$ (500 MHZ)

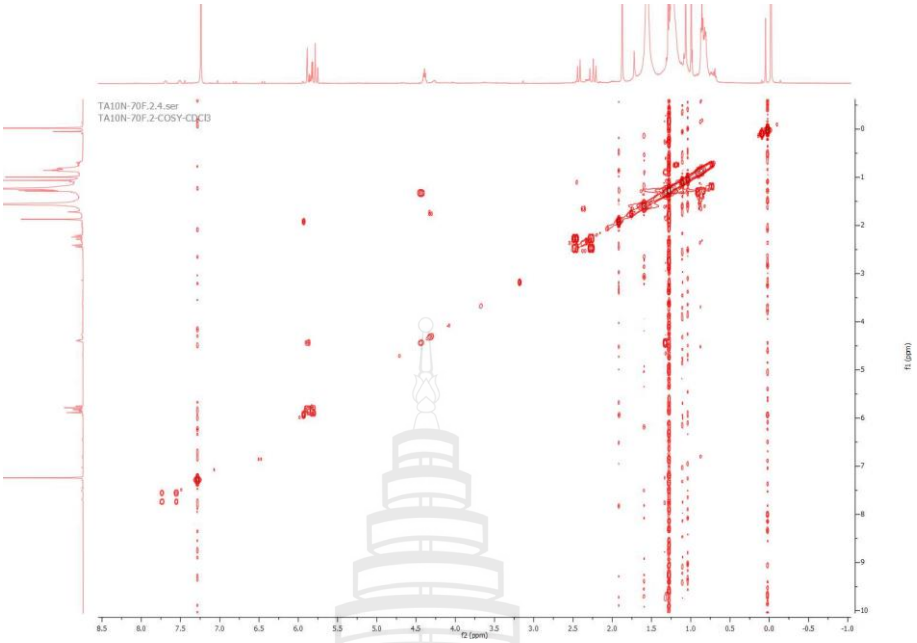

Figure A28 COSY NMR Spectrum of Compound **T-6** in $CDCl_3$

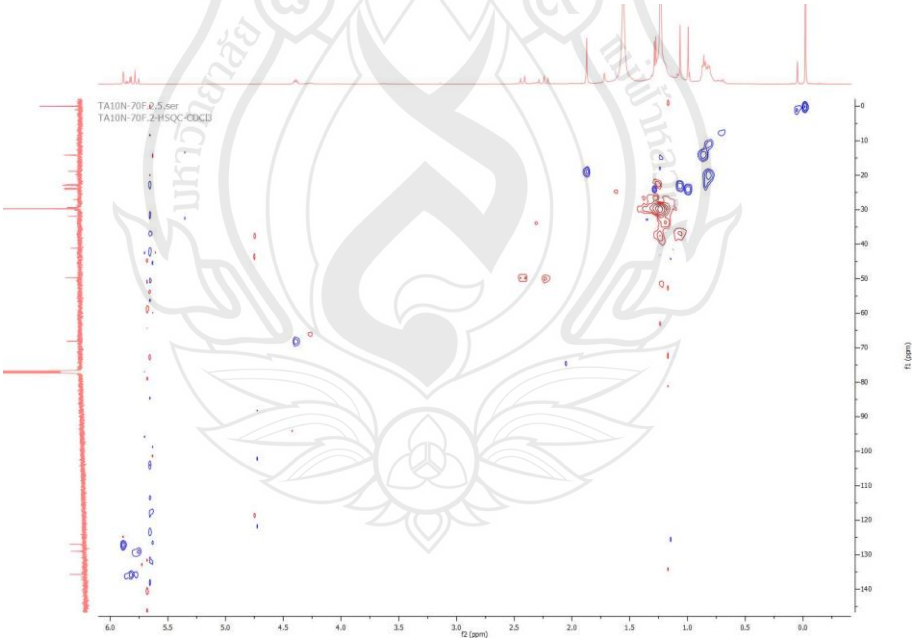

Figure A29 HSQC NMR Spectrum of Compound **T-6** in $CDCl_3$

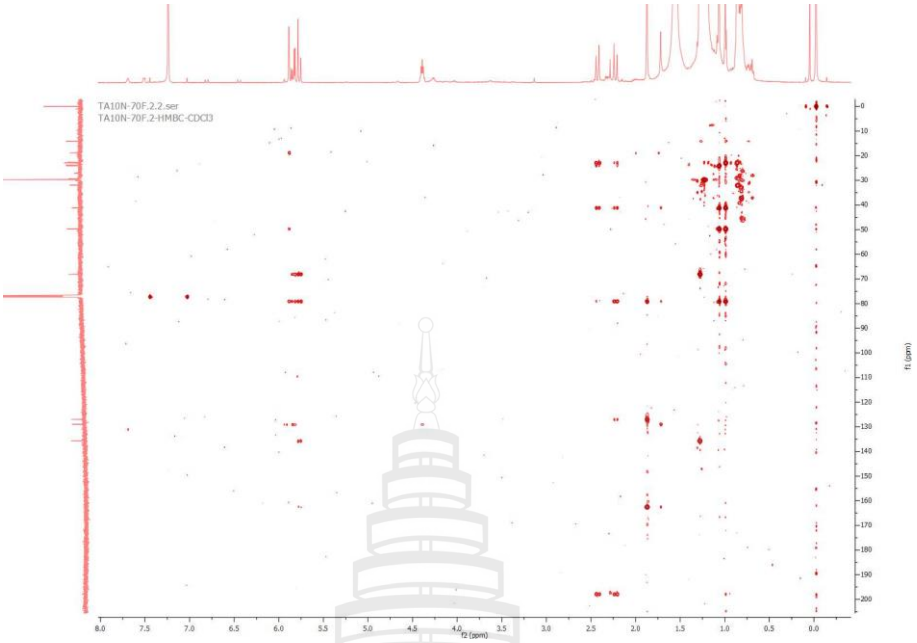

Figure A30 HMBC NMR Spectrum of Compound **T-6** in $CDCl_3$

APPENDIX B

ELECTRONIC CIRCULAR DICHROISM SPECTRUM OF COMPOUNDS FROM *L. JAPONICUS*

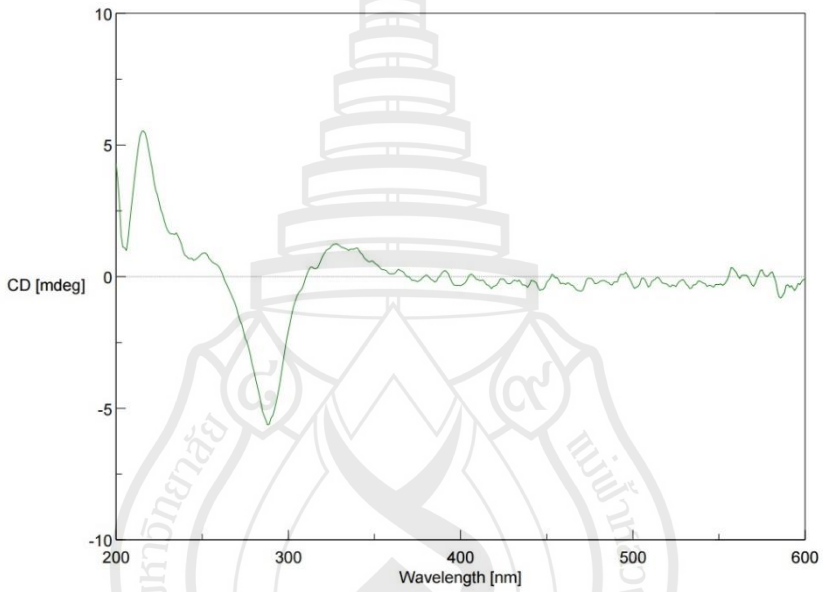

Figure B1 ECD Spectrum of Compound **T-1** in MeOH

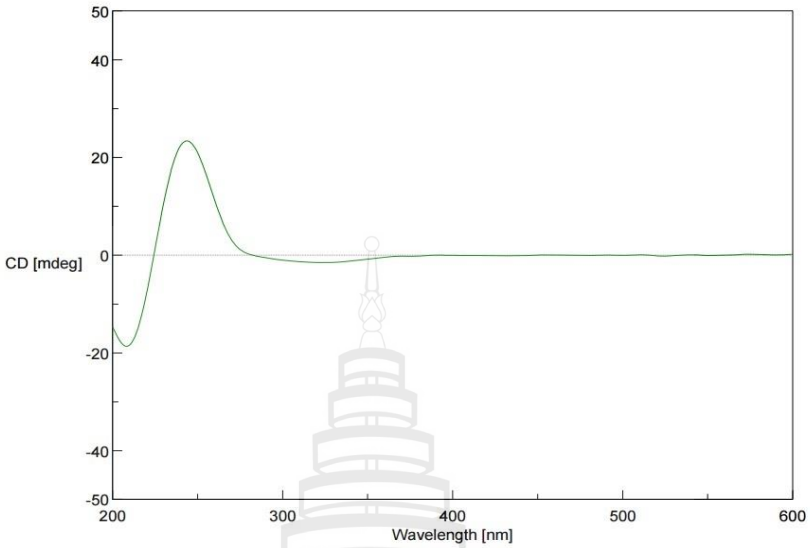

Figure B2 ECD Spectrum of Compound **T-3** in MeOH

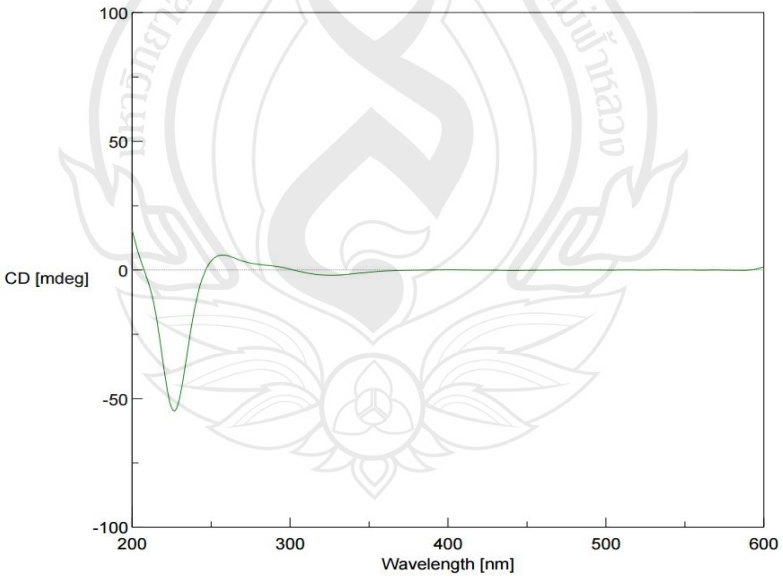

Figure B3 ECD Spectrum of Compound **T-4** in MeOH

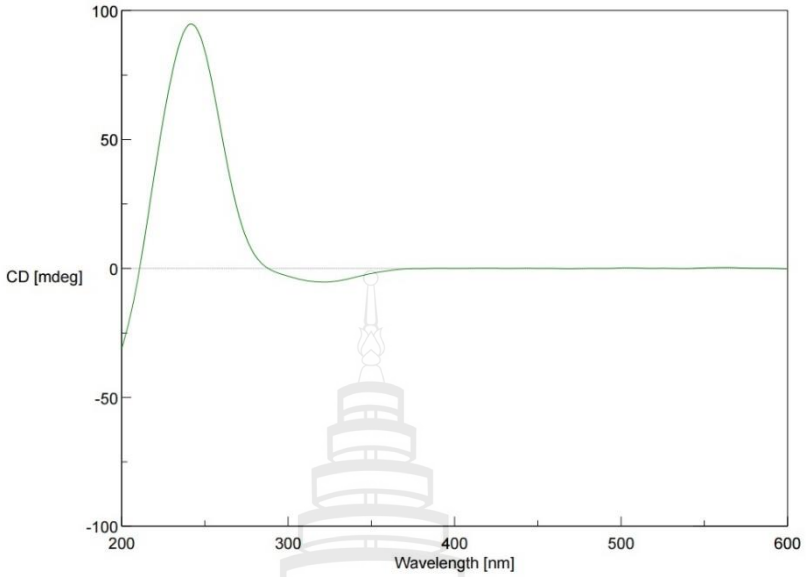

Figure B4 ECD Spectrum of Compound **T-6** in MeOH